**The Dissertation Committee for Yongchao Zhang certifies that this is the approved version of the following dissertation:**

# Amperometric DNA Sensing Using Wired Enzyme Based Electrodes

**Committee:**

Adam Heller, Supervisor

Marye Anne Fox

George Georgiou

Keith Stevenson

Steve Kornguth

# Amperometric DNA Sensing Using Wired Enzyme Based Electrodes

**by**

**Yongchao Zhang, B.S.; M.S.**

**Dissertation**

Presented to the Faculty of the Graduate School of

The University of Texas at Austin

in Partial Fulfillment

of the Requirements

for the Degree of

**Doctor of Philosophy**

**The University of Texas at Austin**

**December, 2003**

# Dedication

This work is dedicated to my wife, Xian, my parents, and my unborn child.

# Acknowledgements

I would like to thank my supervisor Professor Adam Heller for all his guidance and support over the last 5 years, and my former supervisor Professor Marye Anne Fox for her advice and understanding. I would like to thank the other members of my committee, Professors George Georgiou, Keith Stevenson, and Steve Kornguth for taking time to review my work. I would also like to thank my friends and colleagues at The University of Texas at Austin: Ting Chen, Hyug-Han Kim, Nicolas Mano, Zhiqiang Gao, Woonsup Shin, Keith Friedman, Gary Binyamin, Scott Calabrese Barton, Doron Gal, Chuck Campbell, Norma Horn, Colleen Schultz, Susan Odom and Vonda Totten.

I would like to thank my parents for their love and support. Finally I want to express my love and gratitude to my wife, Xian, without whom I could not have completed this work.

# Amperometric DNA Sensing Using Wired Enzyme Based Electrodes

Publication No._____

Yongchao Zhang, Ph.D.

The University of Texas at Austin, 2003

Supervisor: Adam Heller

A water soluble copolymer of acrylamide and 4-vinylpyridine complexed with $[Os(bpy)_2Cl]^{+/2+}$ (bpy = 2,2'-bipyridine), was synthesized. An electrodeposition method of making redox polymer films on electrodes was developed. This method was also shown to be effective in incorporating enzymes and amine-terminated DNA sequences in the redox polymer film.

A 38-base DNA sequence was detected at 20 pM concentration in 15-35 μL droplets by an electrochemical enzyme-amplified sandwich-type assay on a mass-manufacturable screen printed carbon electrode with a diameter of 3.5 mm. A DNA-capturing oligonucleotide was attached to the pre-deposited redox polymer film using the electrodeposition method. The electrode was exposed to the droplet containing the tested DNA sample, and was then treated with a droplet containing horseradish peroxidase-labeled detection sequence. Formation of the

capture-target-detection sandwich brought the horseradish peroxidase-label of the detection sequence in electrical contact with the redox polymer, making the sandwich an electrocatalyst for the reduction of hydrogen peroxide to water at + 0.2 V (Ag/AgCl).

The radial diffusion of electrons through the redox polymer film on the microelectrode allowed the electrodeposition of a thicker film of the redox polymer, an increase in the loading of the capture sequence, and increased the collection efficiency of the electron vacancies originating in the electroreduced $H_2O_2$. With a 10-μm diameter carbon fiber microelectrode, as few as 3000 copies of the 38-basse DNA sequence were detected at 0.5 fM concentration in a 10 μL sample.

A biofuel cell operating at a power density of 50 μW $cm^{-2}$ at 0.5 V under physiological conditions (air saturated, pH 7.4, 0.14 M NaCl, 37.5°C, 15 mM glucose) was developed. The cell had a glucose electro-oxidizing anode and an $O_2$ electro-reducing cathode. The anode and the cathode were 7 μm diameter, 2 cm long carbon fibers, on which the catalytic enzyme-redox polymer adducts were cross-linked. When the miniature cell operated at 0.5 V, the power output dropped to about 60% of its initial value after 2 days of continuous operation at 37.5°C.

# Table of Contents

List of Tables ..... xii

List of Figures ..... xiii

List of Schemes ..... xxii

Chapter 1: A Brief Review of DNA Sensors ..... 1

1.1 Thermal Sensors ..... 2

1.2 Optical Sensors ..... 2

1.2.1 Luminescent Labels ..... 2

1.2.2 Molecular Beacons ..... 3

1.2.3 Fiber Optics ..... 3

1.2.4 Evanescent Wave Devices ..... 4

1.2.5 Surface Plasmon Resonance (SPR) ..... 4

1.3 Acoustic-wave Sensors ..... 5

1.4 Electrochemical Sensors ..... 5

1.5 References ..... 7

Chapter 2: Enzyme-Amplified Detection of a 38-Base Oligonucleotide at 20 pM Concentration in a 30 μL Droplet on a Screen-Printed Electrode ..... 18

2.1 Abstract ..... 18

2.2 Introduction ..... 19

2.3 Experimental ..... 21

2.3.1 Chemicals ..... 21

2.3.2 Preparation of the Redox Polymer ..... 22

2.3.3 Screen-Printed Electrode ..... 24

2.3.4 Equipment ..... 24

2.3.5 Preparation of the DNA Sensing Electrode ..... 25

2.3.6 Hybridizations and Detection ..... 25

2.4 results and discussion ..... 26
2.4.1 Electrodeposition of the Redox Polymer ..... 26
2.4.2 Attachment of the Capture Sequence to the Redox Polymer Film ..... 28
2.4.3 Noise Reduction through Use of the PAA-PVP-Os Redox Polymer ..... 29
2.4.4 Extending the Period of the "Plating" of the Capture Sequence ..... 30
2.4.5 Comparison of Sandwiches Made with One and Two Redox Polymer Layers ..... 30
2.4.6 Detection of Mismatched Base Pairs ..... 33
2.5 conclusions ..... 34
2.6 References ..... 34

Chapter 3: Enzyme-Amplified Amperometric Detection of 3000 Copies of DNA at a 10-μm Diameter Microelectrode ..... 53
3.1 Abstract ..... 53
3.2 Introduction ..... 54
3.3 Experimental ..... 59
3.3.1 Chemicals ..... 59
3.3.2 Redox Polymers ..... 60
3.3.3 Electrodes ..... 60
3.3.4 Instrumentation ..... 60
3.3.5 Electrode Preparation ..... 61
3.3.6 Assay ..... 61
3.4 Results and discussion ..... 62
3.4.1 Electrodeposition of the Redox Polymer and the Capture Sequence ..... 62
3.4.2 Detection of 3000 Copies of Target DNA ..... 64
3.4.3 Mismatched Target Sequences ..... 67
3.4.4 One-Minute DNA Assay ..... 67

3.5 Conclusion ..... 68
3.6 References ..... 69

Chapter 4: Conclusions and Recommended Future work ..... 83

Chapter 5: A Miniature Membrane-less Biofuel Cell Operating under Physiological Conditions at 0.5 V ..... 85
5.1 Abstract ..... 85
5.2 Introduction ..... 86
5.3 Experimental ..... 90
5.3.1 Chemicals ..... 90
5.3.2 Synthesis of the Redox Polymer PVI-[Os(4,4′-diamino2,2′-bipyridine)$_2$Cl]$^{+/2+}$ ..... 91
5.3.3 Synthesis of the Redox Polymer PAA-PVI-[Os(4,4-dichloro-2,2-bipyridine)$_2$Cl]$^{+/2+}$ ..... 91
5.3.4 Biofuel Cell ..... 92
5.3.5 Instrumentation and Electrochemical Measurements ..... 93
5.4 Results and Discussion ..... 94
5.4.1 Polarization Curves of the Miniature Biofuel Cell ..... 94
5.4.2 Effect of the Partial Pressure of $O_2$ ..... 95
5.4.3 Absence of Inhibition in Physiological Solution ..... 95
5.4.4 Stability of the Biofuel Cell ..... 96
5.5 Conclusions ..... 96
5.6 References ..... 97

Chapter 6: Charge Transfer Complexation of Ruthenium Tris-bipyridine by a Stable Carbene ..... 109
6.1 Abstract ..... 109
6.2 Introduction ..... 109
6.3 Experimental ..... 111
6.3.1 Solvents and Chemicals ..... 111
6.3.2 Instrumentation ..... 111

6.3.3 Synthesis of the Stable Carbene ..... 111
6.4 Results and discussion ..... 112
6.4.1 Absorption and Fluorescence Spectra ..... 112
6.4.2 NMR Spectra ..... 114
6.4.3 Cyclic Voltammetry ..... 115
6.5 Conclusion ..... 116
6.6 References ..... 117
Bibliography ..... 129
Vita ..... 145

# List of Tables

Table 2.1: The Capture, Target and HRP-Labeled Detection Sequences ..... 38

Table 3.1: The Capture, Target and HRP-Labeled Detection Sequences ..... 72

Table 3.2: Dependence of the Current Increments on the Concentration of the Analyzed Sequence and on the Presence of Mismatched Bases ..... 73

# List of Figures

Figure 1.1: Schematic representation of biosensors ..... 15

Figure 1.2: Scheme of molecular beacon (MB) based DNA sensors. Q: quencher; F: fluorophore ..... 16

Figure 1.3: Schematic representation of sandwich-type enzyme-amplified DNA detection ..... 17

Figure 2.1: (A) Scheme of the sandwich-type assay. The capture probe is covalently bound to the redox polymer; after hybridization, the HRP label on the detection probe electrically contacts the redox polymer, making it a catalyst for the reduction of $H_2O_2$ to $H_2O$. (B) Steps of electron transfer in the electroreduction of $H_2O_2$ to $H_2O$ ..... 39

Figure 2.2: Structures of PAA-PVP and PAA-PVP-Os ..... 40

Figure 2.3: Schemes of (A) an array of screen-printed electrodes on polyester film, and (B) a SPE droplet-based cell ..... 41

Figure 2.4: Mechanism of electron-induced crosslinking of PAA-PVP-Os ..... 42

Figure 2.5: Attachment of the $NH_2$-terminated capture sequence to the PAA-PVP-Os redox polymer ..... 43

Figure 2.6: Cyclic voltammogramms of a sceen printed electrode at different scan rates. The electrode was coated with PAA-PVP-Os by applying 25 µL 1 mg/mL PAA-PVP-Os PBS solution on the electrode while the electrode was poised at –1.4 V for 30 sec. The electrode was extensively washed with water after deposition, and the cyclic voltammograms were taken in PBS. Scan rate (from bottome to top): 5, 10, 20, 30, 40, 50, 60, 70, 80, 100 mV/S..... 44

Figure 2.7: Dependence of the peak current on the scan rate. Conditions are the same as in Figure 2.5. Solid circles (●): anodic peak current; open circles (○): cathodic peak current ..... 45

Figure 2.8: Dependence of the peak current on the polymer concentration. PAA-PVP-Os was deposited on screen printed electrodes by applying 25 µl polymer solutions to the electrodes and poising the electrodes at –1.4 V for 2 min. Anodic peak currents were measured in cyclic voltammograms which were recorded in PBS at 10 mV $sec^{-1}$ scan rate..... 46

Figure 2.9: Dependence of the peak current on the deposition time. PAA-PVP-Os was deposited on screen printed electrodes by applying 25 µl 1 mg/mL polymer solution to the electrodes and poising the electrodes at –1.4 V for various durations. Anodic peak currents were measured in cyclic voltammograms which were recorded in PBS at 10 mV $sec^{-1}$ scan rate ..... 47

Figure 2.10: Cyclic voltammograms of a screen printed electrode after (a) electrodeposition of PAA-PVP-Os, (b) incorporation of the capture probe, (c) electrodeposition of a second layer of PAA-PVP-Os, and (d) hybridizations with the target, T, and with the detection probe. PAA-PVP-Os film was deposited by applying 25 μL 1 mg/mL polymer solution to the electrode and poising the electrode at –1.4 V (vs. Ag/AgCl) for 2 min. Capture sequence was attached by applying 25 μL 1 μM capture sequence solution to the electrode and poising the electrode at –1.4 V for 20 min. Hybridizations were carried out, sequentially, with the target sequence at 46 °C for 30 min, with the detection sequence at 37 °C for 40 min ..... 48

Figure 2.11: Dependence of the $H_2O_2$ electroreduction current on the deposition time of the capture sequence. PAA-PVP-Os was electrodeposited on the screen printed electrodes by applying -1.4 V (Ag/AgCl) for 2 min. The capture sequence was incorporated by applying the same potential for 2, 4, 10, and 20 min, respectively. The electrodes were allowed to hybridize with 1 nM target (T) and 50 nM detection probe. The current was measured with the electrodes poised at 0.2 V (Ag/AgCl), PBS buffer, 0.2 mM $H_2O_2$ ..... 49

Figure 2.12: Dependence of the $H_2O_2$ electroreduction current on the concentration of the target (T). The electrodes were coated with PAA-PVP-Os by applying -1.4 V (Ag/AgCl) for 2 min, then loaded with the capture probe by applying the same potential for 20 min. (+): Before hybridization, the electrodes were coated with a second layer of PAA-PVP-Os; and (Δ): No second layer of PAA-PVP-Os was coated. The currents were measured while the electrodes were poised at 0.2 V (Ag/AgCl); PBS buffer; 0.2 mM $H_2O_2$ ..... 50

Figure 2.13: Schemes of sandwich assays made with (A) a single layer of the redox polymer, and (B) two layers of the redox polymer ..... 51

Figure 2.14: $H_2O_2$ reduction currents of the sandwich hybrids with 0, 1, and 2 mismatched base pairs, T, M1, and M2, respectively. Standard deviations: T, 9 nA; M1, 3 nA; and M2, 2 nA. Target concentrations 1 nM. Other conditions as in Figure 7 ..... 52

Figure 3.1: (A) Tip of a 10-μm diameter glassy carbon microelectrode. The 10-μm diameter carbon fiber is embedded in glass. (B) The tip of a microelectrode is placed in 10 μL sample solution as during the hybridization. The size of the tip is shown against the ruler..... 74

Figure 3.2 (A): Cyclic voltammograms of a microelectrode coated with the redox polymer, PAA-PVP-Os, at different scan rates. The redox polymer was deposited by placing the microelectrode in 200 µL of a 1 mg $mL^{-1}$ polymer solution in PBS and applying a constant potential of –1.4 V (vs. Ag/AgCl) for 2 min. Scan rate (from bottom to top): 2, 5, 10, 15, 20, 30, 40, 50, and 60 mV $S^{-1}$ ..... 75

Figure 3.2 (B): Cyclic voltammograms of a microelectrode coated with the redox polymer, PAA-PVP-Os, at different scan rates. The redox polymer was deposited by placing the microelectrode in 200 µL of a 1 mg $mL^{-1}$ polymer solution in PBS and applying a constant potential of –1.4 V (vs. Ag/AgCl) for 2 min. Scan rate (from bottom to top): 80, 100, 150, 200, 250, 300, and 400 mV $S^{-1}$ ..... 76

Figure 3.3: Dependence of the peak current of cyclic voltammograms on the scan rate. The 10-µm microelectrode was coated with the redox polymer, PAA-PVP-Os, by placing the microelectrode in 200 µL of a 1 mg $mL^{-1}$ polymer solution in PBS and applying a constant potential of –1.4 V (vs. Ag/AgCl) for 2 min. ●: Anodic peak currents; ○: cathodic peak currents ..... 77

Figure 3.4: Dependence of the peak current of cyclic voltammograms on the square root of scan rate. The 10-μm microelectrode was coated with the redox polymer, PAA-PVP-Os, by placing the microelectrode in 200 μL of a 1 mg $mL^{-1}$ polymer solution in PBS and applying a constant potential of –1.4 V (vs. Ag/AgCl) for 2 min. ●: Anodic peak currents; ○: cathodic peak currents..... 78

Figure 3.5: Cyclic voltammograms of a microelectrode after (a) electrodeposition of the redox polymer, and (b) incorporation of the capture oligonucleotide. The redox polymer, PAA-PVP-Os, was deposited by placing the microelectrode in 200 μL of a 1 mg $mL^{-1}$ polymer solution in PBS and applying a constant potential of –1.4 V (vs. Ag/AgCl) for 2 min. The capture oligonucleotide was subsequently deposited by placing the electrode in 200 μL of a 1 μM solution of the capture sequence and applying the same potential for 20 min. PBS, scan rate 10 $mV \cdot s^{-1}$ ..... 79

Figure 3.6: Current increments upon raising [$H_2O_2$ ] from 0 to 1 mM. (a) Without the analyzed sequence in the droplet (b) with 1 x $10^{-14}$ M perfectly matched analyzed sequence; (c) as in (b), but with a mismatched base (M1); (d) as in (b), with two mismatched bases (M2). Electrodes were activated by depositing the redox polymer and the capture sequence, as described in Figure 3.5. Electrodes poised at 0.12 V vs. Ag/AgCl. PBS, 25ºC. $H_2O_2$ added at t = 200 s..... 80

Figure 3.7: Dependence of the current increment on the concentration of the analyzed sequence (the perfectly matched target sequence). Electrodes were made as in Figure 3.6 ..... 81

Figure 3.8: One-minute DNA assay. Electrodes were made receptive by electrodepositing the redox polymer and the capture sequence as described before. Current was measured while the electrodes were held at 0.12 V (Ag/AgCl) after (a) the electrode was exposed to the HRP-labeled detection sequence for 5 sec and no target sequence was present; and (b), a 1 nM target sequence solution was contacted for 10 sec followed by 5 sec exposure to the detection sequence solution. $H_2O_2$ was added at t = 30 sec to produce a 1 mM concentration ..... 82

Figure 5.1: Structure of the bilirubin oxidase-"wiring" redox polymer, PAA-PVI-[Os(dCl-bpy)$_2$Cl]$^{+/2+}$, redox potential E°′= +350 mV vs. Ag/AgCl ..... 101

Figure 5.2: Structure of the GOx-"wiring" redox polymer, PVI-[Os(da-bpy)$_2$Cl]$^{+/2+}$, redox potential E°′= -160 mV vs. Ag/AgCl..... 102

Figure 5.3: (a) Schematic drawing of the miniature cell structure; (b) A segment of the cell, consisting of two 7-µm diameter carbon fibers ..... 103

Figure 5.4: Polarization curves of the anode and cathode. Quiescent solution, under air, 37.5 °C, PBS buffer, 15 mM glucose..... 104

Figure 5.5: Dependence of the power density on the cell voltage. Quiescent solution, under air, PBS buffer, 15 mM glucose ..... 105

Figure 5.6: $O_2$ pressure dependence of the power density. Quiescent solution, under air, PBS buffer, 15 mM glucose, 37.5 °C..... 106

Figure 5.7: Dependence of the power density of the cell on the $Cl^-$ concentration. Quiescent solution, air, 37.5 °C, PBS buffer, 15 mM glucose ..... 107

Figure 5.8: Stability of the biofuel cell operating at 0.5 V. Quiescent solution, air, 37.5 °C, PBS buffer, 15 mM glucose..... 108

Figure 6.1: Absorption spectra of 5.4 mM carbene **1** in deaerated acetonitrile before (1) and after (2) exposure to air ..... 122

Figure 6.2: Emission spectra of a 2.7 mM solution of carbene **1** in deaerated THF with increasing amounts of $CuCl_2$. (1) No Cu2+; Carbene-to-$Cu^{2+}$ ratio : (2) 10:1; (3) 5:1; (4) 1:1. Excitation: 345 nm ..... 123

Figure 6.3: Emission spectra of a 4.0 mM solution of carbene **1** in deaerated THF with increasing amounts of $Hg(OAc)_2$: (1) 0; (2) 0.64 mM; (3) 1.6 mM; (4) 4.0 mM $Hg^{2+}$. Excitation: 345 nm..... 124

Figure 6.4: Absorption spectra of in deaerated DMSO of: (a) 1.4 mM carbene **1**; (b) 0.05 mM $[Ru(bpy)_3]^{2+}$; (c) mixture containing 1.4 mM carbene **1** and 0.05 mM $[Ru(bpy)_3]^{2+}$; and (d) sample c after treatment of air ..... 125

Figure 6.5: $^{1}H$ NMR spectra of a 0.05 mM solution in deaerated DMSO-d6 of carbene **1** containing $[Ru(bpy)_3]^{2+}$ with a carbene-to-$[Ru(bpy)_3]^{2+}$ ratio of (a) 0.5:1; and (b) 1:1; and (c) $[Ru(bpy)_3]^{2+}$. All solutions contain trace amount of free 2,2'-bipyridine ..... 126

Figure 6.6: Cyclic voltammograms of a 2.0 mM carbene **1** solution in $CH_3CN$ before (a) and after (b) treatment of air. Electrolyte: 0.1 M $Bu_4$ $NPF_6$..... 127

Figure 6.7: Cyclic voltammograms of (a) 0.8 mM $[Ru(bpy)_3]Cl_2$, and (b) a mixture of 0.8 mM $[Ru(bpy)_3]Cl_2$ and 1.6 mM carbene **1**. solvent: $CH_3CN$. Electrolyte: 0.1 M $Bu_4$ $NPF_6$ ..... 128

# List of Schemes

Scheme 5.1: Electron-transfer steps in the electrooxidation of glucose (top) and in the Electroreduction of $O_2$ (bottom) ..... 100

# Chapter 1: A Brief Review of DNA Sensors

Sequence-based DNA identification is relevant to clinical diagnosis, therapy of genetic disorders and infectious diseases,[1-8] detection of environmental hazardous pathogens (bacterial and viruses),[9-12] monitoring of drug discovery,[13-16] and analysis of forensic samples.[17-19] In general, methods for DNA sequence determination are based on either direct sequencing or DNA hybridization.[20] Because of their simplicity, hybridization-based DNA assays, which utilize the strong and specific interactions between two complementary nucleic acid strands, are more commonly used.

The polymerase chain reaction (PCR) is the most widely used DNA amplification method which, by applying a series of thermal cycles to allow thermal denaturing, annealing and primer extension, amplifies exponentially specific DNA or RNA sequences.[21-24] PCR is powerful and, coupled with DNA detection methods, capable of detecting a single copy of DNA. Quantification can be difficult and requires careful isolation and purification of the original sample sequence and optimization of the amplification conditions.[23,25-28] Other drawbacks include the proneness to contaminations.

A biosensors has a ***biolayer*** (usually immobilized on the surface of a solid support), which binds the ***analyte(s)*** of interest through specific molecular recognition (avidin/biotin, nucleotides, enzymes, etc), and a ***transducer*** which transforms the binding event between the biolayer and the analyte into a

quantifiable and processable, ultimately electrical, signal for acquisition and interpretation (Figure 1.1).[29,30]

Non-radioactive transducers of DNA sensors can be categorized, according to their energy transduction modes (signal transducers), into four major groups: thermal, electrochemical, optical and acoustic.[30,31]

## 1.1 THERMAL SENSORS

Thermal biosensors, which are based on the heat of the reactions involved, have a long history in biosensing.[32] Thermal DNA sensors, however, are rare.

## 1.2 OPTICAL SENSORS

Photonic transduction has been the mainstay of bioanalysis,[30] offering some of the most sensitive DNA sensors.

### 1.2.1 Luminescent Labels

Luminescent reactions (chemiluminescent or bioluminescent) or components of luminescent reactions, such as acridinium esters,[33-35] stabilized dioxetanes,[34] aequorin,[36] have been used to report DNA/RNA hybridization events. Enzymes that catalyze luminescent reactions or luminescent compounds generating reactions, such as alkaline phosphatase,[37-40] luciferase,[41,42] horseradish peroxidase,[43-45] and glucose oxidase[46] have all been used as labels.

Chelates of lanthanide ions ($Eu^{3+}$, $Tb^{3+}$, $Sm^{3+}$ and $Dy^{3+}$) have been used as luminescent labels, and with the use of time-resolved fluorometry (TRF) the background fluorescence was efficiently eliminated and high signal-to-noise ratio and wide dynamic range were achieved.[47-49]

### 1.2.2 Molecular Beacons

A class of DNA probes called molecular beacons, which are single stranded oligonucleotides with a stem-and-loop structure (Figure 1.2), has been introduced.[50-52] The loop portion of the molecular beacons can hybridize to the target ssDNAs. Upon hybridization the conformational change of the stem portion separates the fluorophore from the quencher and the beacon becomes fluorescent.

### 1.2.3 Fiber Optics

DNA optical sensors often incorporate fiber-optic devices (optodes), in which the emission (signal) from a luminescent label propagates to the detector.[30,31,53-56] Significant advantages of using optical fibers include probing of small sample domains, remote sensing and miniaturization. With high density arrays of DNA sensing optical fibers it is possible to monitor multiple DNA sequences in parallel,[57] as well as the detection of amounts as low as zeptomoles.[58]

### 1.2.4 Evanescent Wave Devices

Upon total internal reflection in an optical fiber or other waveguide an electromagnetic wave is generated at each reflection point. Part of this wave penetrates the optically less dense medium outside the waveguide. The wave originating from just outside the multiple reflection points is referred to as the evanescent wave.[30,31] The evanescent wave originates from the near-waveguide 100-200 nm layer, decaying exponentially in the outer space, making it an excellent tool for monitoring, with minimal interference from distant substances, physical property changes, usually the changes in refractive index, of the thin film on the detector surface which can be caused by hybridization in the film.

### 1.2.5 Surface Plasmon Resonance (SPR)

One evanescent wave-based technique is surface plasmon resonance (SPR). It received considerable attention and evolved into a powerful, surface-characterization method for the real-time monitoring of bioaffinity events without the use of labels.[59,60] An ultra thin layer (5-10 nm) of bio-selective material such as biotin and DNA capture probe is deposited on a thin layer (~50 nm) of a metal, mostly gold or silver, which is on top of a prism. Because the surface plasma wave (SPW) is generated at the interface, it is used to measure changes in the biolayers. Its detection limits are at femtomolar concentrations.[61] Drawbacks include the size and cost of the required instrumentation.

## 1.3 ACOUSTIC-WAVE SENSORS

Acoustic-wave sensors oscillate in a narrow frequency range within the $10^6$-$10^9$ Hz domain.[30,62] They are based on piezoelectricity, which is the generation of polarization upon stress, and the converse piezoelectric effect, which is the mechanical deformation induced by an external electric field. Among the piezoelectric crystals quartz is most commonly used. The frequency of oscillation of acoustic wave devices depends on the mass of the oscillator and therefore the material on the surface of the crystal. A linear relationship existed between the frequency decrease and the deposited mass,[63,64] which is the reason such a device is called a quartz-crystal microbalance (QCM). Many QCM-based DNA sensors have been reported in recent years.[65-68] In general, QCM techniques allow real-time, label-free detection, although non-specific binding is usually high,[69] the detection limit is not as good as optical sensors, and the miniaturization is naturally limited.[62]

## 1.4 ELECTROCHEMICAL SENSORS

Electrochemical DNA sensors measure current or resistance changes accompanying DNA hybridization at the surface of electrodes.[70]

Early examples of electrochemical detection of DNA hybridizations were reported by Mikkelsen and co-workers, where $Co(phen)_3^{3+}$ was used as an redox indicator to broadcast the hybridization event, based on the fact that $Co(phen)_3^{3+}$ binds to the capture-target DNA duplex preferably over single stranded DNA.[71,72] Other DNA ligands have been used as redox markers,[73-76] and low detection limits

have been reached.[77] Electrochemical detection of DNA hybridization and single-base mismatch based on the long-range electron transfer through ds-DNA has been reported.[78-81] The electrocatalytic oxidation of guanine by $Ru(bpy)_3^{3+}$ has also been used to detect the DNA hybridization.[82-84]

Conductivity-based DNA detection has been reported by Mirkin and co-workers, in which capture oligonucleotides immobilized in the 20-μm gap between two microelectrodes hybridize first with the target oligonucleotides and then with Au nanoparticle-labeled probe oligonucleotides.[85] Upon hybridization the Au nanoparticles line up between and bridge the microelectrodes.

Amperometric DNA sensors are based on the specificity and selectivity of enzymes and measure the electron flow between the redox centers of enzymes and electrodes.[31] Typically, to minimize the handling and pretreatment of the assayed DNA, a sandwich-type assay is adopted where an enzyme is used as a redox-active label and is attached to a detection oligonucleotide, and a capture oligonucleotide is immobilized on the electrode (Figure 1.3). The sequences of both the capture and the detection oligonucleotides are complementary to that of the analyzed DNA (the "target"), and in the presence of the target DNA a capture-target-probe hybrid forms, bringing the enzyme label into electrical contact with the electrode. The detection involves the poising of the electrode at a constant potential where the substrate-oxidized/reduced enzyme is electro-reduced/oxidized, resulting in the flow of a current.

The redox centers of many enzymes are buried inside thick insulating protein or glycoprotein shells and direct electron transfer between the redox

centers and the electrode is negligibly slow.[86,87] This problem was overcome by electron mediators which effectively transport electrons between the enzyme and the electrode. The initially used diffusional electron mediators were later replaced by electron-conducting redox polymers.[87-92]

The main advantages of electrochemical DNA sensors over optical sensors are their high sensitivity, ease of design, feasibility of miniaturization, low cost, low power requirements, portability allowing on-site and in-situ detection, and independence of sample turbidity.[70,93-96]

This dissertation is focused on the development of "wired" enzyme amplified amperometric DNA/RNA sensors. In chapter 2 a new osmium bis-bipyridine complex-based redox polymer is synthesized as an enzyme "wire". The feasibility of mass-producing DNA biosensors is tested by electrodepositing the redox polymer onto manufacturable screen-printed carbon electrodes. In chapter 3 microelectrodes are used as substrates for DNA sensors instead of the much larger screen-printed electrodes and it is shown by using microelectrodes that the sensitivity is more than one thousand fold improved. Chapter 4 outlines future directions in DNA-sensing. Chapter 5 describes a miniature membrane-less biofuel cell operating under physiological conditions at 0.5 V. In chapter 6 a stable carbene is synthesized and its photochemistry is studied.

## 1.5 REFERENCES

(1) Malcolm, S. *Eur. J. Biochem.* **1990**, *194*, 317-321.

(2) Wood, S.; Langlois, S. *J. Chromatography* **1991**, *569*, 421-447.

(3) Schochetman, G. *Clin. Chim. Acta* **1992**, *211*, 1-26.

(4) Burchill, S. A.; Selby, P. J. *J. Pathol.* **2000**, *190*, 6-14.

(5) Tawata, M.; Aida, K.; Onaya, T. *Combinat. Chem. High Throughput Screen.* **2000**, *3*, 1-9.

(6) Clarke, J. R. *Expert Rec. Mol. Diagn.* **2002**, *2*, 233-239.

(7) Zammatteo, N.; Hamels, S.; de Longueville, F.; Alexandre, I.; Gala, J.-l.; Brasseur, F.; Remacle, J. *Biotech. Ann. Rev.* **2002**, *8*, 85-101.

(8) Opalinska, J. B.; Gewirtz, A. M. *Nat. Rev. Drug. Disc.* **2002**, *1*, 503-514.

(9) Smith, C. L.; Kricka, L.; Krull, U. J. *Gen. Anal. Biomol. Eng.* **1995**, *12*, 33-37.

(10) Ivnitski, D.; Abdel-Hamid, I.; Atanasov, P.; Wilkins, E. *Biosens. Bioelectron.* **1999**, *14*, 599-624.

(11) Olsen, J. E. *Food Research International* **2000**, *33*, 257-266.

(12) Candrian, U. *Journal of Microbiological Methods* **1995**, *23*, 89-103.

(13) Gambari, R. *Am. J. Pharmacogen.* **2001**, *1*, 119-135.

(14) Gmuender, H. *BioTech.* **2002**, *32*, 152-154, 156, 158.

(15) Johnson, P. H.; Walker, R. P.; Jones, S. W.; Stephens, K.; Meurer, J.; Zajchowski, D. A.; Luke, M. M.; Eeckman, F.; Tan, Y.; Wong, L.; Parry, G.; Morgan, T. K., Jr.; McCarrick, M. A.; Monforte, J. *Mol. Cancer Therap.* **2002**, *1*, 1293-1304.

(16) Durick, K.; Negulescu, P. *Biosens. Bioelectron.* **2001**, *16*, 587-592.

(17) Benecke, M. *Naturwiss.* **1997**, *84*, 181-188.

(18) Laszik, A.; Falus, A.; Keresztury, L.; Sotonyi, P. *Acta Biol. Hun.* **1998**, *49*, 89-95.

(19) Gockel, A.; Berschick, P. *Nucl. Acids. Isol. Meth.* **2003**, 153-177.

(20) Christopoulos, T. K. *Anal. Chem.* **1999**, *71*, 425R-438R.

(21) Poljak, M.; Seme, K.; Koren, S. *Period. Biol.* **1996**, *98*, 183-190, P.190.

(22) Wabuyele, M. B.; Soper, S. A. *Single Mol.* **2001**, *2*, 13-21.

(23) Raeymaekers, L. *Mol. Biotech.* **2000**, *15*, 115-122.

(24) Johnson, J. R. *J. Microbiol. Meth.* **2000**, *41*, 201-209.

(25) Raeymaekers L. *Anal. Biochem.* **1993**, *214*, 582-585.

(26) Jung, R.; Soondrum, K.; Neumaier, M. *Clin. Chem. Lab. Med.* **2000**, *38*, 833-836.

(27) Ayala-Torres, S.; Chen, Y.; Svoboda, T.; Rosenblatt, J.; Van Houten, B. *Methods* **2000**, *22*, 135-147.

(28) Lovatt, A. *Rev. Mol. Biotech.* **2002**, *82*, 279-300.

(29) Ramsay, G., Ed. *Commercial Biosensors: Applications to Clinical, Bioprocess, and Environmental Samples*; John Wiley & Sons, Inc: New York, 1998.

(30) Cunningham, A. J. *Introduction to Bioanalytical Sensors*; John Wiley & Sons, Inc: New York, 1998.

(31) Sethi, R. S. *Biosens. Bioelectron.* **1994**, *9*, 243-264.

(32) Danielsson, B.; Mosbach, K. In *Biosensors: Fundamentals and Applications.*; Turner, A. P. F., Karube, I., Wilson, G. S., Eds.; Oxford University Press: New York, 1989.

(33) Arnold, L. J., Jr.; Hammond, P. W.; Weise, W. A.; Nelson, N. C. *Clin. Chem.* **1989**, *35*, 1588-1594.

(34) Nelson, N. C.; Kacian, D. L. *Clin. Chim. Acta* **1990**, *194*, 73-90.

(35) Ou, C. Y.; McDonough, S. H.; Cabanas, D.; Ryder, T. B.; Harper, M.; Moore, J.; Schochetman, G. *AIDS Res. Human Retrovir.* **1990**, *6*, 1323-1329.

(36) Actor, J. K.; Kuffner, T.; Dezzutti, C. S.; Hunter, R. L.; McNicholl, J. M. *J. Immunol. Meth.* **1998**, *211*, 65-77.

(37) Hauber, R.; Geiger, R. *Nucl. Acids. Res.* **1988**, *16*, 1213.

(38) Clyne, J. M.; Running, J. A.; Stempien, M.; Stephens, R. S.; Akhavan-Tafti, H.; Schaap, A. P.; Urdea, M. S. *J. Biolumi. Chemilumi.* **1989**, *4*, 357-366.

(39) Ishii, J. K.; Ghosh, S. S. *Bioconjugate Chem.* **1993**, *4*, 34-41.

(40) Chiu, N. H. L.; Christopoulos, T. K.; Peltier, J. *Analyst* **1998**, *123*, 1315-1319.

(41) Chiu, N. H. L.; Christopoulos, T. K. *Anal. Chem.* **1996**, *68*, 2304-2308.

(42) Verhaegen, M.; Christopoulos, T. K. *Anal. Chem.* **2002**, *74*, 4378-4385.

(43) Pollard-Knight, D.; Read, C. A.; Downes, M. J.; Howard, L. A.; Leadbetter, M. R.; Pheby, S. A.; McNaughton, E.; Syms, A.; Brady, M. A. W. *Anal. Biochem.* **1990**, *185*, 84-89.

(44) Casperson, M. E.; Coughlin, R. W.; Davis, E. M. *Trends Anal. Chem.* **1991**, *10*, 133-136.

(45) Girotti, S.; Musiani, M.; Ferri, E.; Gallinella, G.; Zerbini, M.; Roda, A.; Gentilomi, G.; Venturoli, S. *Anal. Biochem.* **1996**, *236*, 290-295.

(46) DeFillipo, K. A.; Grayeski, M. L. *Anal. Chim. Acta* **1991**, *249*, 155-162.

(47) Elbanowski, M.; Makowska, B. *J. Photochem. Photobiol. A* **1996**, *99*, 85-92.

(48) Hakala, H.; Virta, P.; Salo, H.; Lonnberg, H. *Nucl. Acids. Res.* **1998**, *26*, 5581-5588.

(49) Hakala, H.; Mäki, E.; Lönnberg, H. *Bioconjugate Chem.* **1998**, *9*, 316-321.

(50) Tyagi, S.; Kramer, F. R. *Nat. Biotechnol.* **1996**, *14*, 303-309.

(51) Liu, X.; Tan, W. *Anal. Chem.* **1999**, *71*, 5054-5059.

(52) Tan, W.; Fang, X.; Li, J.; Liu, X. *Chem. Eur. J.* **2000**, *6*, 1107-1111.

(53) Wang, J. *Nucl. Acids. Res.* **2000**, *28*, 3011-3016.

(54) Vercoutere, W.; Akeson, M. *Cur. Opin. Chem. Biol.* **2002**, *6*, 816-822.

(55) Marazuela, M. D.; Moreno-Bondi, M. C. *Anal. Bioanal. Chem.* **2002**, *372*, 664-682.

(56) Wolfbeis, O. S. *Anal. Chem.* **2002**, *74*, 2663-2677.

(57) Ferguson, J. A.; Steemers, F. J.; Walt, D. R. *Anal. Chem.* **2000**, *72*, 5618-5624.

(58) Epstein, J. T.; Lee, M.; Walt, D. R. *Anal. Chem.* **2002**, *74*, 1836-1840.

(59) Kambhampati, D. K.; Knoll, W. *Cur. Opin. Coll. Interf. Sci.* **1999**, *4*, 273-280.

(60) Homola, J.; Yee, S. S.; Gauglitz, G. *Sens. Actuat. B* **1999**, *54*, 3-15.

(61) Song, F.; Zhou, F.; Wang, J.; Tao, N.; Lin, J.; Vellanoweth, R. L.; Morquecho, Y.; Wheeler-Laidman, J. *Nucl. Acids. Res.* **2002**, *30*, e72-.

(62) Janshoff, A.; Galla, H.-J.; Steinem, C. *Angew. Chem. Int. Ed.* **2000**, *39*, 4004-4032.

(63) Schumacher, R. *Angew. Chem. Int. Ed.* **1990**, *29*, 329.

(64) Buttry, D. A.; Ward, M. D. *Chem. Rev.* **1992**, *92*, 1355-1379.

(65) Caruso, F.; Rodda, E.; Furlong, D. N.; Niikura, K.; Okahata, Y. *Anal. Chem.* **1997**, *69*, 2043-2049.

(66) Wang, J.; Nielsen, P. E.; Jiang, M.; Cai, X.; Fernandes, J. R.; Grant, D. H.; Ozsoz, M.; Beglieter, A.; Mowat, M. *Anal. Chem.* **1997**, *69*, 5200-5202.

(67) Patolsky, F.; Lichtenstein, A.; Willner, I. *J. Am. Chem. Soc.* **2000**, *122*, 418 -419.

(68) Mannelli, I.; Minunni, M.; Tombelli, S.; Mascini, M. *Biosens. Bioelectron.* **2003**, *18*, 129-140.

(69) Byfield, M. P.; Abuknesha, R. A. *Biosens. Bioelectron.* **1994**, *9*, 373-399.

(70) Palecek, E. *Talanta* **2002**, *56*, 809-819.

(71) Millan, K. M.; Mikkelsen, S. R. *Anal. Chem.* **1993**, *65*, 2317-2323.

(72) Millan, K. M.; Saraullo, A.; Mikkelsen, S. R. *Anal. Chem.* **1994**, *66*, 2943-2948.

(73) Erdem, A.; Kerman, K.; Meric, B.; Akarca, U. S.; Ozsoz, M. *Anal. Chim. Acta* **2000**, *422*, 139.

(74) Erdem, A.; Kerman, K.; Meric, B.; Ozsoz, M. *Electroanalysis* **2001**, *13*, 219.

(75) Takagi, M. *Pure App. Chem.* **2001**, *73*, 1573-1577.

(76) Takenaka, S. *Bull. Chem. Soc. Jpn.* **2001**, *74*, 217-224.

(77) Takenaka, S.; Yamashita, K.; Takagi, M.; Uto, Y.; Kondo, H. *Anal. Chem.* **2000**, *72*, 1334-1341.

(78) Kelley, S. O.; Boon, E. M.; Barton, J. K.; Jackson, N. M.; Hill, M. G. *Nucl. Acids. Res.* **1999**, *27*, 4830-4837.

(79) Kelley, S. O.; Jackson, N. M.; Hill, M. G.; Barton, J. K. *Angew. Chem. Int. Ed.* **1999**, *38*, 941-945.

(80) Boon, E. M.; Ceres, D. M.; Drummond, T. G.; Hill, M. G.; Barton, J. K. *Nat. Biotechnol.* **2000**, *18*, 1096-1100.

(81) Boon, E. M.; Barton, J. K. *Cur. Opin. Struc. Biol.* **2002**, *12*, 320-329.

(82) Johnston, D. H.; Glasgow, K. C.; Thorp, H. H. *J. Am. Chem. Soc.* **1995**, *117*, 8933-8938.

(83) Napier, M. E.; Loomis, C. R.; Sistare, M. F.; Kim, J.; Eckhardt, A. E.; Thorp, H. H. *Bioconjugate Chem.* **1997**, *8*, 906-913.

(84) Armistead, P. M.; Thorp, H. H. *Anal. Chem.* **2000**, *72*, 3764-3770.

(85) Park, S.-J.; Taton, T. A.; Mirkin, C. A. *Science* **2002**, *295*, 1503-1506.

(86) Degani, Y.; Heller, A. *J. Am. Chem. Soc.* **1988**, *110*, 2615-2620.

(87) Heller, A. *Acc. Chem. Res.* **1990**, *23*, 128-134.

(88) De Lumley-Woodyear, T.; Campbell, C. N.; Heller, A. *J. Am. Chem. Soc.* **1996**, *118*, 5504-5505.

(89) Caruana, D. J.; Heller, A. *J. Am. Chem. Soc.* **1999**, *121*, 769-774.

(90) De Lumley-Woodyear, T.; Caruana, D. J.; Campbell, C. N.; Heller, A. *Anal. Chem.* **1999**, *71*, 394-398.

(91) Campbell, C. N.; Gal, D.; Cristler, N.; Banditrat, C.; Heller, A. *Anal. Chem.* **2002**, *74*, 158-162.

(92) Dequaire, M.; Heller, A. *Anal. Chem.* **2002**, *74*, 4370 -4377.

(93) Wang, J. *Chem. Eur. J.* **1999**, *5*, 1681-1685.

(94) Wang, J. *Trends Anal. Chem.* **2002**, *21*, 226-232.

(95) Wang, J. *Anal. Chim. Acta* **2002**, *469*, 63-71.

(96) Popovich , N. D.; Thorp, H. H. *The Electrochemical Society Interface* **2002**, *11*, 30-34.

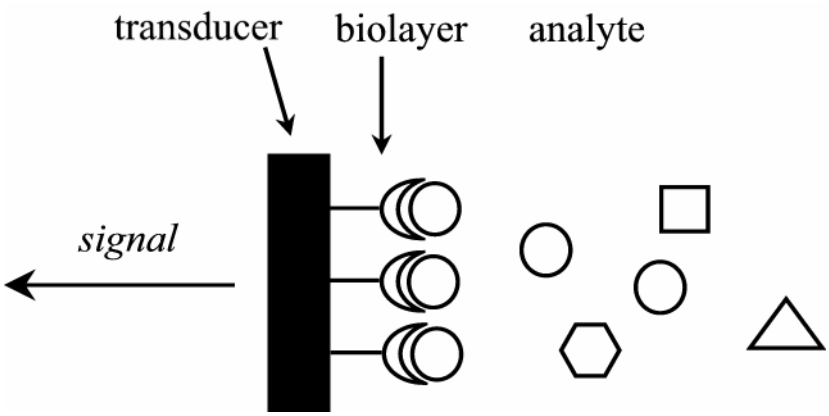


Figure 1.1: Schematic representation of biosensors.

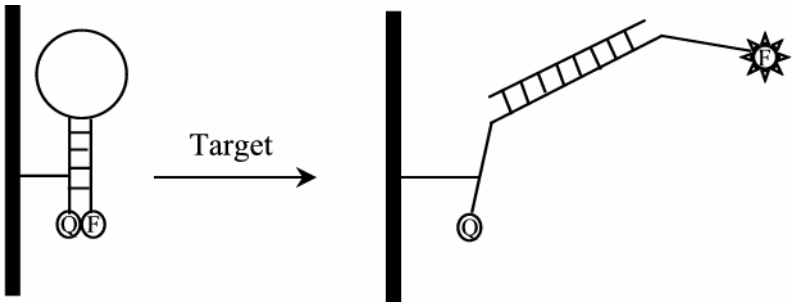


Figure 1.2: Scheme of molecular beacon (MB) based DNA sensors. Q: quencher; F: fluorophore.

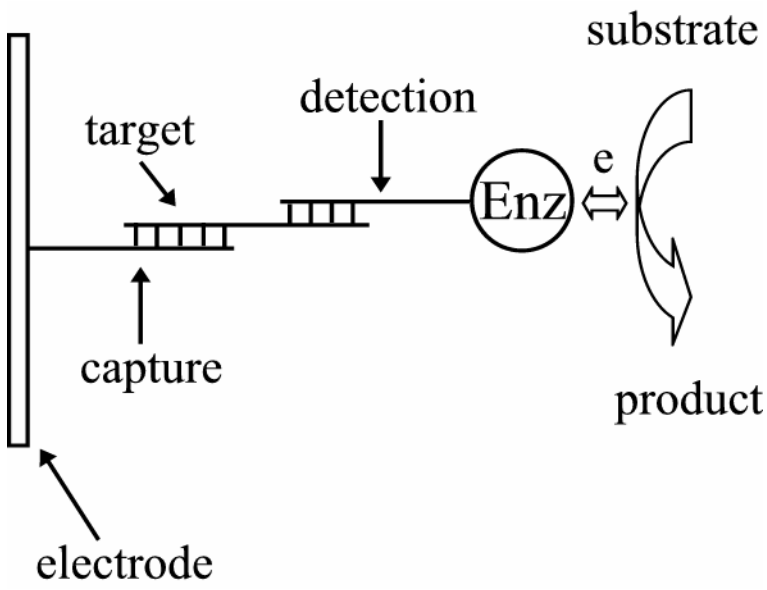


Figure 1.3: Schematic representation of sandwich-type enzyme-amplified DNA detection.

# Chapter 2: Enzyme-Amplified Detection of a 38-Base Oligonucleotide at 20 pM Concentration in a 30 μL Droplet on a Screen-Printed Electrode

## 2.1 ABSTRACT

A 38-base DNA sequence was detected at 20 pM concentration in 15-35 μL droplets by an electrochemical enzyme-amplified sandwich-type assay on a mass-manufacturable screen printed carbon electrode. Formation of the sandwich brought the horseradish peroxidase-label of the detection sequence in electrical contact with a pre-electrodeposited redox polymer, making the sandwich an electrocatalyst for the reduction of hydrogen peroxide to water at + 0.2 V (Ag/AgCl).

A 20-fold improvement over the sensitivity in a related system of Dequaire and Heller resulted of (a) five-fold reduction of the noise by substituting the formerly used poly(N-vinyl imidazole)-co-acrylamide comprising redox co-polymer with a poly(4-vinyl pyridine)-co-acrylamide comprising redox polymer, allowing the poising of the electrodes at a more oxidizing potential where noise (the rate of non-enzyme catalyzed electro-reduction currents of dissolved oxygen and hydrogen peroxide) was lower ; (b) doubling of the catalytic electroreduction current upon electrodepositing a second layer of the redox polymer on the capture sequence containing film; and (c) doubling of the current by increasing the coverage by the capture sequence.

## 2.2 INTRODUCTION

Sandwich-type, sequence-specific DNA and RNA assays[1-3] are widely used because, unlike simple capture assays, they do not require the chemical modification of the analyzed strand. Three sequences are bound by hybridization in these assays: a capture sequence, often immobilized on a surface; the target sequence; and a detection sequence, usually tagged with a radioactive label, or a label generating an optical, electrochemical, or electrical signal, indicating the completion of the sandwich. Reported labels include radioactive isotopes,[1,2] transition metal complexes,[3-5] liposomes,[6,7] enzymes,[7-11] DNA fragments[12] and gold nanoparticles.[13-16] Recently Park et al.[17] aligned the capture oligonucleotides in a 20-μm gap between two microelectrodes; after hybridization with the target and the detection sequence, gold nanoparticles bound to the detection sequences lined up and bridged the gap between the microelectrodes. By measuring the resistance, DNA was detected at concentrations as low as 0.5 pM.

Electron-conducting redox polymers have been widely used to construct biosensors and biofuel cells.[18-25] When the polymers are hydrated, flexible segments of the redox polymer move relatively freely and collide randomly, resulting in the transfer of electrons between reduced and oxidized segments.[26,27] When redox polymers and redox enzymes are co-immobilized on electrode, these reduced and oxidized mobile segments of the polymer can penetrate the enzymes and mediate the electron transfer between the redox centers of the enzymes and

the electrode. The immobilization of the redox polymers and enzymes usually involve the use of cross-linkers; in these experiments small amount of cross-linkers are mixed with redox polymers and enzymes in buffer solutions on the surface of electrodes and the electrodes are allowed to cure for 20-40 hours. This "dropping procedure" (mostly manual) may hinder its application in terms of miniaturization and mass production.[21] Recently fast and highly reproducible methods of co-immobilizing redox polymers and enzymes have been explored.[28] The fundamental reason is that transition metal ions may exchange ligands when electroreduced and/or electrooxidized,[29-33] or when irradiated with visible light.[34] Therefore, replacement of the inner-sphere $Cl^-$ of the redox polymer-bound Os complexes by coordination ligands of ambient polymer chains, whether be it amine, pyridine or imidazole, results in the coordinative cross-linking of the redox polymer and subsequent depositin on the electrode surface.

Enzyme-amplified amperometric DNA and RNA sensors were based earlier on incorporating capture probes in enzyme "wiring" polymers and labeling of detection probes with enzymes that were "wired" to the electrodes by redox polymers.[11,35] The scheme of these assays is shown in Figure 2.1 A. A film of the redox polymer was cast or electrodeposited on an electrode. A capture probe was then bound to the film covalently, coordinatively, or by an affinity (e,g. avidin-biotin) reaction. Capture of the target sequence made the film receptive to the selective hybridization of the enzyme-tagged detection sequence, which made the film an electrocatalyst, usually for the electroreduction of hydrogen peroxide to water. The electron flow is illustrated in Figure 2.1 B. Detection of a reduction

current when $H_2O_2$ is added indicates the presence of the analyzed target sequence.

In recent years screen printing technologies have drawn a lot of attention.[35-43] In making screen-printed electrodes (SPEs), a conducting pad is formed on a base, usually flexible polyester films, by pressing a carbon paste or ink, platinum or other metal paste, through a pre-patterned screen.[40] Mediators, enzymes, polymers, cross-linkers, or other components are applied after. Multiple layers can be fabricated. Because of their versatility, the ability to be miniaturized, and the low cost of possible mass production, screen-printed electrodes are likely to find applications in making inexpensive, rapid, and disposable biosensors in biological and medical research, in diagnostic, genetic and forensic testing, and in environmental analysis.

In this chapter we show that screen-printing techniques, together with the electrodeposition methods, can be used to mass-produce redox polymer-based DNA/RNA sensing electrodes with incredible ease and high reproducibility. The detection limit of the assay was ~20 pM, with 0.6 femtomoles of the target DNA detected in simple, 15-35 μL droplet cells.

## 2.3 EXPERIMENTAL

### 2.3.1 Chemicals.

The desalted 38-base target oligonucleotide sequences, including the perfectly matched sequence (T), the 1-base mismatched sequence (M1), and the 2-base mismatched sequence (M2); the 20-base capture oligonucleotide, having a

5'-amine-terminated 12-T spacer (C); and the 18-base horseradish peroxidase-labeled detection sequence (D) were custom prepared by Synthetic Genetics, San Diego, CA. Their sequences are shown in Table 2.1. The specific activity of the horseradish peroxidasse (HRP) label of the detection sequence was reported to be 15,000 units $mg^{-1}$ against 3,3',5,5'-Tetramethylbenzidine (TMB).

Potassium hexachloroosmate ($K_2OsCl_6$), 2,2'-bipyridine, sodium dithionite ($Na_2S_2O_4$), acrylamide, 4-vinylpyridine, and N,N,N',N'-tetramethylethylenediamine were purchased from Aldrich (Milwaukee, WI). The buffer salts and all other inorganic chemicals were purchased from Sigma (St. Louis, MO) or Aldrich (Milwaukee, WI) and were used as received unless otherwise stated. The pH 7.4 phosphate buffered saline solution (PBS) had 8 mM sodium phosphate, 2 mM potassium phosphate, 140 mM sodium chloride and 10 mM potassium chloride concentrations, and was purchased from Pierce (Rockford, IL). The hybridization buffer (4.3 mM $NaH_2PO_4$, 15.1 mM $Na_2HPO_4$, 500 mM NaCl, and 10mM EDTA), the washing buffer (4.3 mM $NaH_2PO_4$, 15.1 $Na_2HPO_4$, 500 mM NaCl, and 0.5% Tween 20®), TE buffer (10mM TRIS, 1 mM EDTA, pH 7.7), and all other solutions were prepared using deionized water (Barnstead, Nanopure II, Van Nuys, CA).

### 2.3.2 Preparation of the Redox Polymer.

***$Os(bpy)_2Cl_2$*** The preparation of $Os(bpy)_2Cl_2$ was carried out under argon. 200 mg potassium hexachloroosmate ($K_2OsCl_6$) and 130 mg 2,2'-bipyridine were mixed in 10 mL ethylene glycol. The solution was degassed by

bubbling argon and was refluxed under argon for 1 hour. The mixture was then cooled to room temperature, and 10 mL 1M aqueous solution of sodium dithionite ($Na_2S_2O_4$) was added. The osmium complex was reduced and precipitated, and was collected by vaccum filtration, washed with cold water and ether, and dried. The yield was 85%.

***PAA-PVP*** Poly(4-vinyl pyridine)-co-acrylamide or PAA-PVP copolymer was synthesized according to published procedures[44] with modifications. 2.3 g of acrylamide (32 mmoles) and 0.5 mL of 4-vinylpyridine (4.6 mmoles) were dissolved in a 1:1 v/v acetone-water solution. The solution was de-aerated by bubbling argon for 30 min, then 55 mg of ammonium persulfate and 60 μL of N,N,N',N'-tetramethylethylenediamine in 10 mL water were added. De-aeration was continued for 10 min. The solution was then stirred at 40 $^oC$ for 13 h. The resulting viscous solution was poured into 800 mL acetone, stirred, and most of the solvent was evaporated. The residue was added to another 800 mL of acetone, the precipitate was collected, washed with acetone, and dried overnight under vacuum at room temperature. The molar ratio of the acrylamide unit to the pyridine unit was found to be 5.2 : 1 based on NMR results (Figure 2.2).

***PAA-PVP-Os*** 120 mg of the resulting PAA-PVP copolymer was refluxed with 109 mg of $Os(bpy)_2Cl_2$ in 15 mL ethylene glycol for 2 h. The Os-complexed copolymer PAA-PVP-Os was precipitated in ether, re-dissolved in de-ionized water, and purified by ultra-filtration using a 10 K cut-off membrane (Amicon, Beverly, MA). The structure of the redox polymer, confirmed by NMR, is shown in Figure 2.2.

### 2.3.3 Screen-Printed Electrode.

The disposable working electrodes were 3.5 mm-diameter carbon disks screen-printed on flexible polyester films with hydrophilic carbon ink (Electrodag® 423SS from Acheson, Port Huron, MI). An array of 8 SPE's were printed in one stroke (Figure 2.3 A), which were then cured in an oven at 70 °C overnight. These electrodes were used without further treatment. To avoid the spreading of the 10-35 μL droplets beyond the 3.5 mm diameter working electrodes, a hydrophobic circle was drawn around each SPE with a felt-tip pen containing hydrophobic ink (DAKO Pen, S 2002, DAKO Corporation, Carpinteria, CA). The electrochemical cell formed in the confined 10-35 μL droplet had a screen-printed carbon working electrode with an area of 9.6 $mm^2$, a 0.5 mm diameter platinum wire counter electrode, and a Ag/AgCl micro-reference electrode, as shown in Figure 2.3 B.

### 2.3.4 Equipment.

Hybridizations were performed on a block heater (DIGI-BLOCK® JR, from Aldrich). All electrochemical measurements were carried out in a Faraday cage with a CH Instruments (Austin, TX) Model 832A electrochemical detector, interfaced to a Dell computer (Dell, Austin, TX). A 0.5 mm diameter platinum wire counter electrode, and a Ag/AgCl micro-reference electrode (3 M KCl saturated with AgCl) (Cypress, Lawrence, KS), to which all potentials were referenced, were used.

### 2.3.5 Preparation of the DNA Sensing Electrode.

The redox polymer films were electrodeposited from solutions containing 1 mg/mL PAA-PVP-Os and 18 v % phosphate buffer. 25 μL of the solution was pipetted onto the SPE and a potential of -1.4 V was applied for 2 min. The electrode was then rinsed thoroughly with deionized water, and was scanned between 0.1 mV and 0.5 mV to confirm the deposition.

After the redox polymer film was electrodeposited, a 25 μL aliquot of a 1 μM capture probe solution in PBS was pipetted onto the SPE, and a potential of -1.4 V was applied for 2-20 min. The electrode was rinsed with water and the voltammogram of the deposited film in the 0.1 V and 0.5 V region (vs. Ag/AgCl) was measured.

A second layer of the redox polymer was electrodeposited after the incorporation of the capture probe in part of the experiments.

### 2.3.6 Hybridizations and Detection.

The hybridization of the target sequence and its detection were performed in two steps. After the incorporation of the 20-base capture oligonucleotide into the polymer film and, in part of the experiments, after the electrodeposition of the second redox polymer layer, the electrode was placed on the block heater block maintained at 46°C and 30 μL of the target-containing hybridization buffer solution was pipetted onto the SPE. After 30 min at 46°C the block was allowed

to cool and was held at ambient temperature for 10 min. The SPE was rinsed briefly with the hybridization buffer, incubated with 30 μL of a 50 nM solution of the detection sequence in hybridization buffer at 37 °C for 40 min. It was cooled and held at room temperature for 10 min before being rinsed sequentially in washing buffer (10 min) and in PBS (5 min). The $H_2O_2$ electroreduction current was then measured in 30 μL of PBS, 0.2 mM $H_2O_2$, at room temperature, with the electrode poised at 0.2 V (Ag/AgCl).

## 2.4 RESULTS AND DISCUSSION

### 2.4.1 Electrodeposition of the Redox Polymer.

Gao et al. reported that redox polymers comprising osmium complexes having chloride in their inner coordination sphere are cross-linked and electrodeposited by ligand exchange upon their electroreduction at high coverage of the electrode by the adsorbed polymer, and that vitreous carbon must be pre-oxidized for the coverage to be high.[28] Dequaire and Heller have shown that pre-oxidation of hydrophilic graphite ink–printed electrodes is not necessary, because planes of graphite perpendicular to the van der Waals plane are spontaneously oxidized.[35] After its adsorption at open circuit potential, the polymer is easily and completely rinsed off by water or buffer. However, when an electrode is poised at -1.4 V (Ag/AgCl) and the $Os^{3+}$ complex is reduced to $Os^{2+}$ the polymer is irreversibly crosslinked and electrodeposited. Electroreduction of the osmium centers diminishes the coulombic component of the binding energy of the inner-sphere $Cl^-$ and the now labile $Cl^-$ is exchanged by a pyridine, which is likely to be

of a different chain if the graphite plane is densely covered by the redox polymer (Figure 2.4). As discussed in detail,[28,35] the exchange crosslinks the reversibly adsorbed redox polymer, leading to its irreversible electrodeposition. Cyclic voltammogram of the electrode after the electrodeposition process showed characteristic properties of the redox polymer (Figure 2.6), and exhaustive washing with water or buffer did not change the voltammogram, confirming the strong adsorption of the crosslinked polymer to the electrode surface. Figure 2.6 shows the cyclic voltammograms of a screen-printed electrode coated with PAA-PVP-Os at different scan rates (from 5 mV $S^{-1}$ to 100 mV $S^{-1}$). The peak separation and peak currents of the voltammograms increased with scan rate; and both the anodic and cathodic peak currents are proportional to the scan rate (Figure 2.7), characteristic of adsorbed thin layers on electrode surface.[45]

Figure 2.8 shows the dependence of the cyclic voltammogram (anodic) peak current on the concentration of the polymer solution. At low concentrations the peak current increased almost linearly with the polymer concentration, indicating that deposition was determined by the osmium coverage on the surface of the electrode, and only when densely covered would significant amount of redox polymer be cross-linked and electrodeposited. Maximum peak current was reached when the redox polymer concentration was 1 mg/mL, above which peak current would be independent of the polymer concentration.

In general, prolonging the time in which the –1.4 V potential was applied to the electrode increased the amount of polymer deposited on the electrode surface, as shown in Figure 2.9 where the anodic peak current was measured

against different deposition times. Maximum amount of deposited polymer was obtained when the deposition time was 2 min, and longer deposition time would not increase the deposition amount any more. With 2 min deposition time, on average, integration of the oxidation wave yielded a Faradaic charge of 7.4 μC, translating to $8.0 \times 10^{-10}$ moles of the $Os^{2+/3+}$ centers per $cm^2$. Similar results were obtained when a series of alternating square potential waves instead of constant potential were applied to deposit the polymer.[28] Since the repeating unit of the polymer had a formula weight of ~2450, and assuming the density of the fully hydrated redox polymer (the hydrogel) was about 1 g/mL, the thickness of the fully hydrated polymer film was about 0.02 μm, or 200 Å. A standard deviation of ~ 8 % was obtained when more than 100 electrodes were used in the assay using the same protocol, showing great consistency and reproducibility of the screen-printing and the electrodeposition method in making redox polymer based electrodes. The thus made electrodes can be stored at 4 °C for months without significant loss of materials.

### 2.4.2 Attachment of the Capture Sequence to the Redox Polymer Film.

Through similar mechanism, exchange of $Cl^-$ by the terminal amine of the spacer-arm of the capture sequence causes the irreversible binding of the capture sequence to the redox polymer. This process is illustrated in Figure 2.5. Reversible adsorption of the capture sequence, a 20-base polyanion modified at its 5'-end with a spacer arm, ending in a primary amine (Table 2.1) on the polycationic redox polymer, followed by application of –1.4 V (Ag/AgCl) for 20

min, led to the irreversible coordinative binding of the capture sequence to $Os^{2+/3+}$ centers of the polymer. The steady-state cyclic voltammogramms of a SPE coated with the electrodeposited PAA-PVP-Os film, progressively modified with the components of the sandwich, are shown in Figure 2.10. Curve ***a*** is the voltammogram after the electrodeposition of the redox polymer; curve ***b***, after attachment of the capture probe; curve ***c***, after the electrodeposition of the second polymer layer; and curve ***d***, after hybridization with the target and detection sequences. The capture probe was attached by applying –1.4 V (Ag/AgCl) for 20 min.

The bonding of the capture sequence decreased the segmental mobility of the polymer and decreased thereby the diffusivity of electrons, which propagate in hydrated redox polymer films by electron transfer between colliding segments.[26] The higher resistance is reflected in the broadening of the waves (Figure 2.10, b) and in decreased peak heights. The increased resistance was remedied by the electrodeposition of a second redox polymer layer, which doubled the heights of the voltammetric peaks (Figure 2.10, c). Hybridization of the target sequence again decreased the peak heights (Figure 2.10, d).

### 2.4.3 Noise Reduction through Use of the PAA-PVP-Os Redox Polymer.

In previous studies[11,35] where poly(N-vinyl imidazole)-co-acrylamide-complexed $Os(dme\text{-}bpy)_2^{2+/3+}$(PAA-PVI-Os) was used the background current was ~ 40 nA for 3 mm diameter vitreous carbon electrodes and the lowest detectable RNA or DNA concentration was ~500 pM. Use of the redox polymer

PAA-PVP-Os, which has a higher redox potential (+0.30 V versus +0.10 V) allowed the poising of the electrodes at a more oxidizing potential (0.20 V vs. 0.10 V) where the hydrogen peroxide and oxygen reduction currents in the absence of HRP were lower, and the background current was only 8 nA, resulting in a ~5 fold improvement in the signal to noise ratio.

### 2.4.4 Extending the Period of the "Plating" of the Capture Sequence.

In electrodes made with a single redox polymer layer the signal current increased by a factor of 1.8 when the period of capture sequence attachment was increased from 2 to 10 min (Figure 2.11). In these experiments the electrodes were immersed in a 1 μM solution of the capture sequence and were poised at – 1.4 V (Ag/AgCl) for 2-20 min. The $H_2O_2$ electroreduction current observed after hybridization of the target at 1 nM concentration and of the detection sequence at 50 nM concentration increased from 60 nA to 108 nA when the 2 min attachment period was extended to 10 min.

### 2.4.5 Comparison of Sandwiches Made with One and Two Redox Polymer Layers.

Electrodes were made by electrodepositing PAA-PVP-Os at -1.4 V (Ag/AgCl) for 2 min, followed by incorporating the capture sequence by poising the electrode in a 1 μM capture probe solution at the same potential for 20 min. Half of the prepared electrodes were then over-coated (-1.4 V vs. Ag/AgCl, 2 min) with a second layer of PAA-PVP-Os. After the electrodes were allowed to

hybridize first for 30 min with the target sequence T at 20, 50, 100, 200, 400, 800 or 1000 pM concentration, then with the detection sequence at 50 nM concentration for 40 min, their $H_2O_2$ electroreduction currents were measured (Figure 2.12). The current increased linearly with the concentration of the target DNA, whether one or two layers were electrodeposited. For the assay with a single polymer layer, the data fitted ($R^2 = 0.91$) the equation

*measured current (nA) = 0.116 (nA/pM) × [target] (pM) - 0.7 (nA).*

When two layers of the polymer were electrodeposited the best fit ($R^2 = 0.98$) was for the equation

*measured current (nA) = 0.235 (nA/pM) × [target] (pM) + 17.1 (nA).*

For the electrodes with one layer of redox polymer the sensitivity (the slops) is $0.116 \times 10^{-9}$ A/pM target DNA, or $3.9 \times 10^{-9}$ A/femtomole target DNA, while the two layer fabrication provides a sensitivity of $0.235 \times 10^{-9}$ A/pM target DNA, or $7.8 \times 10^{-9}$ A/femtomole target DNA (1 femtomole = $1 \times 10^{-15}$ mole). Thus, the sensitivity increased by a factor of 2 when two layers of the redox polymer were electrodeposited. It should also be noted that when one layer of the redox polymer was deposited the lowest concentration detected was 200 pM, below which the measured current did not change with the concentration and equaled the noise.

69 independent assays were carried out using the double electrodeposition process (Figure 2.12), of which 40 were at target concentrations of 50 pM or less. The average deviation of the current from that predicted by the second equation was ±6.8 nA and the average % deviation from the predicted current was 16%. The linear increase in current with the target concentration shows that the rate of binding of the target was controlled by its transport to the surface of the electrode, not by the kinetics of hybridization after its adsorption. In 10 experiments the average measured current at 10 pM concentration was 16.6 ± 3.1 nA; in 17 experiments at 20 pM, it was 19.8 ± 3.7 nA, and in 13 experiments at 50 pM concentration it was 28.8 ± 7.7 nA.

By electrodepositing a second redox polymer layer, the detected concentration of the target was lowered to 20 pM, corresponding to 0.6 femtomoles of the target oligonucleotide in the 30 μL droplet. The results suggest that in absence of a second redox polymer layer HRP, a polyanion at neutral pH, is repelled by the DNA-loaded redox polymer. The repulsion is advantageous in minimizing the non-specific adsorption of the detection probe-bound HRP, but is detrimental in that it expels part of the HRP from the redox polymer film, reducing the transfer of electrons to the HRP (Figure 2.13, A). Since a DNA double helix has a rise per residue of about 3.4 Å,[46] and the HRP has a diameter of about 50-60 Å,[47] the 38-base pair "capture-target-detection sandwich" is approximately 200 Å long, equaling the thickness of the deposited redox polymer film. Because the HRP is located at the end of the rod-like 38-base pair double

helix, unless the rod is buried in the redox polymer film, or "lies" on it, the terminal HRP may not be close enough to $Os^{2+}$ redox centers of the polymer to accept their electrons. The repulsion between the polyanionic DNA-loaded redox polymer and the polyanionic HRP-labeled detection sequence, and the fact that the length of the rod-like DNA double helix is the same as the thickness of the redox polymer film, made it impossible for most of the HRP labels to be "wrapped" by the redox polymer; in other words, only a very small portion of the HRP labels were in good electrical contact with the redox polymer film, of essence for the detected electroreduction of $H_2O_2$. Depositing a second layer of the redox polymer after the incorporation of the capture sequence provides a better contact between redox centers of the polymer and the enzyme (Figure 2.13, B), and hence improves the detection.

### 2.4.6 Detection of Mismatched Base Pairs.

When sandwiches differing in their number of mismatched base pairs in the target sequences (Table 2.1) were used at 1 nM target solution concentration, the current for the sandwich without a mismatch was 245 ± 9 nA; with a single mismatched base pair it was 80 ± 3 nA; and with two mismatched base pairs it was 36 ± 2 nA, readily allowing discrimination between the three targets (Figure 2.14).

## 2.5 CONCLUSIONS

An osmium bis-bipyridine-based redox polymer was synthesized and was shown to effectively "wire" the redox enzyme, HRP, when forming a thin film on the carbon electrodes. The electrodes were reproducibly screen-printed and activated by electrodepositing on their surface a redox polymer film and a DNA-capture sequence. A 38-base oligonucleotide was amperometrically detected at 20 pM concentration in 30 μL droplets on the screen printed carbon based electrodes.

## 2.6 REFERENCES


(1) Dunn, A. R.; Hassell, J. A. *Cell* **1977**, *12*, 23-36.

(2) Ranki, M.; Palva, A.; Laaksonen, M.; Virtanen, M.; Söderlund, H. *Gene* **1983**, *21*, 77-85.

(3) Dahlén, P.; Syvänen, A.-C.; Hurskainen, P.; Kwiatkowski, M.; Sund, C.; Ylikoski, J.; Söderlund, H.; Lövgren, T. *Mol. Cell. Probes* **1987**, *1*, 159-168.

(4) Ihara , T.; Nakayama , M.; Murata , M.; Nakano, K.; Maeda, M. *Chem. Commun.* **1997**, 1609-1610.

(5) Hakala, H.; Virta, P.; Salo, H.; Lonnberg, H. *Nucl. Acids. Res.* **1998**, *26*, 5581-5588.

(6) Rule, G. S.; Montagna, R. A.; Durst, R. A. *Anal. Biochem.* **1997**, *244*, 260-269.

(7) Alfonta, L.; Singh, A. K.; Willner, I. *Anal. Chem.* **2001**, *73*, 91-102.

(8) Ishii, J. K.; Ghosh, S. S. *Bioconjugate Chem.* **1993**, *4*, 34-41.

(9) Alexandre, I.; Zammatteo, N.; Moris, P.; Brancart, F.; Remacle, J. *J. Virol. Meth.* **1997**, *66*, 113-122.

(10) Fisher, M.; Harbron, S.; Taylorson, C. J. *Anal. Biochem.* **1997**, *251*, 280-287.

(11) Campbell, C. N.; Gal, D.; Cristler, N.; Banditrat, C.; Heller, A. *Anal. Chem.* **2002**, *74*, 158-162.

(12) Chiu, N. H. L.; Christopoulos, T. K. *Anal. Chem.* **1996**, *68*, 2304-2308.

(13) He, L.; Musick, M. D.; Nicewarner, S. R.; Salinas, F. G.; Benkovic, S. J.; Natan, M. J.; Keating, C. D. *J. Am. Chem. Soc.* **2000**, *122*, 9071-9077.

(14) Taton, T. A.; Mirkin, C. A.; Letsinger, R. L. *Science* **2000**, *289*, 1757-1760.

(15) Han, S.; Lin, J.; Zhou, F.; Vellanoweth, R. L. *Biochem. Biophys. Res. Comm.* **2000**, *279*, 265-269.

(16) Taton, T. A.; Lu, G.; Mirkin, C. A. *J. Am. Chem. Soc.* **2001**, *123*, 5164-5165.

(17) Park, S.-J.; Taton, T. A.; Mirkin, C. A. *Science* **2002**, *295*, 1503-1506.

(18) Degani, Y.; Heller, A. *Journal of the American Chemical Society* **1989**, *111*, 2357-2358.

(19) Heller, A. *Acc. Chem. Res.* **1990**, *23*, 128-134.

(20) Heller, A. *J. Phys. Chem.* **1992**, *96*, 3579-3587.

(21) Habermuller, K.; Mosbach, M.; Schuhmann, W. *Fresenius J. Anal. Chem.* **2000**, *366*, 560-568.

(22) Barton, S. C.; Kim, H.-H.; Binyamin, G.; Zhang, Y.; Heller, A. *J. Am. Chem. Soc.* **2001**, *123*, 5802-5803.

(23) Chen, T.; Barton, S. C.; Binyamin, G.; Gao, Z.; Zhang, Y.; Kim, H.-H.; Heller, A. *J. Am. Chem. Soc.* **2001**, *123*, 8630-8631.

(24) Nagels, L. J.; Staes, E. *Trends Anal. Chem.* **2001**, *20*, 178-185.

(25) Schuhmann, W. *Rev. Mol. Biotech.* **2002**, *82*, 425-441.

(26) Aoki, A.; Heller, A. *J. Phys. Chem.* **1993**, *97*, 11014-11019.

(27) Aoki, A.; Rajagopalan, R.; Heller, A. *J. Phys. Chem.* **1995**, *99*, 5102-5110.

(28) Gao, Z.; Binyamin, G.; Kim, H.-H.; Barton, S. C.; Zhang, Y.; Heller, A. *Angew. Chem. Int. Ed.* **2002**, *41*, 810-813.

(29) Heineman, W. R.; Burnett, J. N.; W. Murray, R. *Anal. Chem.* **1968**, *40*, 1970-1973.

(30) Bontempelli, G.; Magno, F.; De Nobili, M.; Schiavon, G. *J. Chem. Soc. Dalton Trans.* **1980**, 2288-2293.

(31) Hershberger, J. W.; Amatore, C.; Kochi, J. K. *J. Organomet. Chem.* **1983**, *250*, 345-371.

(32) Kirk, J. R.; Page, D.; Prazak, M.; Katovic, V. *Inorg. Chem.* **1988**, *27*, 1956-1963.

(33) Bartlett, P. N.; Eastwick-Field, V. *Electrochim. Acta* **1993**, *38*, 2515-2523.

(34) Haas, O.; Kriens, M.; Vos, J. G. *J. Am. Chem. Soc.* **1981**, *103*, 1318-1319.

(35) Dequaire, M.; Heller, A. *Anal. Chem.* **2002**, *74*, 4370 -4377.

(36) Del Carlo, M.; Lionti, I.; Taccini, M.; Cagnini, A.; Mascini, M. *Anal. Chim. Acta* **1997**, *342*, 189-197.

(37) Abass, A. K.; Hart, J. P.; Cowell, D. C.; Chappell, A. *Analytica Chimica Acta* **1998**, *373*, 1-8.

(38) Bagel, O.; Degrand, C.; Limoges, B.; Joannes, M.; Azek, F.; Brossier, P. *Electroanalysis* **2000**, *12*, 1447-1452.

(39) Dequaire, M.; Degrand, C.; Limoges, B. *J. Am. Chem. Soc.* **1999**, *121*, 6946-6947.

(40) Albareda-Sirvent, M.; Merkoci, A.; Alegret, S. *Sens. Actuat. B* **2000**, *69*, 153-163.

(41) Azek, F.; Grossiord, C.; Joannes, M.; Limoges, B.; Brossier, P. *Anal. Biochem.* **2000**, *284*, 107-113.

(42) Mascini, M.; Palchetti, I.; Marrazza, G. *Fresenius' Journal of Analytical Chemistry* **2001**, *369*, 15-22.

(43) Wang, J.; Xu, D.; Erdem, A.; Polsky, R.; Salazar, M. A. *Talanta* **2002**, *56*, 931-938.

(44) Ramaraj, R.; Natarajan, P. *J. Pol. Sci.: Pol. Chem.* **1991**, *29*, 1339-1346.

(45) Bard, A.; Faulkner, L. R. *Electrochemical Methods: Fundamentals and Applications*; 2nd ed.; John Wiley & Sons, Inc.: New York, 2001.

(46) Harry, M. R.; Freedland, R.; Roger, M. L. *Biochemistry: A Short Course*; Wiley-Liss, Inc.: New York, 1997.

(47) Farb, A.; Kolodgie, F. D.; Jones, R. M.; Jenkins, M.; Virmani, R. *J. Mol. Cell. Cardiol.* **1993**, *25*, 343-353.

Table 2.1 The Capture, Target and HRP-Labeled Detection Sequences. [a]

| *Symbol* | *Sequence (5'→ 3')* |
|---|---|
| C | TTT TTT TTT TTT CAC TTC ACT TTC TTT CCA AGA G |
| T | AGG CAT AGG ACC CGT GTC CTC TTG GAA AGA AAG TGA AG |
| M1 | AGG CAT AGG ACC CGT GTC CTC TTG GAA ***T***GA AAG TGA AG |
| M2 | AGG CAT AGG ACC CGT GTC CTC T***C***G GAA AGA AAG ***A***GA AG |
| D | GAC ACG GGT CCT ATG CCT |

[a] The capture sequence had a 5'-amine-terminated 6-carbon spacer. A 12-T spacer was appended to the 5'-end of the capture sequence. The detection sequence was 3'-labeled with a 6-carbon spacer ending in HRP . The targets T, M1, and M2 had, respectively, no, one and two mismatched bases.

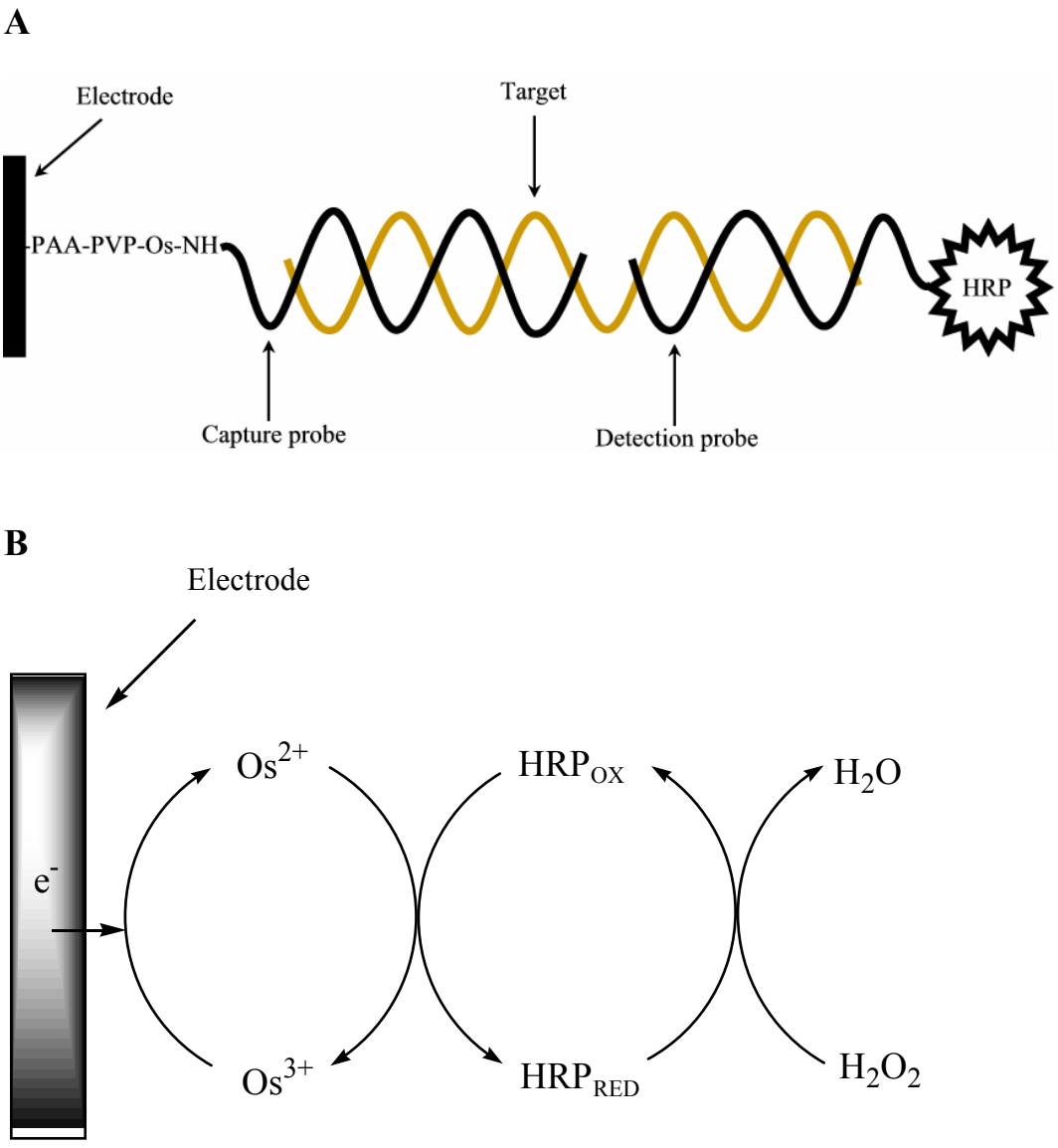


Figure 2.1: (A) Scheme of the sandwich-type assay. The capture probe is covalently bound to the redox polymer; after hybridization, the HRP label on the detection probe electrically contacts the redox polymer, making it a catalyst for the reduction of $H_2O_2$ to $H_2O$. (B) Steps of electron transfer in the electroreduction of $H_2O_2$ to $H_2O$.

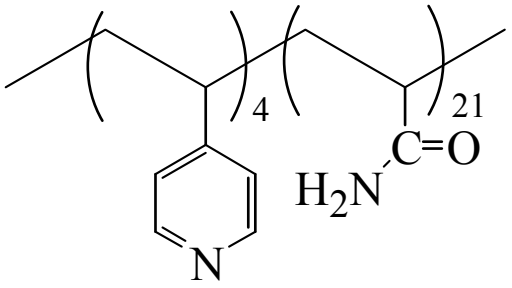


**PAA-PVP**

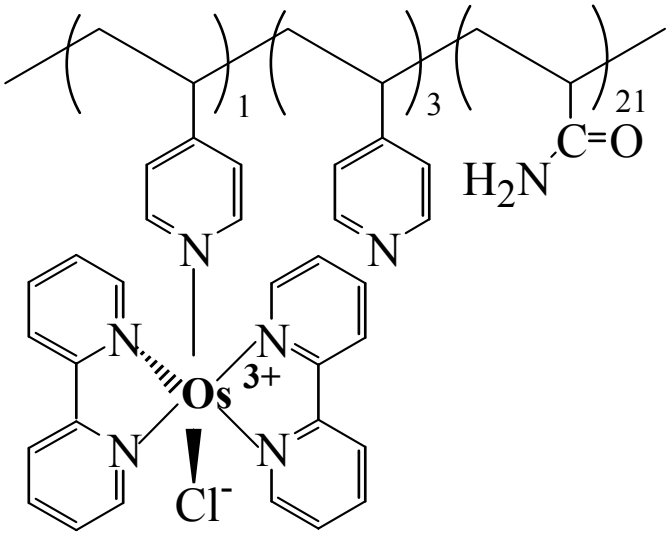


**PAA-PVP-Os**

Figure 2.2: Structures of PAA-PVP and PAA-PVP-Os.

**A**

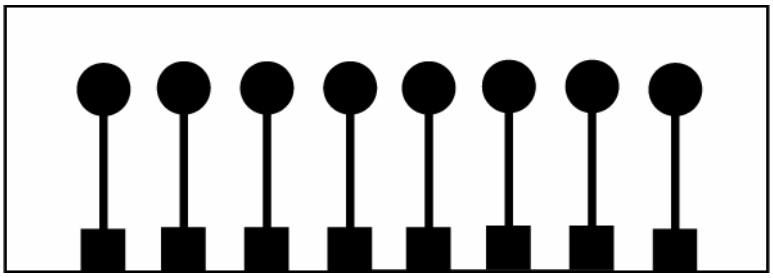

**B**

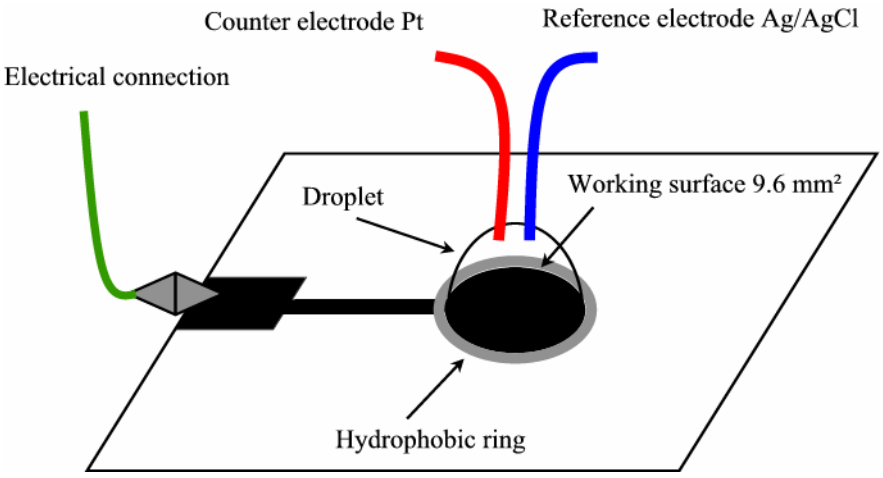


Figure 2.3: Schemes of (A) an array of screen-printed electrodes on polyester film, and (B) a SPE droplet-based cell.

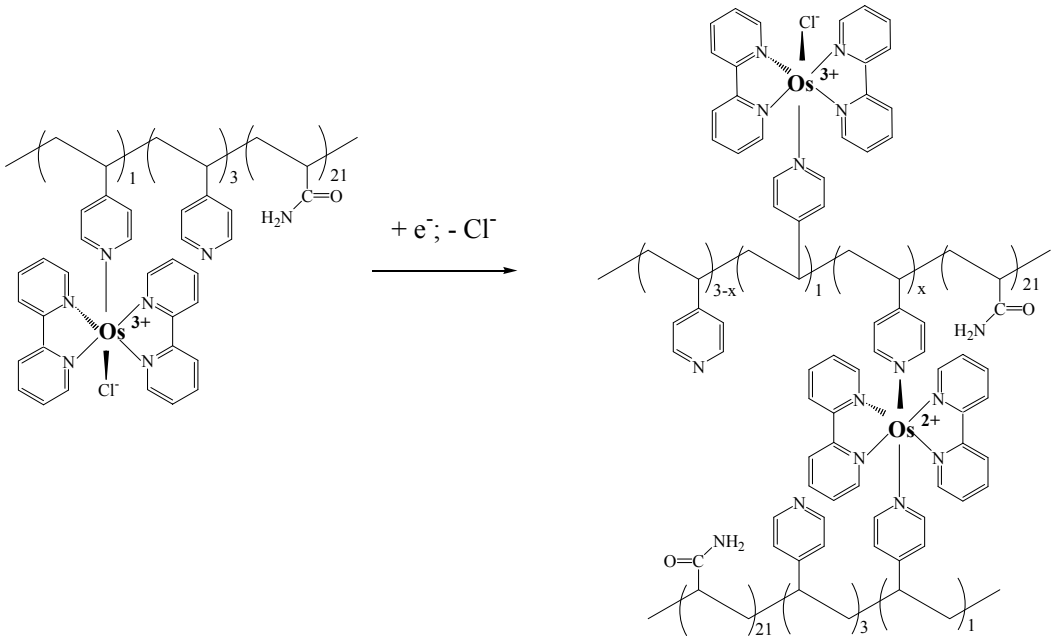


Figure 2.4: Mechanism of electron-induced crosslinking of PAA-PVP-Os.

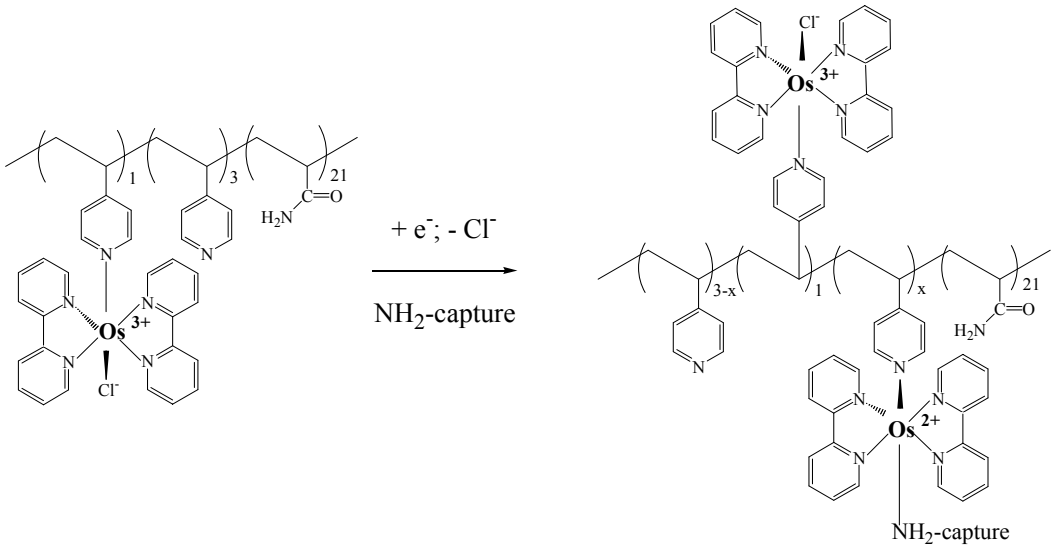


Figure 2.5: Attachment of the $NH_2$-terminated capture sequence to the PAA-PVP-Os redox polymer.

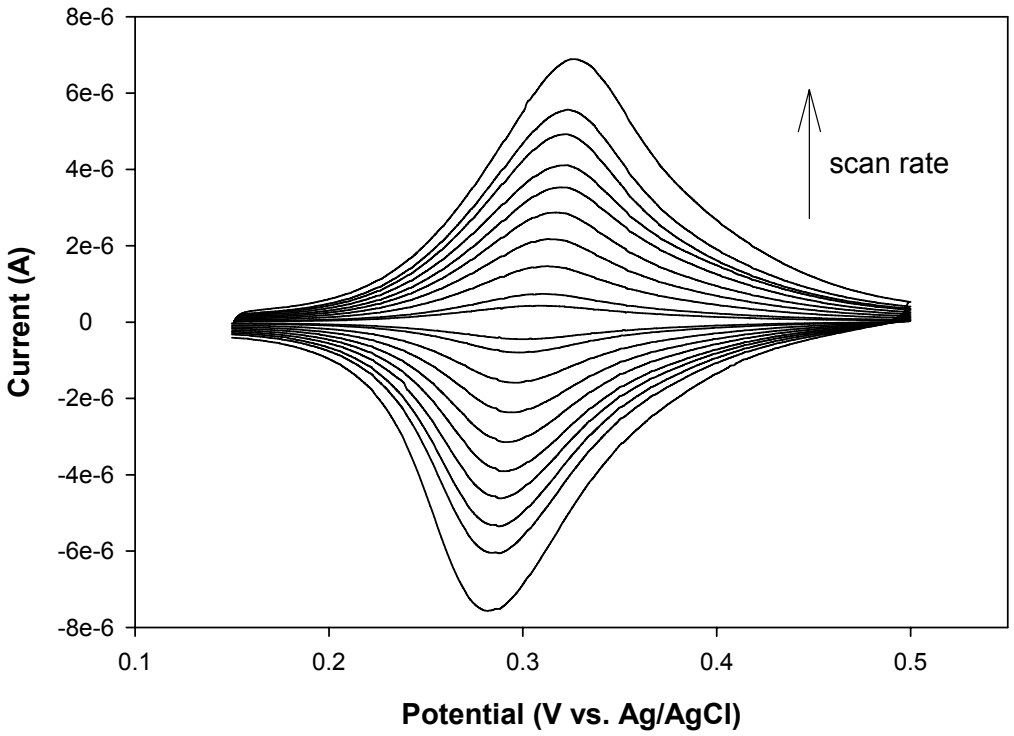


Figure 2.6: Cyclic voltammogramms of a sceen printed electrode at different scan rates. The electrode was coated with PAA-PVP-Os by applying 25 µL 1 mg/mL PAA-PVP-Os PBS solution on the electrode while the electrode was poised at –1.4 V for 30 sec. The electrode was extensively washed with water after deposition, and the cyclic voltammograms were taken in PBS. Scan rate (from bottome to top): 5, 10, 20, 30, 40, 50, 60, 70, 80, 100 mV/S.

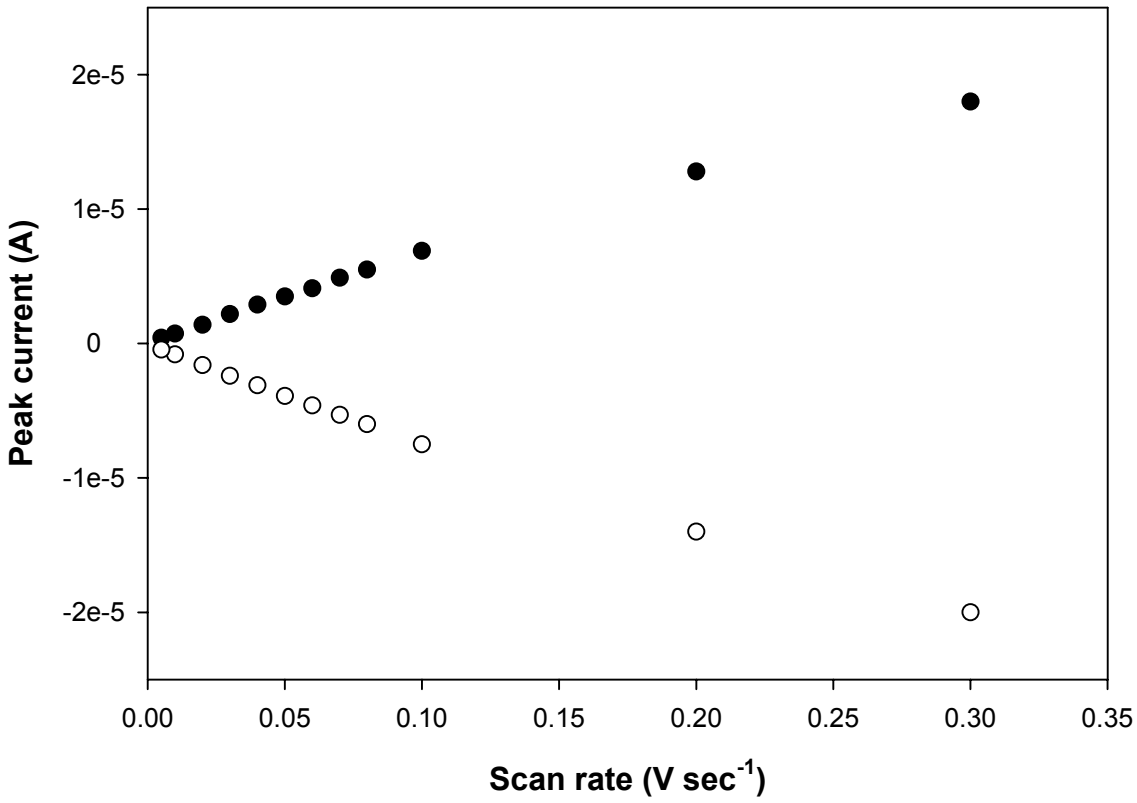


Figure 2.7: Dependence of the peak current on the scan rate. Conditions are the same as in Figure 2.5. Solid circles (●): anodic peak current; open circles (○): cathodic peak current.

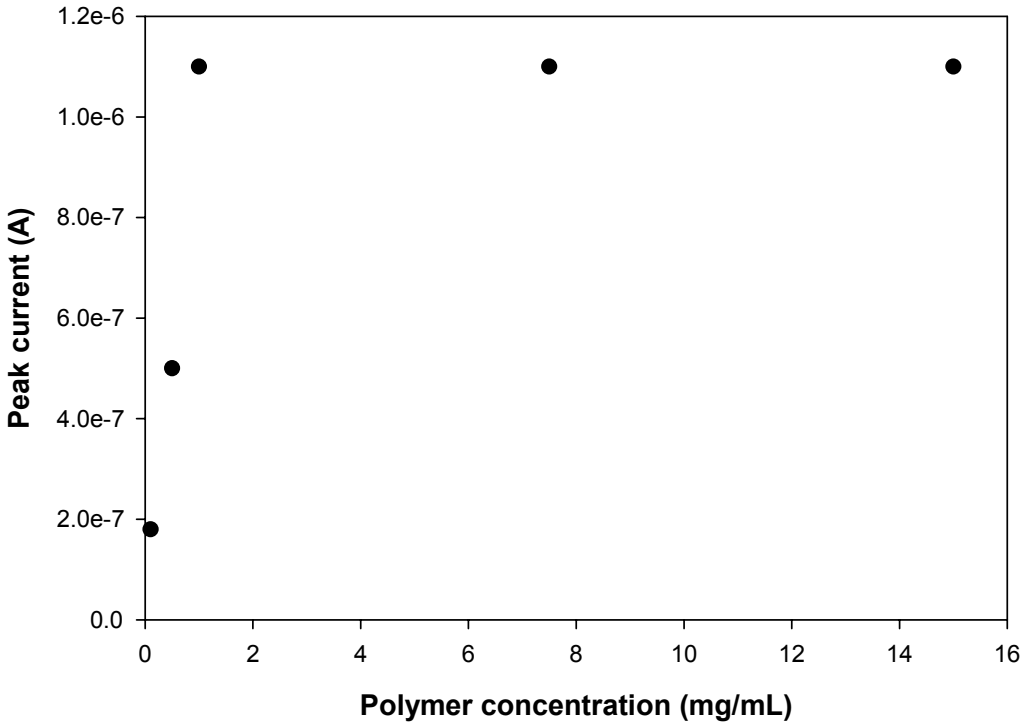


Figure 2.8: Dependence of the peak current on the polymer concentration. PAA-PVP-Os was deposited on screen printed electrodes by applying 25 µl polymer solutions to the electrodes and poising the electrodes at –1.4 V for 2 min. Anodic peak currents were measured in cyclic voltammograms which were recorded in PBS at 10 mV $sec^{-1}$ scan rate.

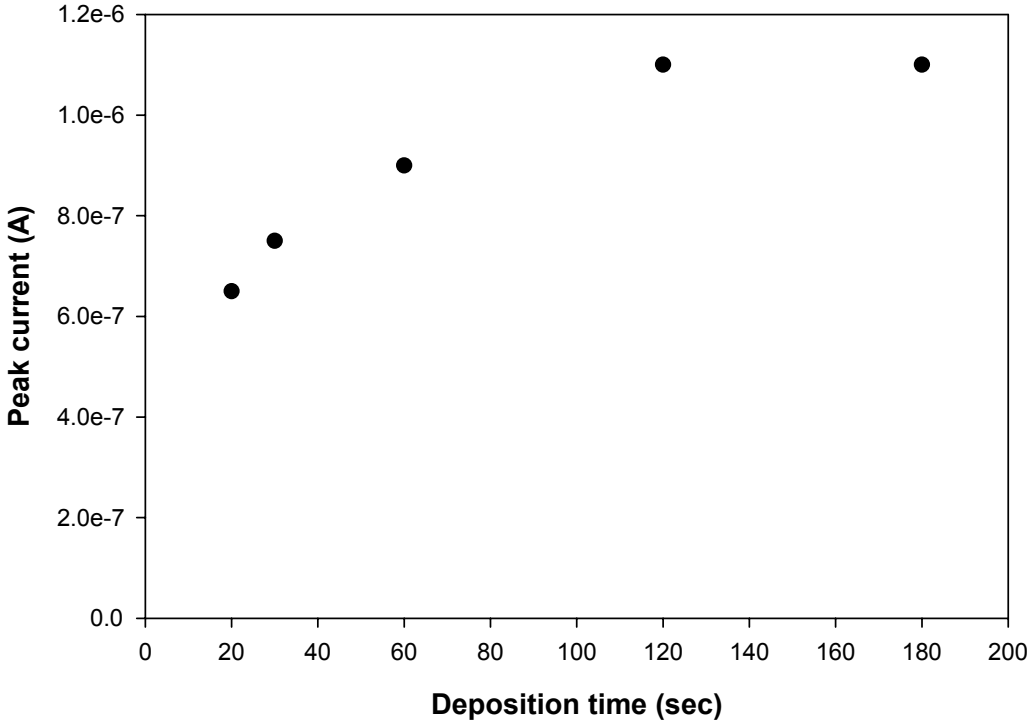


Figure 2.9: Dependence of the peak current on the deposition time. PAA-PVP-Os was deposited on screen printed electrodes by applying 25 µl 1 mg/mL polymer solution to the electrodes and poising the electrodes at –1.4 V for various durations. Anodic peak currents were measured in cyclic voltammograms which were recorded in PBS at 10 mV $sec^{-1}$ scan rate.

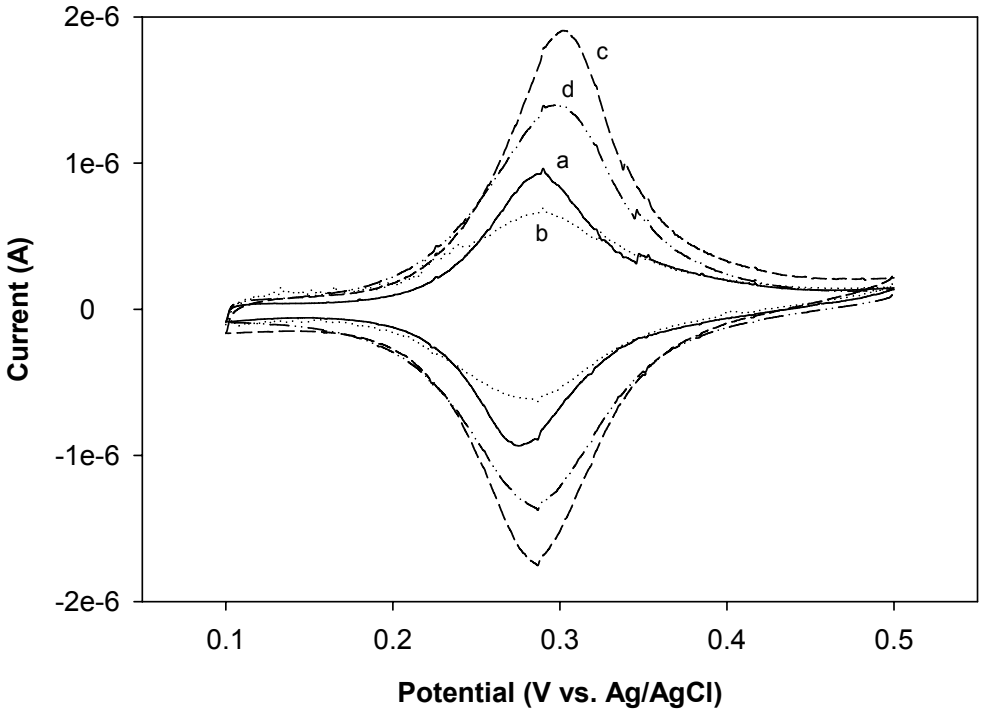


Figure 2.10: Cyclic voltammograms of a screen printed electrode after (a) electrodeposition of PAA-PVP-Os, (b) incorporation of the capture probe, (c) electrodeposition of a second layer of PAA-PVP-Os, and (d) hybridizations with the target, T, and with the detection probe. PAA-PVP-Os film was deposited by applying 25 µL 1 mg/mL polymer solution to the electrode and poising the electrode at –1.4 V (vs. Ag/AgCl) for 2 min. Capture sequence was attached by applying 25 µL 1 µM capture sequence solution to the electrode and poising the electrode at –1.4 V for 20 min. Hybridizations were carried out, sequentially, with the target sequence at 46 °C for 30 min, with the detection sequence at 37 °C for 40 min.

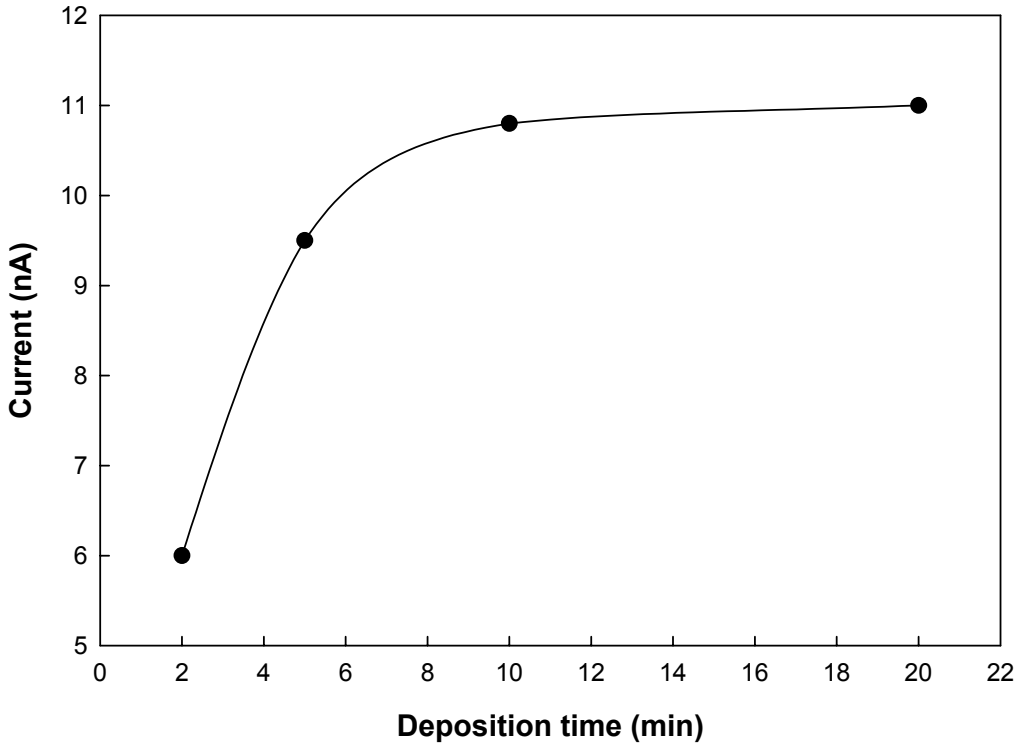


Figure 2.11**:** Dependence of the $H_2O_2$ electroreduction current on the deposition time of the capture sequence. PAA-PVP-Os was electrodeposited on the screen printed electrodes by applying -1.4 V (Ag/AgCl) for 2 min. The capture sequence was incorporated by applying the same potential for 2, 4, 10, and 20 min, respectively. The electrodes were allowed to hybridize with 1 nM target (T) and 50 nM detection probe. The current was measured with the electrodes poised at 0.2 V (Ag/AgCl), PBS buffer, 0.2 mM $H_2O_2$.

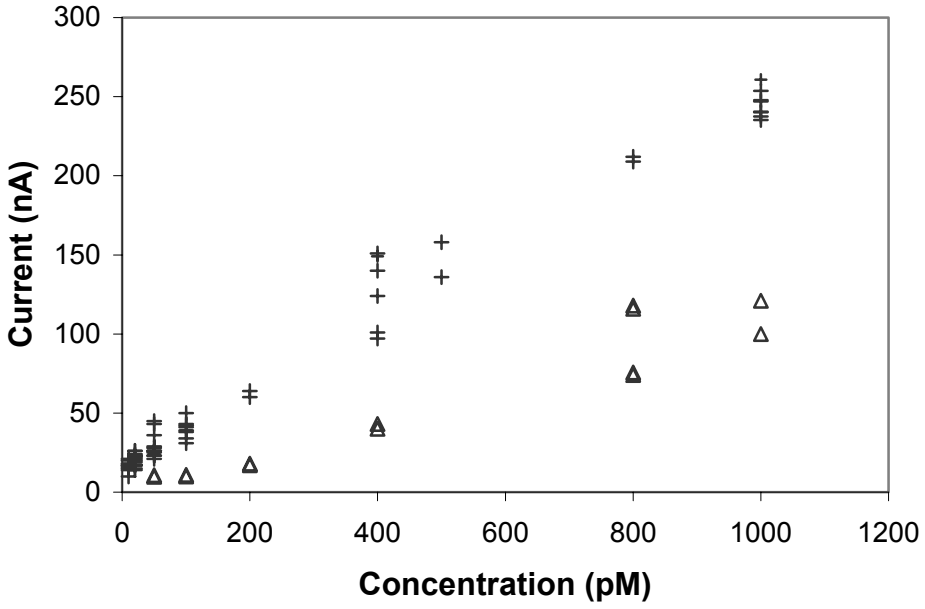


Figure 2.12: Dependence of the $H_2O_2$ electroreduction current on the concentration of the target (T). The electrodes were coated with PAA-PVP-Os by applying -1.4 V (Ag/AgCl) for 2 min, then loaded with the capture probe by applying the same potential for 20 min. (+): Before hybridization, the electrodes were coated with a second layer of PAA-PVP-Os; and (Δ): No second layer of PAA-PVP-Os was coated. The currents were measured while the electrodes were poised at 0.2 V (Ag/AgCl); PBS buffer; 0.2 mM $H_2O_2$.

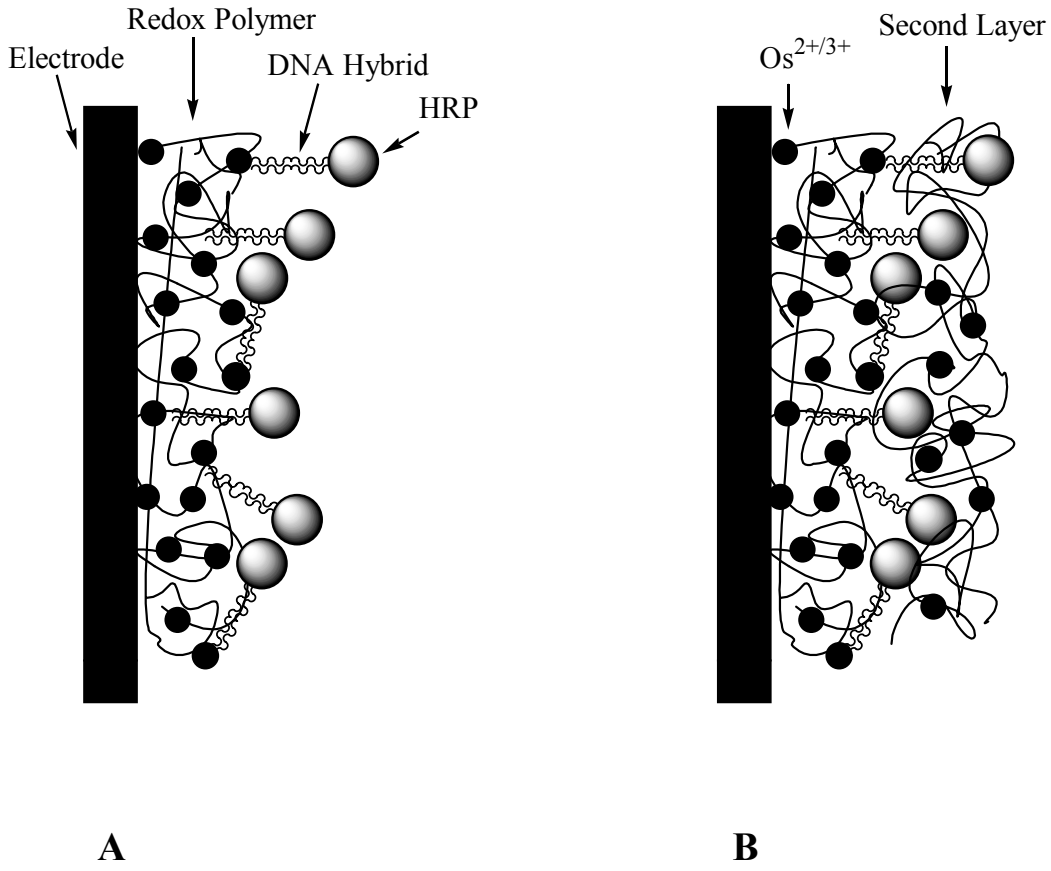


Figure 2.13: Schemes of sandwich assays made with (A) a single layer of the redox polymer, and (B) two layers of the redox polymer.

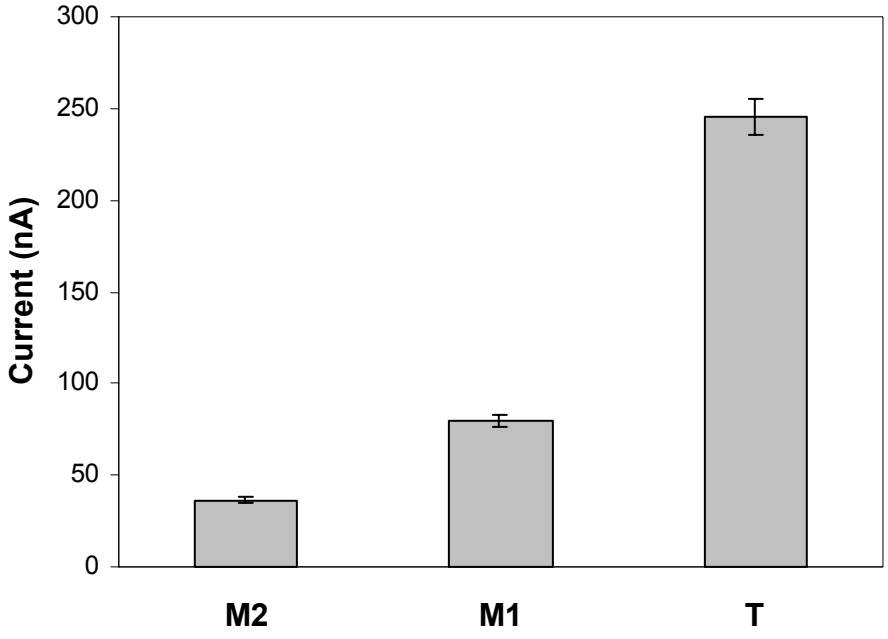


Figure 2.14: $H_2O_2$ reduction currents of the sandwich hybrids with 0, 1, and 2 mismatched base pairs, T, M1, and M2, respectively. Standard deviations: T, 9 nA; M1, 3 nA; and M2, 2 nA. Target concentrations 1 nM. Other conditions as in Figure 7.

# Chapter 3: Enzyme-Amplified Amperometric Detection of 3000 Copies of DNA at a 10-µm Diameter Microelectrode

## 3.1 ABSTRACT

As few as 3000 copies of 38-base DNA sequence were detected at 0.5 fM concentration in a 10 µL sample by means of a relatively simple electrochemical enzyme-amplified sandwich-type assay. The tip of a 10 µm diameter carbon fiber electrode was activated by co-electrodeposition of a redox polymer and a DNA-capturing sequence. The activated electrode was exposed to the droplet of the tested solution to capture the analyzed DNA, then probed with a droplet containing the horseradish peroxidase labeled detection sequence. Formation of the capture-target-detection sandwich brought the horseradish peroxidase label of the detection sequence into electrical contact with the pre-electrodeposited redox polymer, making the sandwich an electrocatalyst for the reduction of hydrogen peroxide to water at 0.12 V (Ag/AgCl). The radial diffusion of electrons through the film on the microelectrode allowed the electrodeposition of a thicker film of the redox polymer, an increase in the loading of the capture sequence, and increased the collection efficiency of the electron vacancies originating in the electroreduced $H_2O_2$.

## 3.2 INTRODUCTION

Simple, inexpensive and sensitive sequence-specific DNA/RNA detection is sought for diagnosing disease and for combating terrorism. Ideally, the test would be quantitative and detect a single copy of DNA/RNA. PCR, the most widely used method of selectively amplifying DNA, can detect a few copies,[1] even one copy, in less than one hour, when coupled with a detection method.[2] Rapid PCR adds, however, to the complexity of the required instrumentation, is not free of error and does not always quantify accurately the amount of DNA in the sample.[2,3]

Ongoing research aims at reducing the number of copies detected by methods not requiring PCR.[4,5] With an optical fiber fluorescence sensor 3.2 attomoles of DNA were detected at 30fM concentration.[6] At $10^{-16}$ M concentration $10^3$ copies of nucleic acids were assayed by single molecule imaging with a CCD camera.[7] In 28 femtoliter volume wells, 50 copies of DNA were monitored.[8] Using gold nanoparticle-labeled oligonucleotides as detection sequences, DNA was detected at 20 fM concentration.[9] Chemiluminescence and bioluminescence based systems detect attomoles ($10^{-18}$ moles $\approx 10^6$ copies) of DNA at <1 pM concentrations.[10,11] Surface plasmon resonance (SPR),[12] quartz crystal microbalance (QCM),[13] and terahertz resonance[14] based methods detect nucleic acids at <1 pM concentrations.

Electrochemical DNA/RNA detection[15-17] could be equally sensitive and selective, but should be simpler and require smaller and less expensive instrumentation. The underlying reason for the potentially smaller size and lower

cost of electrochemical detectors is that faradaic processes yield currents (fluxes of electrons). The currents need not be converted to a different flux, then reconverted to currents, as is the case in photonic and other detection methods. Indeed, PCR amplified DNA was detected by differential pulse voltammetry already at 0.6 fM concentration,[18] and the electrochemical detection of ~31,000 copies of DNA has been reported recently.[19]

A microelectrode is an electrode with at least one dimension, called the critical dimension, smaller than 25 μm.[20-22]

Consider a spherical electrode with a radius of $r_s$. According to Fick's laws of diffusion in spherical conditions,[20]

$$\frac{\partial c}{\partial t} = D\frac{\partial^2 c}{\partial r^2} + \frac{2D}{r}\frac{\partial c}{\partial r} \tag{3.1}$$

and

$$-J_{r=r_s} = \frac{I_d}{nF} = D\left[\frac{\partial c}{\partial r}\right]_{r=r_s} \tag{3.2}$$

where $-J_{r=r_s}$ is the net mass transfer at the surface of the spherical electrode, $I_d$ is the current density, $r$ is the distance from the center of the sphere, $D$ is the diffusion coefficient of the electroactive species, $c$ is its concentration as a function of $r$ and time $t$, and the bulk concentration is $c^{\infty}$.

The initial condition is

$$\text{at} \quad t = 0 \quad \text{and} \quad r > r_s, \; c = c^{\infty}$$

and the boundary conditions are for $t > 0$,

at $r = \infty,\ c = c^{\infty}$

and

at $r = r_s,\ c = 0$

By Laplace transform the current density, $I_d$, is given by

$$I_d = \frac{nFDc^{\infty}}{r_s} + \frac{nFD^{1/2}c^{\infty}}{\pi^{1/2}t^{1/2}} \tag{3.3}$$

At short times the second term in the equation is much greater than the first term, and the current density is given by the Cottrell equation

$$I_d = \frac{nFD^{1/2}c^{\infty}}{\pi^{1/2}t^{1/2}} \tag{3.4}$$

and a transient current is observed.

When $t$ is large enough, the transient current becomes negligible and the current density reaches a steady state,

$$I_d = \frac{nFDc^{\infty}}{r_s} \tag{3.5}$$

With spherical electrodes of millimeter diameters or larger, the time required to reach the steady state is so long that the steady state is rarely reached, if no forced convection, e.g., rotating disk electrode, is applied.[20] As the sphere gets smaller and smaller, the time needed to reach the steady state current density gets shorter and shorter. For example, for a spherical electrode with a radius of 1 mm, the time required to reach the steady state current is about $4 \times 10^4$ sec; if the radius decreases to 100 μm, it takes 400 sec; if the radius decreases further to 10 μm, it takes only 4 sec; and the steady state can be reached in 40 msec at a 1 μm microspherical electrode.[23,24]

There are benefits of using microelectrodes:

- A steady state is attained rapidly. In other words, the flux density to a microelectrode is much higher than to a macroelectrode, and the current at a microelectrode becomes independent of convection in practical time scales.[25] Therefore flowing streams can be followed and analyzed with microelectrodes without knowing the flow rate.
- The actual potential tracks rapidly the nominal applied potential. As a result, rapid electron transfer and fast coupled chemical reaction mechanisms and kinetics can be studied using microelectrodes.
- Because of the very small current flowing through the system and the much reduced double-layer capacity, ohmic polarization (the "*iR* drop")

and capacitive interferences are less problematic,[24] and the electrochemical signal-to-noise ratio is greatly improved.

- The sheer small physical size of microelectrodes allows the analysis of small volumes of samples, in vivo investigations and clinical use.[23,26-29] Because of its small size and the fact that the current flowing through it is very minute, the use of microelectrode is relatively noninvasive.

Because of their unique properties, microelectrodes have found applications in biology and medicine, including cell biology, neurobiology, pharmacology, and tissue engineering.[28] The excellent spatial and temporal resolution of microelectrodes makes quantitative chemical analysis of biological systems at the single-cell level possible, as intracellular processes and extracellular and intercellular communications, both in vivo and in vitro, have been monitored with microelectrodes.[26,28-30]

We have earlier detected DNA amperometrically by a sandwich-type enzyme-amplified assay at 20 pM concentration.[31] Here we show that when the macroelectrode is replaced by a 10-μm diameter microelectrode as few as 3000 copies (or 5 zeptomoles = $5 \times 10^{-21}$ moles) of DNA can be detected already at 0.5 fM ($0.5 \times 10^{-15}$ M) concentration.

## 3.3 EXPERIMENTAL

### 3.3.1 Chemicals.

The desalted 38-base target oligonucleotide sequences, including the perfectly matched sequence (T), the 1-base mismatched sequence (M1), and the 2-base mismatched sequence (M2); the 20-base capture oligonucleotide, having a 5'-amine-terminated 12-T spacer (C); and the 18-base horseradish peroxidase-labeled detection sequence (D) were custom prepared by Synthetic Genetics, San Diego, CA. Their sequences are shown in Table 3.1. The specific activity of the horseradish peroxidasse (HRP) label of the detection sequence was reported to be 15,000 units $mg^{-1}$ against 3,3',5,5'-Tetramethylbenzidine (TMB). The buffer salts and inorganic chemicals were purchased from Sigma (St. Louis, MO) or Aldrich (Milwaukee, WI) and were used as received unless otherwise stated. The pH 7.4 phosphate buffered saline solution (PBS) had 8 mM sodium phosphate, 2 mM potassium phosphate, 140 mM sodium chloride and 10 mM potassium chloride concentrations, and was purchased from Pierce (Rockford, IL). The hybridization buffer (4.3 mM $NaH_2PO_4$, 15.1 mM $Na_2HPO_4$, 500 mM NaCl, and 10mM EDTA), the washing buffer (4.3 mM $NaH_2PO_4$, 15.1 $Na_2HPO_4$, 500 mM NaCl, and 0.5% Tween 20®), TE buffer (10mM TRIS, 1 mM EDTA, pH 7.7), and all other solutions were prepared using deionized water (Barnstead, Nanopure II, Van Nuys, CA).

### 3.3.2 Redox Polymers.

The redox polymer, PAA-PVP-Os (a copolymer of poly-4-vinylpyridine and polyacrylamide, with part of the pyridines complexed with [Os(4,4'-bipyridine)$_2$ Cl]), was prepared as described in Chapter 2.

### 3.3.3 Electrodes.

The 10-μm diameter glassy carbon microelectrodes (catalog # EE017) and the miniaure Ag/AgCl reference electrode (catalog # EE008) were purchased from Cypress Systems (Lawrence, KS). The microelectrodes were polished thoroughly with 1.0, 0.3, and 0.05 μm alumina paste, with sonication between each polishing step. The polished electrodes were rinsed extensively with water and were stored in deionized water.

### 3.3.4 Instrumentation.

The 0.5 mL polypropylene PCR tubes (Catalog # PCR-06) and the 1.5 mL polypropylene microcentrifuge tubes (Catalog # MCT-149) used for all DNA solutions and hybridizations were purchased from United Scientific Products (San Leandro, CA).

All electrochemical experiments and measurements were carried out in a Faraday cage with a CH Instruments (Austin, TX) Model 832A electrochemical detector, interfaced to a computer (Dell OptiPlex Gxi, Austin, TX).

### 3.3.5 Electrode Preparation.

The redox polymer, then the 20 base long capture sequence, were electrodeposited on the 10 μm diameter electrodes in a miniature electrochemical cell comprising also a miniature Ag/AgCl reference electrode and a Pt wire counter-electrode. The polymer was electrodeposited from 200 μL of a 1 mg $mL^{-1}$ of PAA-PVP-Os solution in PBS (20 mM phosphate, 100 mM NaCl, pH 7.4) with the microelectrode placed in the solution and poised at –1.4 V vs. Ag/AgCl for 2 min. The electrode was washed extensively with deionized water before cyclic voltammogram was taken to confirm the deposition. The capture sequence was then electrodeposited to the redox polymer film by placing the microelectrode in 200 μL of the 1 μM capture sequence solution in PBS and poising the electrode at –1.4 V (Ag/AgCl) for 20 min. The electrodes were rinsed and stored in PBS at 4 °C till use.

### 3.3.6 Assay.

The 10 μL droplet (pH 7, 10 mM HEPES, 1 M NaCl, 1 mM EDTA) tested for the presence of the DNA was placed in a 0.5 mL polypropylene test tube (United Scientific Products, San Leandro, CA). The tip of the microelectrode was exposed to the tested liquid for 1 hour at 46°C to allow the hybridization of the capture and the analyzed sequences, and was annealed for 30 min at room temperature. The tip was then exposed for 20 min to 400 μL of the 10 nM HRP-labeled 18 base long detection sequence solution (20 mM phosphate, 0.1 M NaCl, pH 7.4, 37°C, magnetic stirring), PBS rinsed for 10 min. Detection was

performed in 200 μL PBS where the electrode was poised at +0.12 V (Ag/AgCl) and the current was measured before and after addition of $H_2O_2$ (final concentration 1 mM).

## 3.4 RESULTS AND DISCUSSION

### 3.4.1 Electrodeposition of the Redox Polymer and the Capture Sequence.

As discussed in Chapter 2 and previously,[32,33] applying a potential of –1.4 V (vs. Ag/AgCl) to solutions of the redox polymer, PAA-PVP-Os, reduces its Os from 3+ to 2+. As a result, the coulombic component of the bonding energy between Os and the inner sphere $Cl^-$ is weakened, and the Os-Cl bond becomes labile. When the electrode surface is densely covered by the redox polymer, the labile $Cl^-$ is easily exchanged by pyridines of neighboring polymer chains, resulting in coordinative crosslinking of the redox polymer and in irreversible deposition of the crosslinked polymer on the electrode surface. Cyclic voltammograms of the microelectrodes after electrodeposition showed the characteristic redox peak of PAA-PVP-Os at ~ 0.3 V (Ag/AgCl), and exhaustive washing with water and buffer did not change the voltammogram (Figure 3.5, a). Integration of the oxidation wave at 10 mV $S^{-1}$ yielded a Faradaic charge of (3.5 ± 0.4) × $10^{-10}$ C, or ~ 4.6 × $10^{-9}$ mole of $Os^{3+/2+}$ centers per $cm^2$. Note that this polymer coverage is significantly greater than for the 3.5 mm screen-printed electrodes described in Chapter 2, where the polymer coverage is about 8.0 × $10^{-10}$ mole $Os^{3+/2+}$ / $cm^2$. This six-fold increase in polymer coverage results of the

enhanced flux at microelectrodes, as discussed in the introduction. The thickness of the fully hydrated redox polymer film is calculated to be ~100 nm (1000 Å) based on the same assumptions that were made in Chapter 2. Thus the film is significantly thicker than that of the redox polymer films obtained on the 3.5 mm diameter screen-printed electrodes.

The cyclic voltammograms of the redox polymer-modified microelectrodes at different scan rates are shown in Figure 3.2. As expected, the peak current and peak separation increased with scan rate. The correlation between the peak current and the scan rate is intriguing. At slow scan rates (< 0.1 V $S^{-1}$) both the anodic and cathodic peak currents are proportional to scan rate, as shown in Figure 3.3, indicative of surface-bound thin layers. However this linearity does not hold when the scan rate is greater than 0.1 V $S^{-1}$; in fact, there is a linear correlation between the peak current and the square root of the scan rate when the scan rate is greater than 0.1 V $S^{-1}$, or the square root of the scan rate is greater than 0.3 (Figure 3.4), suggesting a more solution-like behavior of the hydrogel of the redox polymer. The mixed characteristics of the polymer film are attributed to the thicker film on the microelectrode.

As discussed previously, reversible adsorption of the capture sequence, a 20-base polyanion modified at its 5'-end with a spacer arm and ending in a primary amine (Table 3.1) on the polycationic redox polymer, followed by application of –1.4 V (Ag/AgCl) for 20 min, led to the irreversible coordinative binding of the capture sequence to part of the $Os^{2+/3+}$ centers of the polymer. The bonding of the capture sequence decreased the segmental mobility of the polymer

and decreased thereby the diffusivity of electrons, which propagate in hydrated redox polymer films by electron transfer between colliding segments.[34] The higher resistance is reflected in the broadening of the waves and in decreased peak heights (Figure 3.5). When the electrode was immersed in the capture sequence solution for 20 min without applying the negative potential, the adsorbed capture sequence was easily removed by rinsing the electrode in buffer solution, and no change (peak broadening or decrease) was observed in the voltammogram, confirming that application of the negative potential is necessary for deposition of the capture sequence in the redox polymer film.

### 3.4.2 Detection of 3000 Copies of Target DNA.

Figure 3.7 shows the current-time response in the assays. The electrodes modified with the redox polymer film and with the capture sequence were hybridized sequentially with the target sequence and the detection sequence. The microelectrodes were then placed in 200 μL of a PBS solution and were poised at 0.12 V (vs. Ag/AgCl). The current stabilized between –5 pA and 15 pA, and $H_2O_2$ was added at $t$ = 200 sec to bring the final concentration to ~1 mM. In control experiments where the hybridization with the target sequence was omitted, the current increment was only 2 ± 1 pA (Figure 3.6, curve a), in agreement with previous results.[35,36] This $H_2O_2$ reduction current is believed to be caused by non-specific adsorption of the HRP-labeled detection sequence on the redox polymer.

When the target sequence was present in the 10 μL tested solution, the current increased much more, as seen in curve b of Figure 3.6 for a target

concentration of $10 \times 10^{-14}$ M, or 10 fM. The dependence of the current increments on the concentration of the target sequence is shown in Table 3.2 and Figure 3.7. When the target sequence concentration was 0.5 fM, the measured $H_2O_2$ reduction current was 9 ± 4 pA, four times the background current ("noise") caused by non-specific adsorption; when the target sequence concentration was 0.2 fM, the measured reduction current was 7 ± 3 pA, indistinguishable from the current generated by 0.5 fM sample. In other words, the lower limit of detection of this assay is about 0.5 fM, or 3000 copies (5 zeptomole) of DNA are detected in 10 μL sample volume. To our best knowledge this is the most sensitive electrochemical DNA/RNA detection method reported so far.

The greatly improved sensitivity of the microelectrode-based sensors over the SPE-based sensors described in Chapter 2 is the result of thicker redox polymer films deposited on microelectrodes (~1000 Å). A DNA double helix has a rise per residue of about 3.4 Å,[37] and HRP has a diameter of about 50-60 Å.[38] Thus the 38-base pair "capture-target-detection sandwich" is approximately 200 Å long. On the screen-printed electrodes the thickness of the deposited redox polymer film was ~ 200 Å. The repulsion between the polyanionic DNA-loaded redox polymer and the polyanionic HRP-labeled detection sequence would make most of the HRP labels "stick out" of the redox polymer film, as discussed in Chapter 2, and thus out of the electrical contact range of the $Os^{2+/3+}$ centers of the redox polymer. The majority of the HRP-labeled sandwiches could not catalyze the reduction of $H_2O_2$ because the HRP could not contact the $Os^{2+/3+}$ of the redox polymer. Hence, only a small portion of the HRP was actively contributing to the

reduction current detected. When the electrodes were coated with two layers of redox polymer film the "communication" between the redox polymer film and the redox centers of the enzyme improved, as evidenced by the improved sensitivity and lowered detection limit (Chapter 2, Figure 2.11). With microelectrodes, however, the thickness of the deposited redox polymer film was about 1000 Å, significantly greater than the length of the 38-base pair "capture-target-detection sandwich"; therefore most of the DNA hybrids were buried in the redox polymer, and most of their HRP labels were well "wired" by the redox polymer, resulting in good electrical communications between the electrode and all or most of the redox centers of the duplex-bound HRP, greatly improving the sensitivity.

It is interesting to note that with the 3.5-mm diameter screen-printed electrode the detection limit was $6 \times 10^{-16}$ mole (30 µL of 20 pM target solution), or $3.8 \times 10^{9}$ copies of target DNA / $cm^2$; with the 10-µm diameter microelectrode the detection limit was $5 \times 10^{-21}$ mole (3000 copies), corresponding to $3.8 \times 10^{9}$ copies of target DNA / $cm^2$. Using microelectrodes did not significantly change the density of the DNA coverage on the electrode surface; rather, the improved sensitivity resulted solely of the improved communications between the HRP redox centers and the electrode. The fraction of the connected HRP-labels increased about 50 fold, possibly from ~2% to ~100%.

With microelectrode-based sensors the measured $H_2O_2$ reduction current increased linearly with the concentration of target sequence through the 0.5 fM –

20 fM range (5-200 zeptomole, or 3000 – 120,000 copies), as shown in Table 3.2 and Figure 3.7. Above 50 fM a plateau of ~600 pA, attributed to the saturation of the hybridization sites, was reached.

### 3.4.3 Mismatched Target Sequences.

The specificity of the assay was determined at 10 fM DNA concentration by replacing the fully complementary analyzed sequence with sequences in which either one or two of their 38 bases were mismatched (Table 3.1). The current increment for the perfectly complementary sequence was 178 ± 14 pA (Figure 3.6, curve b). When one base was mismatched, the increment dropped to 53 ± 10 pA (Figure 3.6, curve c); and when 2 bases were mismatched it was only 17 ± 9 pA (Figure 3.6, curve d), readily allowing discrimination between the three targets.

### 3.4.4 One-Minute DNA Assay.

The feasibility of a one-minute DNA assay was put to test. A microelectrode was made receptive to the target sequence by electrodepositing the redox polymer and the capture sequence as described earlier. The electrode was exposed for 5 seconds to a rapidly stirred solution of 10 nM HRP-labeled detection sequence which was maintained at 37 °C, and was then quickly removed and placed in 200 μL PBS solution, and the current-time curve was recorded while a potential of 0.12 V (vs. Ag/AgCl) was applied. After the current stabilized, $H_2O_2$ was added to produce a 1 mM concentration. No current

increment was observed (Figure 3.8, curve a). The electrode was rinsed in PBS solution. It was then exposed for 10 seconds to a rapidly stirred solution of 1 nM target sequence at 37 °C, followed by 5-second exposure to the 10 mM solution of HRP-labeled detection sequence. The electrode was quickly removed and placed in 200 μL PBS solution and the current-time response was recorded again with the electrode poised at 0.12 V. After adding $H_2O_2$ at t = 30 sec a reduction current of ~ 8 pA was observed, clearly indicating the presence of the target sequence (Figure 3.8, curve b). The whole process, including hybridizations and detection, took about 1 minute. This test shows that simple, qualitative, and very fast electrochemical DNA assays are feasible. These are of relevance to on-the-spot, point-of-care detection of biological warfare agents and other environmental hazardous pathogenic organisms.

### 3.5 CONCLUSION

In summary, a few thousand copies of DNA were selectively detected with simple, potentially inexpensive and compact electrochemical instrumentation. Because a cell or bacterium contains ~ $10^4$ of copies of ribosomal RNA, the method may allow the detection of the *r*RNA of a single cell or bacterium without PCR amplification.

Handheld electrochemical glucose monitors, smaller than the palm and weighing only a few ounces, are available in pharmacies for < $50. Their compact low noise potentiostats, LCD displays, processors and memories are built of components costing < $ 10. Low noise potentiostats, capable of monitoring pA

currents can be built of components that are likely to be only slightly more expensive. Thus, the electrochemical instrumentation for DNA detection is likely to cost far less and is likely to be smaller than that of comparably sensitive non-electrochemical methods.

### 3.6 REFERENCES


(1) Schutzbank, T. E.; Smith, J. *J. Clin. Microbiol.* **1995**, *33*, 2036-2041.

(2) Wabuyele, M. B.; Soper, S. A. *Single Mol.* **2001**, *2*, 13-21.

(3) Johnson, J. R. *J. Microbiol. Meth.* **2000**, *41*, 201-209.

(4) Wang, J. *Nucl. Acids. Res.* **2000**, *28*, 3011-3016.

(5) Vercoutere, W.; Akeson, M. *Cur. Opin. Chem. Biol.* **2002**, *6*, 816-822.

(6) Kleinjung, F.; Bier, F. F.; Warsinke, A.; Scheller, F. W. *Anal. Chim. Acta* **1997**, *350*, 51-58.

(7) Anazawa, T.; Matsunaga, H.; Yeung, E. S. *Anal. Chem.* **2002**, *74*, 5033-5038.

(8) Lou, H. J.; Tan, W. *Instrumentation Science & Technology* **2002**, *30*, 465-476.

(9) Cao, Y. C.; Jin, R.; Mirkin, C. A. *Science* **2002**, *297*, 1536-1540.

(10) Ishii, J. K.; Ghosh, S. S. *Bioconjugate Chem.* **1993**, *4*, 34-41.

(11) Chiu, N. H. L.; Christopoulos, T. K. *Anal. Chem.* **1996**, *68*, 2304-2308.

(12) Song, F.; Zhou, F.; Wang, J.; Tao, N.; Lin, J.; Vellanoweth, R. L.; Morquecho, Y.; Wheeler-Laidman, J. *Nucl. Acids. Res.* **2002**, *30*, e72-.

(13) Patolsky, F.; Lichtenstein, A.; Willner, I. *J. Am. Chem. Soc.* **2000**, *122*, 418 -419.

(14) Nagel, M.; Bolivar, P. H.; Brucherseifer, M.; Kurz, H.; Bosserhoff, A.; Büttner, R. *App. Optics* **2002**, *41*, 2074-2078.

(15) Palecek, E.; Fojta, M. *Anal. Chem.* **2001**, *73*, 74A-83A.

(16) Wang, J. *TrAC, Trends in Analytical Chemistry* **2002**, *21*, 226-232.

(17) Wang, J. *Anal. Chim. Acta* **2002**, *469*, 63-71.

(18) Azek, F.; Grossiord, C.; Joannes, M.; Limoges, B.; Brossier, P. *Anal. Biochem.* **2000**, *284*, 107-113.

(19) Wang, J.; Polsky, R.; Merkoci, A.; Turner, K. L. *Langmuir* **2003**, *19*, 989-991.

(20) Bard, A.; Faulkner, L. R. *Electrochemical Methods: Fundamentals and Applications*; 2nd ed.; John Wiley & Sons, Inc.: New York, 2001.

(21) Zoski, C. G. *Electroanalysis* **2002**, *14*, 1041-1051.

(22) Speiser, B. *Anal. Bioanal. Chem.* **2002**, *372*, 29-30.

(23) Stulik, K.; Amatore, C.; Holub, K.; Marecek, V.; Kutner, W. *Pure App. Chem.* **2000**, *72*, 1483-1492.

(24) Zoski, C. G. *J. Electroanal. Chem. Interf. Electrochem.* **1990**, *296*, 317-333.

(25) Montenegro, M. I.; Queiros, M. A.; Daschbach, J. L., Eds. *Microelectrodes : Theory and Applications*; Kluwer Academic: Dordrecht ; Boston ; London, 1991.

(26) Huang, L.; Kennedy, R. T. *Trends Anal. Chem.* **1995**, *14*, 158-164.

(27) Koudelka-Hep, M.; Van der Wal, P. D. *Electrochim. Acta* **2000**, *45*, 2437-2441.

(28) Lindner, E.; Buck, R. P. *Anal. Chem.* **2000**, *72*, 336A-345A.

(29) Cannon, D. M., Jr.; Winograd, N.; Ewing, A. G. *Ann. Rev. Biophys. Biomol. Struc.* **2000**, *29*, 239-263, 232 Plates.

(30) Pancrazio, J. J.; Whelan, J. P.; Borkholder, D. A.; Ma, W.; Stenger, D. A. *Ann. Biomed. Eng.* **1999**, *27*, 697-711.

(31) Zhang, Y.; Kim, H.-H.; Mano, N.; Dequaire, M.; Heller, A. *Anal. Bioanal. Chem.* **2002**, *374*, 1050-1055.

(32) Gao, Z.; Binyamin, G.; Kim, H.-H.; Barton, S. C.; Zhang, Y.; Heller, A. *Angew. Chem. Int. Ed.* **2002**, *41*, 810-813.

(33) Dequaire, M.; Heller, A. *Anal. Chem.* **2002**, *74*, 4370 -4377.

(34) Aoki, A.; Heller, A. *J. Phys. Chem.* **1993**, *97*, 11014-11019.

(35) De Lumley-Woodyear, T.; Caruana, D. J.; Campbell, C. N.; Heller, A. *Anal. Chem.* **1999**, *71*, 394-398.

(36) Caruana, D. J.; Heller, A. *J. Am. Chem. Soc.* **1999**, *121*, 769-774.

(37) Harry, M. R.; Freedland, R.; Roger, M. L. *Biochemistry: A Short Course*; Wiley-Liss, Inc.: New York, 1997.

(38) Farb, A.; Kolodgie, F. D.; Jones, R. M.; Jenkins, M.; Virmani, R. *J. Mol. Cell. Cardiol.* **1993**, *25*, 343-353.

Table 3.1 The Capture, Target and HRP-Labeled Detection Sequences. [a]

| *Symbol* | *Sequence (5'→3')* |
|---|---|
| C | TTT TTT TTT TTT CAC TTC ACT TTC TTT CCA AGA G |
| T | AGG CAT AGG ACC CGT GTC CTC TTG GAA AGA AAG TGA AG |
| M1 | AGG CAT AGG ACC CGT GTC CTC TTG GAA ***T***GA AAG TGA AG |
| M2 | AGG CAT AGG ACC CGT GTC CTC T***C***G GAA AGA AAG ***A***GA AG |
| D | GAC ACG GGT CCT ATG CCT |

[a] The capture sequence had a 5'-amine-terminated 6-carbon spacer. A 12-T spacer was appended to the 5'-end of the capture sequence. The detection sequence was 3'-labeled with a 6-carbon spacer ending in HRP . The targets T, M1, and M2 had, respectively, no, one and two mismatched bases.

Table 3.2 Dependence of the Current Increments on the Concentration of the Analyzed Sequence and on the Presence of Mismatched Bases

| *Analyzed Sequence In Sample* | *Concentration (x $10^{-15}$ M)* | *Number of copies* | *Current (x $10^{-12}$ A)* |
|---|---|---|---|
| None | 0 | 0 | 2 ± 1 |
| Perfectly matched | 0.2 | $1.2 \times 10^3$ | 7 ± 3 |
| | 0.5 | $3.0 \times 10^3$ | 9 ± 4 |
| | 1.0 | $6.0 \times 10^3$ | 19 ± 5 |
| | 2.0 | $1.2 \times 10^4$ | 40 ± 8 |
| | 5.0 | $3.0 \times 10^4$ | 97 ± 20 |
| | 8.0 | $4.8 \times 10^4$ | 134 ± 16 |
| | 10.0 | $6.0 \times 10^4$ | 178 ± 14 |
| | 15.0 | $9.0 \times 10^4$ | 301 ± 33 |
| | 20.0 | $1.2 \times 10^5$ | 367 ± 27 |
| | 50.0 | $3.0 \times 10^5$ | 542 ± 124 |
| | 100.0 | $6.0 \times 10^5$ | 589 ± 89 |
| 1-base mismatched | 10.0 | | 53 ± 10 |
| 2-bases mismatched | 10.0 | | 17 ± 9 |

[a] Sample volumes 10 μL. The currents are averages for 3-10 electrodes. To avoid systematic error, each solution was individually prepared by a different set of dilutions, and the tests were random, not in the order of increasing or decreasing concentrations.

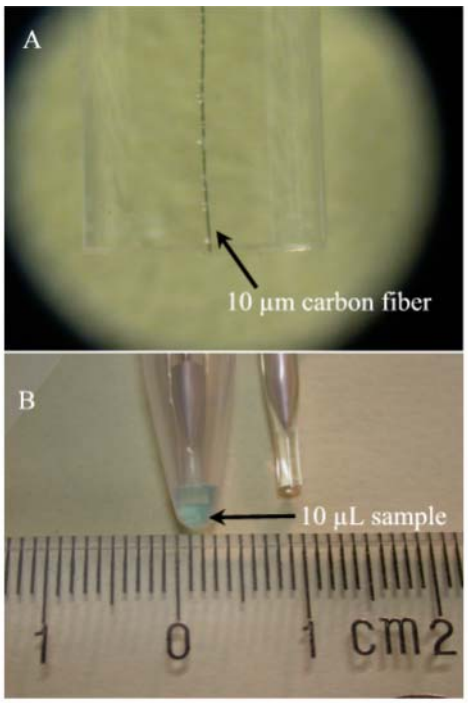


Figure 3.1: (A) Tip of a 10-µm diameter glassy carbon microelectrode. The 10-µm diameter carbon fiber is embedded in glass. (B) The tip of a microelectrode is placed in 10 µL sample solution as during the hybridization. The size of the tip is shown against the ruler.

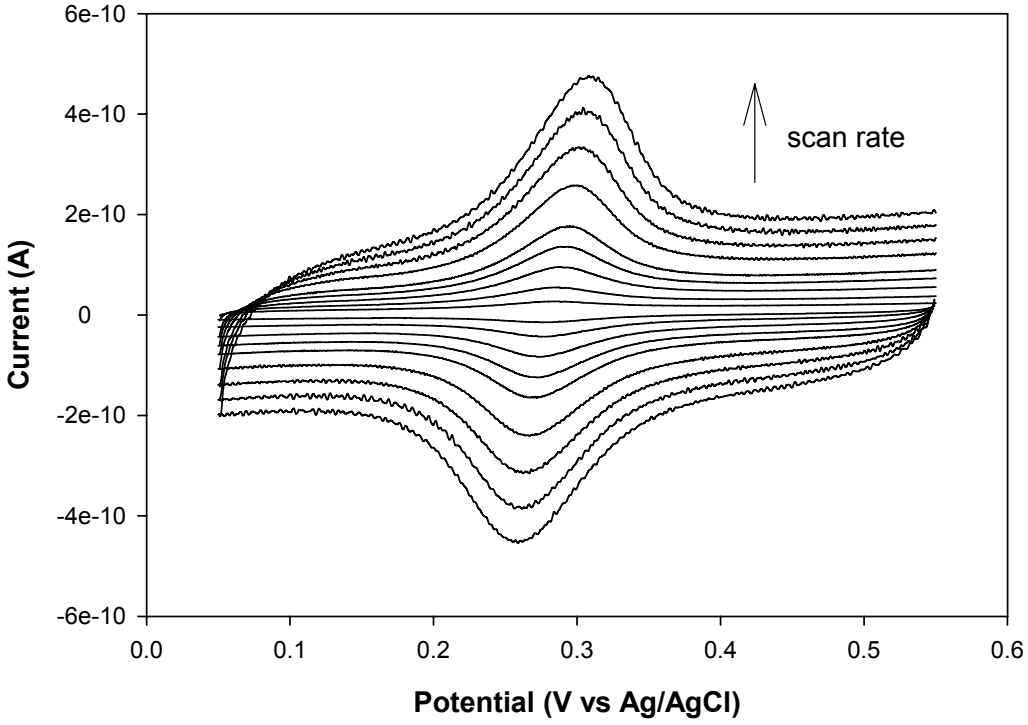


Figure 3.2 (A): Cyclic voltammograms of a microelectrode coated with the redox polymer, PAA-PVP-Os, at different scan rates. The redox polymer was deposited by placing the microelectrode in 200 μL of a 1 mg $mL^{-1}$ polymer solution in PBS and applying a constant potential of –1.4 V (vs. Ag/AgCl) for 2 min. Scan rate (from bottom to top): 2, 5, 10, 15, 20, 30, 40, 50, and 60 mV $S^{-1}$.

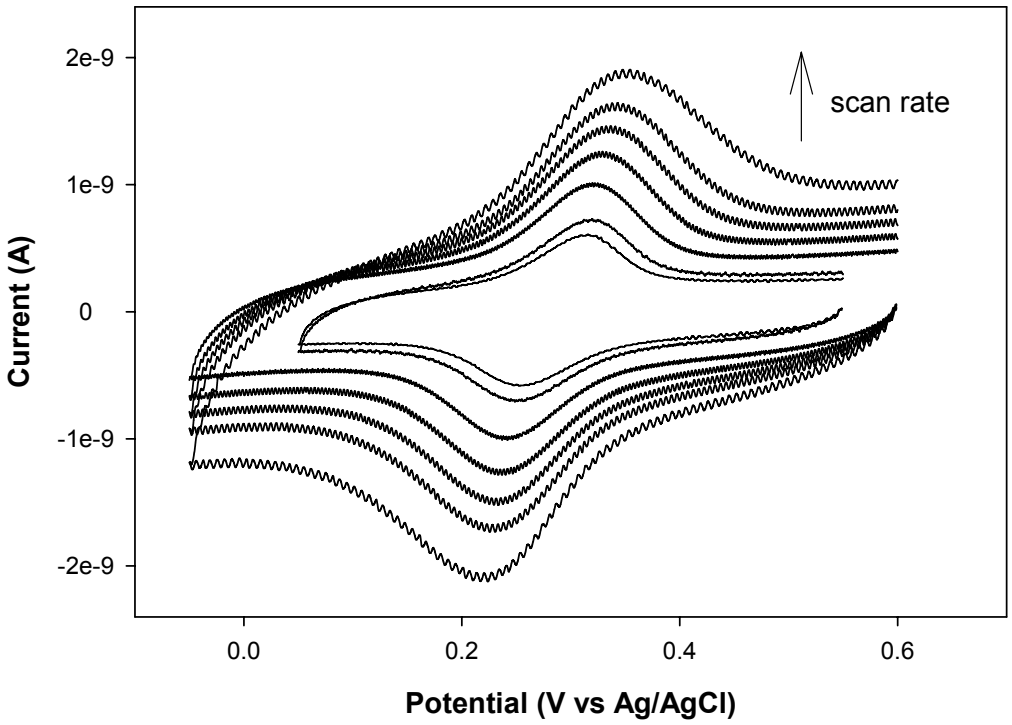


Figure 3.2 (B): Cyclic voltammograms of a microelectrode coated with the redox polymer, PAA-PVP-Os, at different scan rates. The redox polymer was deposited by placing the microelectrode in 200 µL of a 1 mg $mL^{-1}$ polymer solution in PBS and applying a constant potential of –1.4 V (vs. Ag/AgCl) for 2 min. Scan rate (from bottom to top): 80, 100, 150, 200, 250, 300, and 400 mV $S^{-1}$.

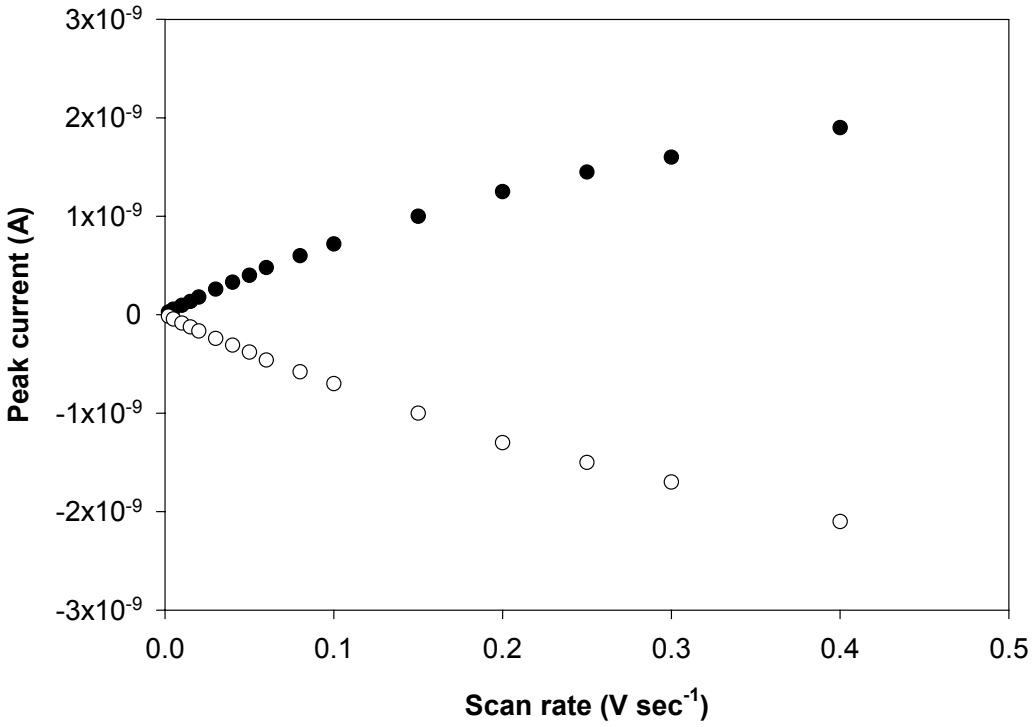


Figure 3.3: Dependence of the peak current of cyclic voltammograms on the scan rate. The 10-µm microelectrode was coated with the redox polymer, PAA-PVP-Os, by placing the microelectrode in 200 µL of a 1 mg $mL^{-1}$ polymer solution in PBS and applying a constant potential of –1.4 V (vs. Ag/AgCl) for 2 min. ●: Anodic peak currents; ○: cathodic peak currents.

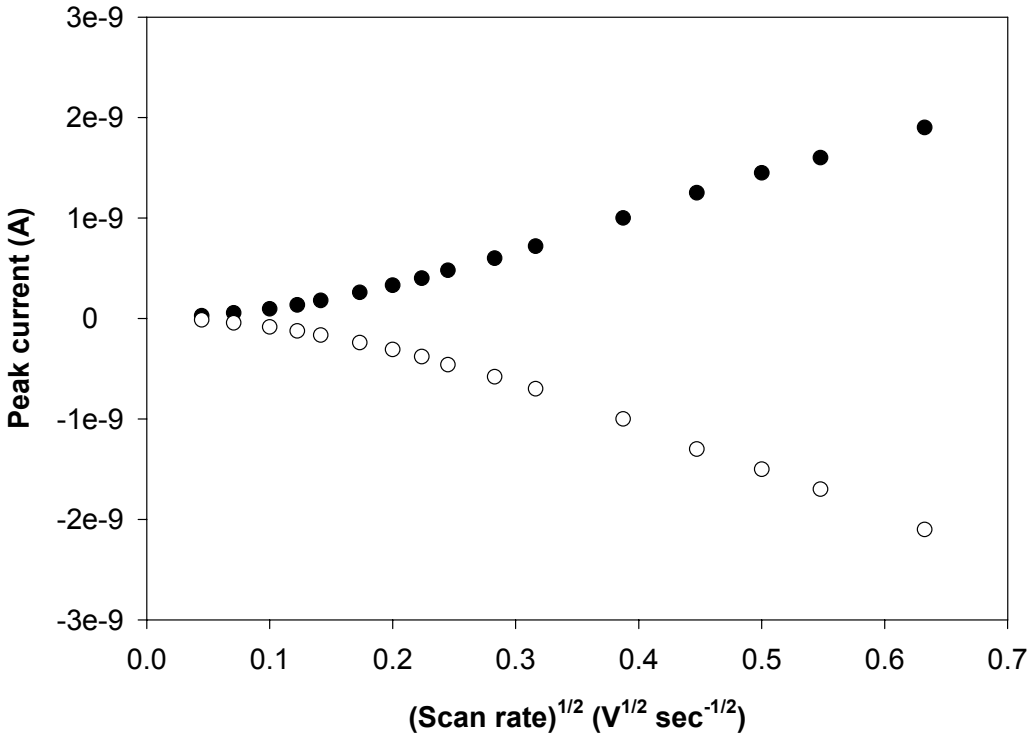


Figure 3.4: Dependence of the peak current of cyclic voltammograms on the square root of scan rate. The 10-µm microelectrode was coated with the redox polymer, PAA-PVP-Os, by placing the microelectrode in 200 µL of a 1 mg $mL^{-1}$ polymer solution in PBS and applying a constant potential of –1.4 V (vs. Ag/AgCl) for 2 min. ●: Anodic peak currents; ○: cathodic peak currents.

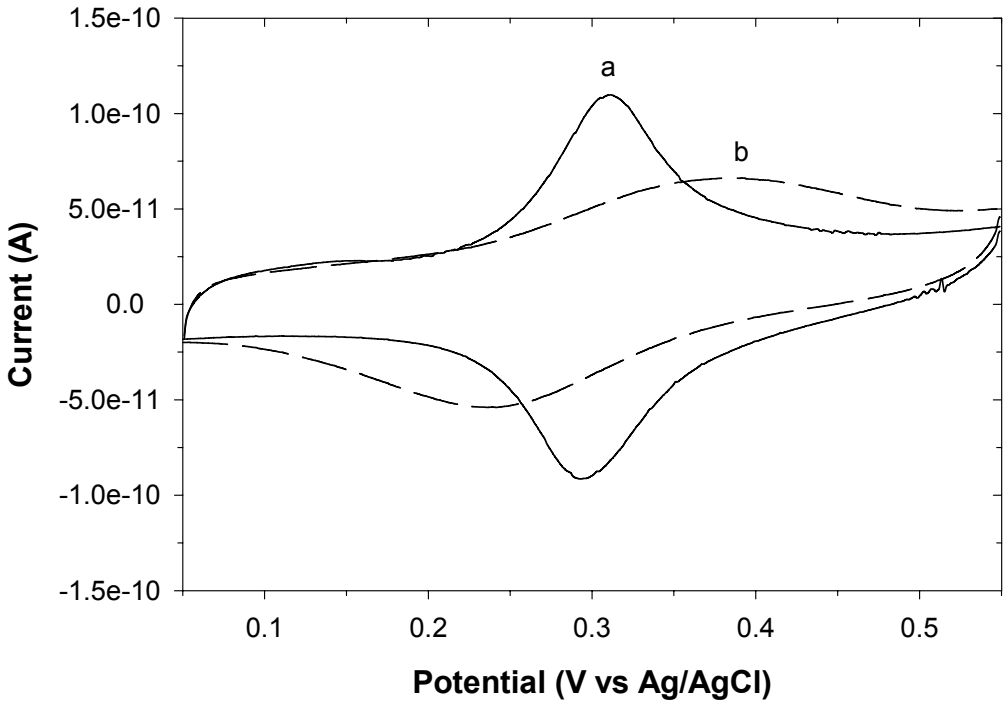


Figure 3.5: Cyclic voltammograms of a microelectrode after (a) electrodeposition of the redox polymer, and (b) incorporation of the capture oligonucleotide. The redox polymer, PAA-PVP-Os, was deposited by placing the microelectrode in 200 µL of a 1 mg $mL^{-1}$ polymer solution in PBS and applying a constant potential of –1.4 V (vs. Ag/AgCl) for 2 min. The capture oligonucleotide was subsequently deposited by placing the electrode in 200 µL of a 1 µM solution of the capture sequence and applying the same potential for 20 min. PBS, scan rate 10 $mV \cdot s^{-1}$.

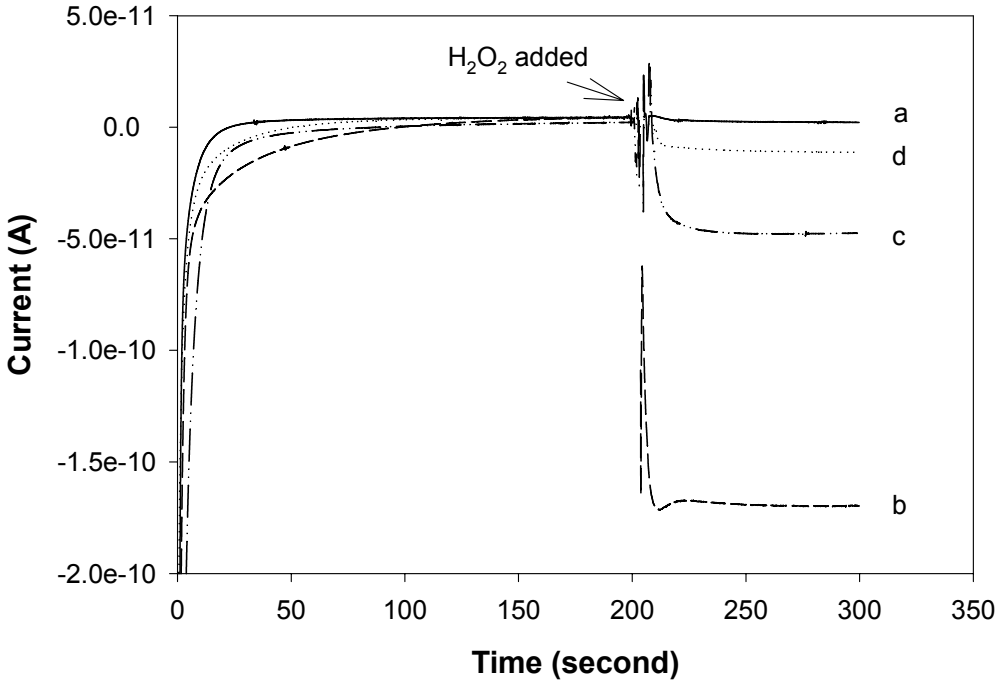


Figure 3.6: Current increments upon raising [$H_2O_2$ ] from 0 to 1 mM. (a) Without the analyzed sequence in the droplet (b) with 1 x $10^{-14}$ M perfectly matched analyzed sequence; (c) as in (b), but with a mismatched base (M1); (d) as in (b), with two mismatched bases (M2). Electrodes were activated by depositing the redox polymer and the capture sequence, as described in Figure 3.5. Electrodes poised at 0.12 V vs. Ag/AgCl. PBS, 25ºC. $H_2O_2$ added at t = 200 s.

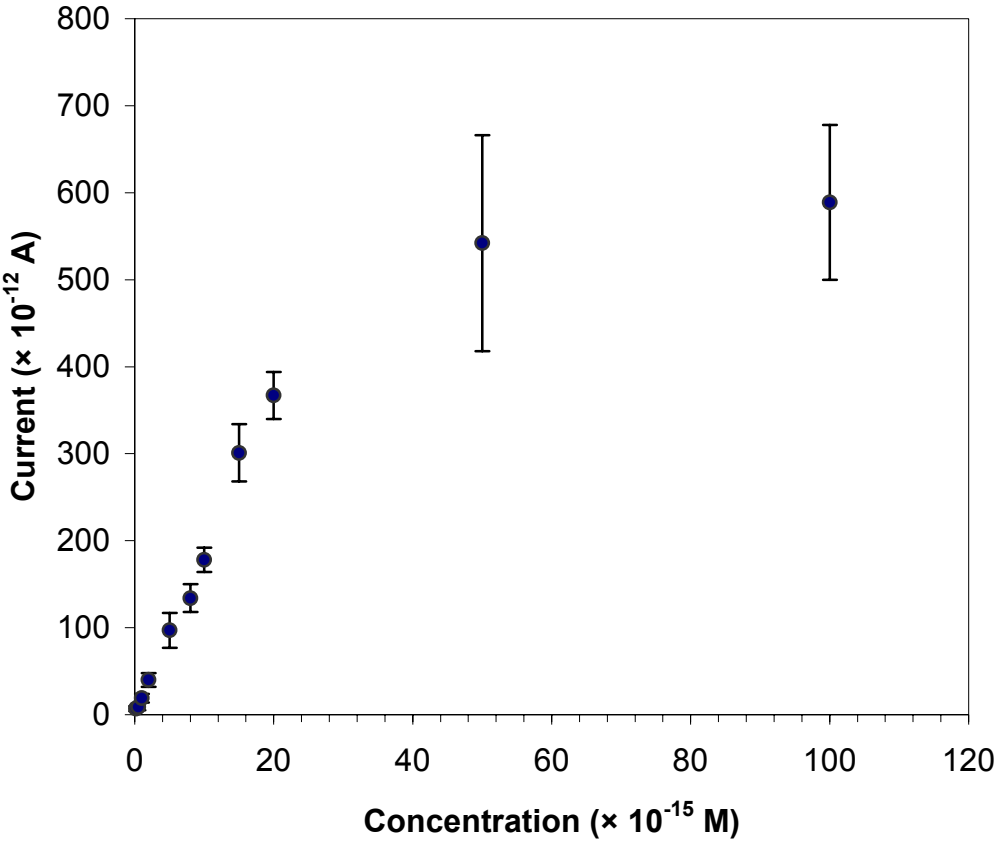


Figure 3.7: Dependence of the current increment on the concentration of the analyzed sequence (the perfectly matched target sequence). Electrodes were made as in Figure 3.6.

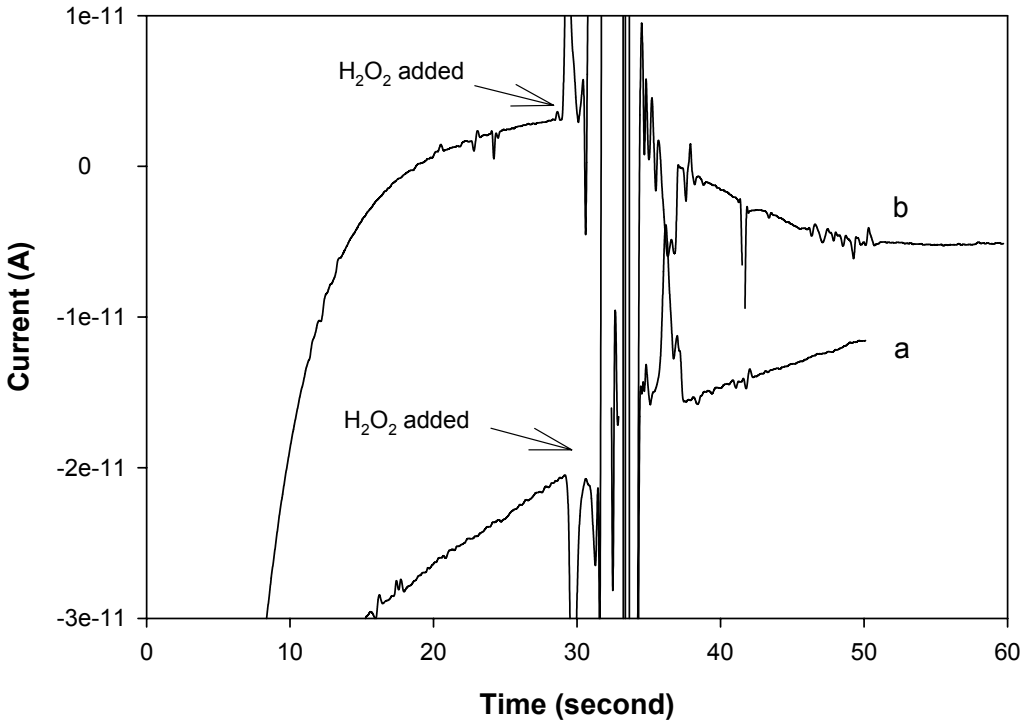


Figure 3.8: One-minute DNA assay. Electrodes were made receptive by electrodepositing the redox polymer and the capture sequence as described before. Current was measured while the electrodes were held at 0.12 V (Ag/AgCl) after (a) the electrode was exposed to the HRP-labeled detection sequence for 5 sec and no target sequence was present; and (b), a 1 nM target sequence solution was contacted for 10 sec followed by 5 sec exposure to the detection sequence solution. $H_2O_2$ was added at t = 30 sec to produce a 1 mM concentration.

# Chapter 4: Conclusions and Recommended Future work

Enzyme-amplified amperometric detection of DNA/RNA has been studied and described in previous chapters of this dissertation. The underlying step of electrodeposition of redox polymers has been shown to be a fast, simple, reproducible and effective method of producing polymer films, which "wire" enzymes. An extremely sensitive DNA/RNA assay based on the electrodeposited redox polymers and capture sequences has been developed. With a 10-μm diameter microelectrode, 3000 copies of the target DNA were detected. This is one of the most sensitive electrochemical DNA/RNA assays to date.

Recommended future research would be aimed at reducing the noise ("background current"). The "background current" caused by the nonspecific adsorption of the HRP-labeled detection sequence, constitutes a major challenge on the way to detecting a few hundred copies of DNA/RNA. As shown in chapter 3, deposition of thicker redox polymer films significantly improved the electrical communications between the electrode and the redox centers of HRP; unfortunately, more of the HRP-labeled detection sequence was non-specifically bound to the thicker redox polymer film. The thickness of the electrodeposited redox polymer film has not been optimized, and its optimization may improve the signal-to-noise ratio. A more promising way, however, would be to use a redox polymer with a neutral or slightly negatively charged backbone, which would repel the also negatively charged enzyme and significantly reduce the nonspecific

adsorption. A few hundreds of copies of the target DNA/RNA might be detectable.

Another focus of research would be detection of DNA/RNA sequences from bacteria and viruses, which are much longer than the 38-base target studied in this dissertation.

So far the vast majority of reported studies on DNA/RNA detection were conducted in clean buffer solutions. Operation of the DNA/RNA sensors in actual biological media is a necessary step on the way to on-the-spot and in-situ analyses.

Much work remains to be done on the actual sampling process and on choosing the restriction enzymes that specifically cleave the nucleic acids, delivering thereby the short actually detected sequences.

Replacing the HRP label on the detection sequence by other enzymes, e.g., bilirubin oxidase (BOD), should be studied. The use of BOD, which catalyzes the reduction of oxygen to water, would allow analysis of $O_2$-containing body fluids, obviating the use of unstable $H_2O_2$ as a substrate and further simplify the assay.

# Chapter 5: A Miniature Membrane-less Biofuel Cell Operating under Physiological Conditions at 0.5 V*

## 5.1 ABSTRACT

A biofuel cell operating at a power density of 50 μW $cm^{-2}$ at 0.5 V under physiological conditions (air saturated, pH 7.4, 0.14 M NaCl, 37.5°C, 15 mM glucose) is described. The cell had a glucose electro-oxidizing anode and an $O_2$ electro-reducing cathode. The anodic electrocatalyst comprised the electrostatic adduct of glucose oxidase (GOx) a polyanion at physiological pH, and the polycationic redox polymer poly (*N*-vinyl imidazole), partially quaternized with 2-bromoethylamine and partially complexed with $[Os(da\text{-}bpy)_2Cl]^{+/2+}$, (da-bpy = 4,4′-diamino-2,2′-bipyridine) ($E^{o\prime}$ = –160 mV *vs.* Ag/AgCl). The cathode electrocatalyst was the electrostatic adduct of bilirubin oxidase (BOD) also a polyanion at physiological pH, and the polycationic redox copolymer of polyacrylamide and poly (*N*-vinylimidazole), complexed with $[Os(dCl\text{-}bpy)_2Cl]^{+/2+}$, where dCl-bpy = 4,4′-dichloro-2,2′-bipyridine ($E^{o\prime}$ = 350 mV *vs.* Ag/AgCl). The anode and the cathode were 7 μm diameter, 2 cm long carbon fibers, on which the catalytic enzyme-redox polymer adducts were cross-linked. When the miniature cell operated at 0.5 V, the power output dropped to about 60% of its initial value after 2 days of continuous operation at 37.5°C.

* The study of this chapter was performed in collaboration with Dr. Nicolas Mano and Dr. Hyug-Han Kim. The author synthesized the polymers "wiring" the enzymes of the anode and the cathode and electrochemically characterized the two electrodes.

## 5.2 INTRODUCTION

A practical limit on the size of manufacturable batteries is posed by the miniaturization of their cases, membranes (or separators), and seals. The reproducible, low cost manufacture of membranes and cases of sub-millimeter dimensions is difficult.[1] Biofuel cells have been studied extensively,[1-8] but most required membranes to separate their anode and cathode compartments and could not be miniaturized. Turner, Higgins, Hill, and their colleagues[9-15] built a series of biofuel cells in which they electro-oxidized methanol at the anode and electroreduced $O_2$ at the cathode.[12-15] The cells required ion-exchange membranes to prevent the anode's substrate-reduced mediators from reaching the cathode compartment, where they would have been oxidized, and to prevent their cathode's mediators from reaching the anode compartment, where they would have been reduced. The membrane was usually Nafion; in some cells the membrane was metallized to reduce cell volume. The anodes were made of platinum gauze or of reticulated carbon, and the cathodes of platinum gauze. Some of the cathode compartments contained dissolved or adsorbed laccase and in some of the laccase-containing cathode compartments electrons were carried to the laccase by the hydroquinone/quinone couple. The anode compartments contained glucose oxidase, pyrroloquinoline quinone (PQQ) alcohol dehydrogenase or PQQ glucose dehydrogenase, the reduced enzymes' electrons being carried to the anode by a redox mediator, such as phenazine/phenazonium ethosulfate, poly-viologen, Wurster's blue (*s*-1,4-bis(dimethylamino)benzene

perchlo- rate) or *N*,*N*,*N'*,*N'*-tetramethyl-*p*-phenylenediamine. In these early cells, the highest (geometric-area based) current density, 20 μA $cm^{-2}$, was reached at pH 9.5 and at 20°C in the methanol/$O_2$ cell. The methanol/$O_2$ cell produced 2 μW $cm^{-2}$ when operating at 0.3 V, its current decreasing by less than 10% per day.[10,11] In more recent work, Willner *et al.* observed power densities of 5 μW $cm^{-2}$ at an operating potential of 0.06 V in a cell having a glucose electro-oxidizing anode made by coupling out the electrons of an immobilized glucose oxidase (GOx) monolayer on a high surface area gold electrode through a PQQ-spacer flavin adenine dinucleotide (FAD) cofactor of the GOx.[3] Rao *et al.* reached power densities of 12 μW $cm^{-2}$ at an operating potential of 0.4 V in metal-oxygen cells.[4]

A miniature biofuel cell comprising a glucose-electrooxidizing anode (Eq. 5.1) and an $O_2$-electroreducing cathode (Eq. 5.2), and operating under

*Anode*: $2\ \text{glucose} \rightarrow 2\ \text{gluconolactone} + 4H^+ + 4e^-$ (5.1)

*Cathode*: $O_2 + 4H^+ + 4e^- \rightarrow 2\ H_2O$ (5.2)

*Cell*: $2\ \text{glucose} + O_2 \rightarrow 2\ \text{gluconolactone} + 2\ H_2O$ (5.3)

physiological conditions may power sensors and actuators implanted in the body. Unlike batteries, such biofuel cells may well be membrane-free, and therefore can be miniaturized substantially.

Recently we described a membrane-less miniature biofuel cell consisting of two 7-μm diameter 2-cm long carbon fibers.[5] The cell had a glucose-oxidation catalyzing fiber anode, made by "wiring" GOx with a redox polymer, and an

oxygen-reduction catalyzing fiber cathode, made by wiring laccase from *Coriolus hirsutus*. It operated at 0.37 V in a pH 5 citrate buffer, producing 64 μW $cm^{-2}$ at 23°C and 137 μW at 37°C. Because laccase is severely inhibited at neutral pH (by $OH^-$) and is also inhibited by $Cl^-$ at its physiological concentration of 0.14 M, the power density under physiological conditions was about 100 times lower than in citrate buffer. The inhibition has been attributed to the strong binding of $OH^-$ at neutral pH, and of $Cl^-$ at its 0.14 M physiological concentration[16,17] to the type 2 $Cu^{+/2+}$ center of laccase.[7,8]

Tsujimura et al.[18] recently described a carbon felt cathode coated with bilirubin oxidase (BOD) from *Myrothecium verrucaria*, an enzyme used in the clinical assay serum bilirubin. The enzyme catalyses the oxidation of bilirubin to biliverdin (Eq. 5.4) and then to a yet unidentified purple pigment. The electrode poised at -0.17 V vs. the reversible potential of the $O_2/H_2O$ electrode operated at 0.5 mA $cm^{-2}$ only for 2 hours in a pH 7 phosphate-buffered 0.1 M KCl solution.

$$\text{Bilirubin} + \tfrac{1}{2}O_2 \rightarrow \text{biliverdin} + H_2O \qquad (5.4)$$

A recent study by our group[19] described the electroreduction of $O_2$ to water under physiological conditions (pH 7.4, 0.14 M NaCl, and 37.5°C) on a carbon cathode modified with the cross-linked electrostatic adduct of BOD and PAA-PVI-Os(dCl-bpy)$_2Cl^{+/2+}$ where dCl-bpy = 4,4′-dichloro-2,2′-bipyridine, $E^{o\prime}$ = 350 mV (Ag/AgCl) (Figure 5.1, Scheme 5.1). The electrode operated at a current density of 5 mA $cm^{-2}$ and at a potential only 0.18 V reducing versus that

of the reversible $O_2/H_2O$ electrode at pH 7, with great pH and $Cl^-$ tolerance and stability (up to days).

Earlier, glucose-oxidizing anodes were made with nonleachable electrocatalysts in which reaction centers of GOx were electrically connected to carbon or gold electrodes through electron conducting redox polymers.[20] The electrocatalysts were electrostatic adducts of polycationic redox polymers and GOx, cross-linked on electrodes to electron-conducting, glucose and ion-permeable redox hydrogels. An example of such an anode was described by Chen *et al.*,[5] who electro-oxidized glucose at pH 5 in citrate buffer. The redox potential of the redox polymer, PAA-PVI-Os(dme-bpy)$_2$Cl$^{+/2+}$, a copolymer of polyacrylamide (PAA) and poly(*N*-vinylimidazole) (PVI) complexed with [Os(4,4′-dimethyl-2,2′-bipyridine)$_2$Cl]$^{+/2+}$, was 95 mV *vs.* Ag/AgCl.

We describe here a membrane-less, miniature biofuel cell comprising two 7-μm diameter, 2-cm long carbon fiber electrodes. The cell operates in physiological solutions (pH 7.4, 0.14 M NaCl, 15 mM glucose, 37.5 °C). The potential of the redox polymer "wire" on the cathode is just negative of that of bilirubin oxidase (BOD) type-2/type-3 $Cu^{+/2+}$ cluster at pH 7 under air, +530 mV (Ag/AgCl).[21-23] The $O_2$-oxidized redox centers of BOD accept electrons from $Os^{2+}$ centers of the [PAA-PVI-Os(dCl-bpy)$_2$Cl]$^+$ wire, and the resulting $Os^{3+}$ centers are electroreduced on the carbon electrode poised near 350 mV (Ag/AgCl). To maximize the power output, a new polymer, PVI-[Os(da-bpy)$_2$Cl]$^{+/2+}$, poly(*N*-vinylimidazole) complexed with [Os(4,4′-diamino-2,2′-bipyridine)$_2$Cl]$^{+/2+}$, $E^{o'}$ = –160 mV *vs.* Ag/AgCl (Figure 5.2, Scheme 5.1), is designed as the redox

polymer "wire" for the anode, with its potential just positive of the –340±100 mV (Ag/AgCl) equilibrium potential of the GOx FAD/$FADH_2$ centers at pH 7.[24-28] The FAD reaction centers of GOx are reduced by glucose to $FADH_2$, which are then oxidized by the $Os^{3+}$ centers of the redox polyer, and the resulting $Os^{2+}$ centers are electro-oxidized at the carbon electrode poised near –160 mV (Ag/AgC/), compared to 95 mV reported earlier (Scheme 5.1). The overpotential for the electro-oxidation of the $FADH_2$ is thus significantly reduced, and the operating potential of the cell increases from 0.37 V to 0.5 V.

## 5.3 EXPERIMENTAL

### 5.3.1 Chemicals

Bilirubin oxidase from *Myrothecium verrucaria* (BOD) (EC 1.3.3.5, Sigma, St. Louis, MO), glucose oxidase (GOx) from *Aspergillus niger* (no. 49182, Fluka, Milwaukee, WI), poly(ethylene glycol) (400) diglycidyl ether (PEGDGE) from Polysciences, Inc. (Warrington, PA), ammonium hexachloroosmate(IV) (Aldrich, Milwaukee, WI), and $NaIO_4$, NaCl (Sigma, St. Louis, MO) were used as received. Fresh solutions of BOD and GOx in pH 7.4 20 mM phosphate buffer containing 0.14 M NaCl (PBS) were prepared daily. All solutions were made with deionized water passed through a purification train (Sybron Chemicals Inc, Pittsburgh, PA).

### 5.3.2 Synthesis of the Redox Polymer PVI-[Os(4,4′-diamino2,2′-bipyridine)$_2$*Cl*]$^{+/2+}$.

4,4′-Dinitro-2,2′-bipyridine-*N*,*N*′-dioxide was prepared as described.[29,30] 4,4′-Diamino-2,2′-bipy-ridine (da-bpy) was synthesized from 4,4′-dinitro-2,2′-bipy-ridine-*N*,*N*′-dioxide by modifying the procedure of Maerker and Case.[31] Os(da-bpy)$_2$Cl$_2$ was prepared as follows: $(NH_4)_2OsCl_6$ and 4,4′-diamino-2,2′-bipyridine (da-bpy) were dissolved in ethylene glycol in a 1:2 molar ratio and refluxed under argon for 1 h (yield 90%). The resulting Os(da-bpy)$_2$Cl$_2$ was then complexed with poly(1-vinylimidazole) (PVI) at 1:4 complex: mer molar ratio and purified as described.[20,30,32] Part of the imidazole rings of the resulting polymer were quaternized by reaction under argon at 45°C with 2-bromoethylamine in stirred ethylene glycol dimethyl formamide (DMF) (3:2 v/v ratio).[33] Figure 5.2 shows the structure and stoichiometry of the partly 2-bromoethylamine-quaternized PVI-[Os(4,4′-diamino-2,2′-bipyridine)$_2$Cl]$^{+/2+}$ wire. The redox potential of the PEGDGE cross-linked polymer was –160 mV *vs.* Ag/AgCl.

### 5.3.3 Synthesis of the Redox Polymer PAA-PVI-[Os(4,4′-dichloro-2,2′-bipyridine)$_2$Cl]$^{+/2+}$.

4,4′-Dichloro-2,2′-bipyridine (dCl-bpy) was synthesized from 4,4′-dinitro-2,2′-bipy-ridine-*N*,*N*′-dioxide by the same procedure of Maerker and Case.[31] Os(dCl-bpy)$_2$Cl$_2$ was prepared as follows: $(NH_4)_2OsCl_6$ and 4,4′-dichloro-2,2′-bipyridine (dcl-bpy) were dissolved in ethylene glycol in a 1:2 molar ratio and refluxed under argon for 1 h (yield 85%). The Os(dcl-bpy)$_2$Cl$_2$ was then

complexed with the 1:7 polyacrylamide-poly(*N*-vinylimidazol) (PAA-PVI) copolymer and purified as described.[34] Figure 5.1 shows the structure and the stoichiometry of the PAA-PVI-[Os(4,4′-dichloro-2,2′-bipyridine)$_2$Cl]$^{+/2+}$ wire of BOD. The redox potential of the PEGDGE cross-linked polymer was 350 mV *vs.* Ag/AgCl.

### 5.3.4 Biofuel Cell.

A cluster of 3-cm long, 7-μm diameter carbon fibers (Goodfellow, Cambridge, UK) were soaked in ethanol to allow for their separation. Two of the separated fibers were placed in two 1 mm × 1 mm grooves machined into a 3 cm long polycarbonate support. One end of each fiber was fixed with epoxy and the other end was electrically connected to copper lead wires using conductive carbon paint (SPI, West Chester, PA). The carbon paint was allowed to dry and was then insulated with a layer of epoxy. The effective length of the carbon fibers was about 2 cm. The active area of each fiber was 0.44 mm$^2$. Prior to their coating with the respective electro-catalysts the carbon fibers were made hydrophilic by plasma oxidation (1 torr $O_2$ plasma, 2.5 min).[35] A photograph, showing part of the anode and the cathode, is seen in Figure 5.3(b).

The anodic catalyst solution was made as follows. 100 μL of 40 mg/mL GOx in 0.1 M $NaHCO_3$ was oxidized by 50 μL of 7 mg/mL $NaIO_4$ in the dark for 1 h; 2 μL of the periodate-oxidized GOx solution was then mixed with 8 μL of 10 mg/mL PVI-[Os(4,4′-diamino-2,2′-bipyridine)$_2$Cl]$^{+/2+}$ and a 0.5 μL droplet of 2.5 mg/mL PEGDGE. 5 μL of the anodic catalytic solution was applied to the carbon

fiber. The cathodic solution consisted of 10 μL of 10 mg $mL^{-1}$ of PAA-PVI-[Os(4,4′-dichloro-2,2′-bipyridine)$_2$Cl]$^{+/2+}$ in water, 2 μL of PBS, 2 μL of 46 mg $mL^{-1}$BOD in PBS, and 2 μL of 7 mg $mL^{-1}$ PEGDGE in water. A 5 μL aliquot of the mixed solution was pipetted onto the hydrophilic carbon fiber, which was promptly wetted and penetrated by the solution. The electrodes were cured for at least 18 h at room temperature before use.

### 5.3.5 Instrumentation and Electrochemical Measurements.

The electrochemical measurements were carried out with a CH Instrument model 832 electrochemical detector (CH Instrument, Austin, TX). The assembled cell was immersed in an aerated 15 mM glucose, pH 7.4, 20 mM phosphate buffered solution. The concentration of NaCl was 0.14 M except in the experiments where the $Cl^-$ dependence of the cell was studied. The temperature was controlled by an isothermal circulator (Fisher Scientific, Pittsburgh, PA). The dissolved $O_2$ concentration was monitored with an oxygen electrode purchased from BAS (West Lafayette, IN). At the start of the experiments argon was bubbled through the solution for a least 15 min, followed by oxygen. To maintain a fixed volume of solution in the cell, the bubbled gases were presaturated with water by passing through a bubbler, which contained PBS. The water-jacketed three-electrode cell had a BAS micro Ag/AgCl (3 M NaCl) reference electrode and a platinum wire counter electrode and was maintained at 37.5°C.

## 5.4 RESULTS AND DISCUSSION

### 5.4.1 Polarization Curves of the Miniature Biofuel Cell.

Figure 5.4 shows the polarization curves of the microcarbon fiber anode and cathode at 37.5°C. The catalytic electro-oxidation current of glucose appeared at –200 mV *vs.* Ag/AgCl and reached its plateau at –50 mV *vs.* Ag/AgCl. The catalytic electroreduction current of $O_2$ appeared at 400 mV *vs.* Ag/AgCl and reached its plateau at 300 mV *vs.* Ag/AgCl. In a quiescent solution the maximum current density of glucose electro-oxidation was about 170 $\mu A/cm^2$ and that of $O_2$ electro-reduction was about 700 $\mu A/cm^2$ under air. Thus, in cells consisting of fiber anode and cathode of equal length, the power output is limited by the rate of glucose electro-oxidation. Higher current and consequently higher power can be achieved by increasing the active electrode area without changing the cell configuration and the cylindrical diffusion profile. Because the glucose concentration was 15 mM and the concentration of $O_2$ in air saturated water at 37°C was only about 0.2 mM, it is evident that the power output was limited not by mass transport but by the kinetics of the anode electrocatalyst.

Figure 5.5 shows the dependence of the power density on the cell voltage. The power density peaked at 10 $\mu W/cm^2$ at $V_{cell}$ = 0.5 V at 23°C, and at 37.5°C it peaked at 50 $\mu W/cm^2$ at $V_{cell}$ = 0.5 V. The fivefold difference between the power densities at the two temperatures reflects the high activation energy for the glucose electro-oxidation, which limits the output.[19,36]

### 5.4.2 Effect of the Partial Pressure of $O_2$.

Figure 5.6 shows the power densities under air and under 1 atm $O_2$. Because the power density was limited by the glucose electro-oxidation kinetics, but not by $O_2$ transport, increasing the partial pressure of $O_2$ resulted not in an increase, but in a slight decrease of the power density. The decrease was caused by the increase in the rate of $FADH_2$ oxidation by $O_2$, which competed with its electro-oxidation via the PVI-[Os(4,4′-diamino-2,2′-bipyridine)$_2$Cl]$^{+/2+}$ wire.[20,30]

### 5.4.3 Absence of Inhibition in Physiological Solution.

"Wired" GOx anodes have an optimum pH range of 6.0 ~ 9.0,[37] and "wired" BOD cathodes reach the maximum activity at pH 7.5 and stay at high activity over a wide pH range between 6 and 10.[19]

The physiological concentration of $Cl^-$ is 0.14 M. The cell maintained its activity in physiological solutions at pH 7.4, 0.14 M NaCl, and 37.5°C. Figure 5.7 shows that the power density was independent of the $Cl^-$ concentration in the cell operating at 0.5 V. The power density declined only by 8% when the $Cl^-$ concentration increased from 0 to 0.9 M. In contrast, the power density of cells comprising laccase-"wiring" cathode decreased by 65% when the $Cl^-$ concentration increased from 0 to 0.128 M, and only 20% of the initial power retained when [$Cl^-$] = 0.5 M; the power density also decreased by more than 90% when the pH increased from 5 to 7.[38]

### 5.4.4 Stability of the Biofuel Cell.

The time-dependence of the power density of the cell poised at 0.5 V cell in a quiescent PBS solution under air at 37.5°C is shown in Figure 5.8. After two days of continuous operations, about 60% of the initial power density retained.

## 5.5 CONCLUSIONS

The miniature membrane-less biofuel cell operated under physiological conditions (pH 7.4, 0.14 M NaCl, 37.5°C) at a power density of 50 μW $cm^{-2}$ and at 0.5 V. The power density in the stagnant solution of the cell was not limited by $O_2$ mass transport, even though the $O_2$ solubility in the physiological buffer solution at 37°C is only 0.2 mM; instead, it was determined by the electrocatalysis of glucose oxidation. The –160 mV (*vs.* Ag/AgCl) redox potential of the glucose oxidase "wiring" PAA-PVI-$[Os(da\text{-}bpy)_2Cl]^{+/2+}$ was only 180 mV oxidizing relative to the redox potential of the $FAD/FADH_2$ centers of GOx at pH 7.4. This allowed the poising of the optimally operating anode at a potential as negative as –50 mV *vs.* Ag/AgCl, and an operating cell voltage of 0.5 V. The cathode utilized PAA-PVI-$[Os(da\text{-}bpy)_2Cl]^{+/2+}$ "wired" BOD, which enabled the operation of the biofuel cell at maximal power output under physiological conditions. By tailoring a similarly reducing but faster GOx wire, it should be possible to increase the power density and maintain the 0.5 V operating potential.

## 5.6 REFERENCES


(1) Palmore, G. T. R.; Whitesides, G. M. *ACS Symposium Series* **1994**, *566*, 271-290.

(2) Palmore, G. T. R.; Kim, H.-H. *Journal of Electroanalytical Chemistry* **1999**, *464*, 110-117.

(3) Willner, I.; Arad, G.; Katz, E. *Bioelectrochemistry and Bioenergetics* **1998**, *44*, 209-214.

(4) Rao, J. R.; Richter, G.; Von Sturm, F.; Weidlich, E.; Wenzel, M. *Biomedical Engineering* **1974**, *9*, 98-103.

(5) Chen, T.; Barton, S. C.; Binyamin, G.; Gao, Z.; Zhang, Y.; Kim, H.-H.; Heller, A. *Journal of the American Chemical Society* **2001**, *123*, 8630-8631.

(6) Kelley, S. C.; Deluga, G. A.; Smyrl, W. H. *Electrochem. Solid State Lett.* **2000**, *3*, 407.

(7) Tarasevich, M. R.; Yaropolov, A. I.; Bogdanovskaya, V. A.; Varfolomeev, S. D. *J. Electroanal. Chem. Interfacial Electrochem.* **1979**, *104*, 393.

(8) Reinhammer, B. R. M. *J. Inorg. Biochem.* **1981**, *15*, 27.

(9) Turner, A. P. F. In *Biotech 83*; Online Publ.: London, 1983, p 643.

(10) Aston, W. J.; Turner, A. P. F. *Biotechnology & Genetic Engineering Reviews* **1984**, *1*, 89-120.

(11) Turner, A. P. F.; Aston, W. J.; Higgins, I. J.; Davis, G.; Hill, H. A. O. *Biotechnology and Bioengineering Symposium* **1982**, *12*, 401-412.

(12) Davis, G.; Hill, H. A. O.; Aston, W. J.; Higgins, I. J.; Turner, A. P. F. *Enzyme and Microbial Technology* **1983**, *5*, 383-388.

(13) Turner, A. P. F.; Ramsay, G.; Higgins, I. J. *Biochem. Soc. Trans.* **1983**, *11*, 445.

(14) Turner, A. P. F.; Aston, W. J.; Bell, J.; Colby, J.; Davis, G.; Higgins, I. J.; Hill, H. A. O. *Anal. Chim. Acta* **1984**, *163*, 161.

(15) Aston, W. J.; Ashby, R. E.; Higgins, I. J.; Scott, L. D. L.; Turner, A. P. F. In *Charge and Field Effects in Biosystem*; Usherwood, P. N. R., Ed.; Abacus Press: Tunbridge Wells, U.K., 1984, p 491.

(16) Koudelka, G. B.; Ettinger, a. M. J. *J. Biol. Chem.* **1988**, *263*, 3698.

(17) Naqui, A.; Varfolomeev, S. D. *FEBS Lett.* **1980**, *113*, 157.

(18) Tsujimura, S.; Tatsumi, H.; Ogawa, J.; Shimizu, S.; Kano, K.; Ikeda, T. *Journal of Electroanalytical Chemistry* **2001**, *496*, 69-75.

(19) Mano, N.; Kim, H.-H.; Zhang, Y.; Heller, A. *Journal of the American Chemical Society* **2002**, *124*, 6480-6486.

(20) Taylor, C.; Kenausis, G.; Katakis, I.; Heller, A. *Journal of Electroanalytical Chemistry* **1995**, *396*, 511-515.

(21) Hirose, J.; Inoue, T.; Sakuragi, H.; Kikkawa, M.; Minakami, M.; Morikawa, T.; Iwamoto, H.; Hiromi, K. *Inorganica. Chim. Acta* **1998**, *273*, 204.

(22) Hiromi, K.; Yamaguchi, S.; Sugiura, Y.; Iwamoto, H.; Hirose, J. *J. Biosci. Biotech. Biochem.* **1992**, *56*, 1349.

(23) Hirose, J.; Minakami, M.; Inoue, K.; Watanabe, H.; Iwamoto, H.; Hiromi, K. *J. Inorg. Biochem.* **1995**, *59*, 718.

(24) Ianiello, R. M.; Lindsay, T. J.; Yacynych, A. M. *Anal. Chem.* **1982**, *54*, 1098.

(25) Heller, A. *Journal of Physical Chemistry* **1992**, *96*, 3579-3587.

(26) Gregg, B. A.; Heller, A. *Journal of Physical Chemistry* **1991**, *95*, 5970-5975.

(27) Vreeke, M. S.; Yong, K. T.; Heller, A. *Analytical Chemistry* **1995**, *67*, 4247-4249.

(28) Miyawaki, O.; Wingard, J. L. B. *Biotech. Bioeng.* **1984**, *26*, 1364.

(29) Anderson, S.; Constable, E. C.; Seddon, K. R.; Turp, E. T.; Baggott, J. E.; Pilling, J. *J. Chem. Soc. Dalton Trans.* **1985**, 2247.

(30) Kenausis, G.; Taylor, C.; Katakis, I.; Heller, A. *Journal of the Chemical Society, Faraday Transactions* **1996**, *92*, 4131-4136.

(31) Maerker, G.; Case, F. H. *J. Am. Chem. Soc.* **1958**, *80*, 2475.

(32) Forster, R. J.; Vos, J. G. *Macromolecules* **1990**, *23*, 4372.

(33) Aoki, A.; Rajagopalan, R.; Heller, A. *Journal of Physical Chemistry* **1995**, *99*, 5102-5110.

(34) Zakeeruddin, S. M.; Fraser, D. M. D. M.; Nazeeruddin, M.-K.; Gratzel, M. *J. Electroanal. Chem.* **1992**, *337*, 253.

(35) Sayka, A.; Eberhart, J. G. *Solid State Technol.* **1989**, *32*, 69.

(36) Mano, N.; Kim, H.-H.; Heller, A. *Journal of Physical Chemistry B* **2002**, *106*, 8842-8848.

(37) Ohara, T. J.; Rajagopalan, R.; Heller, A. *Analytical Chemistry* **1994**, *66*, 2451-2457.

(38) Chen, T., The Development and Application of Glucose Electrodes Based on "Wired" Glucose Oxidase, Doctoral Dissertation, University of Texas: Austin,2001.

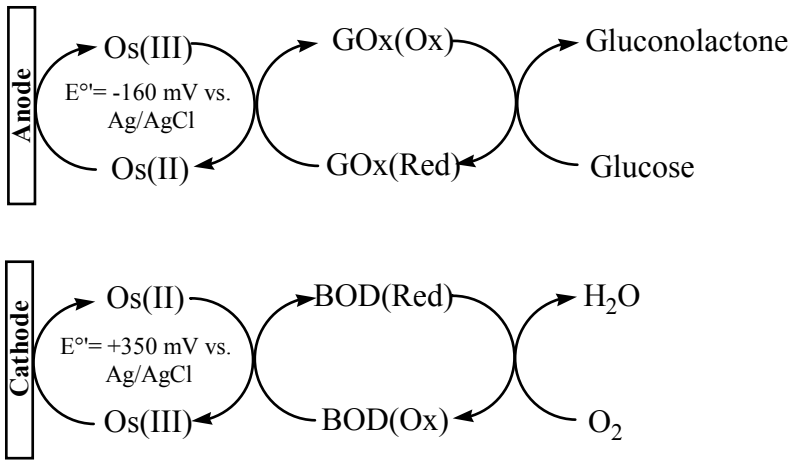


Scheme 5.1: Electron-transfer steps in the electrooxidation of glucose (top) and in the Electroreduction of $O_2$ (bottom).

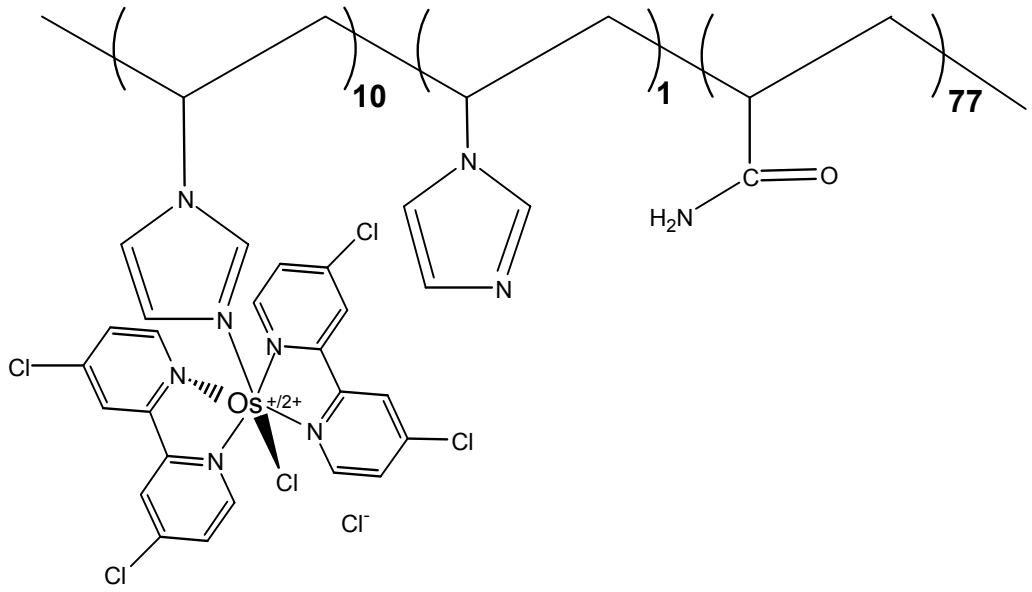


Figure 5.1: Structure of the bilirubin oxidase-"wiring" redox polymer, PAA-PVI-$[Os(dCl\text{-}bpy)_2Cl]^{+/2+}$, redox potential $E^{\circ\prime}$= +350 mV vs. Ag/AgCl.

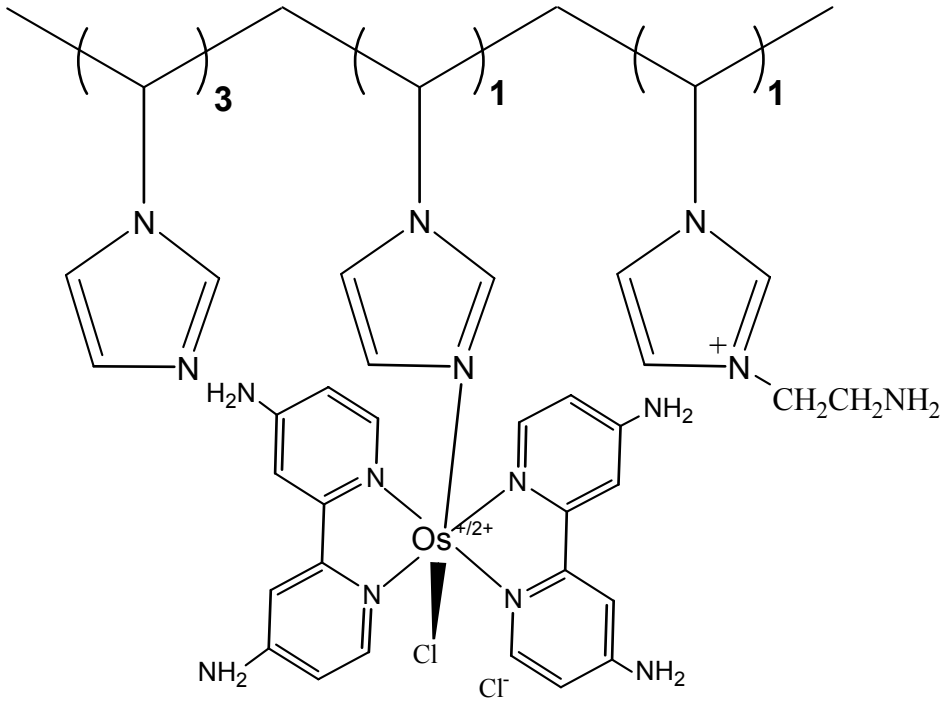


Figure 5.2: Structure of the GOx-"wiring" redox polymer, PVI-[Os(da-bpy)$_2$Cl]$^{+/2+}$, redox potential E°′= -160 mV vs. Ag/AgCl.

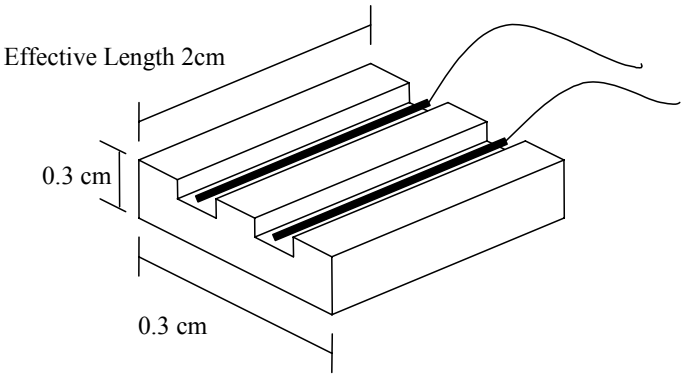


(a)

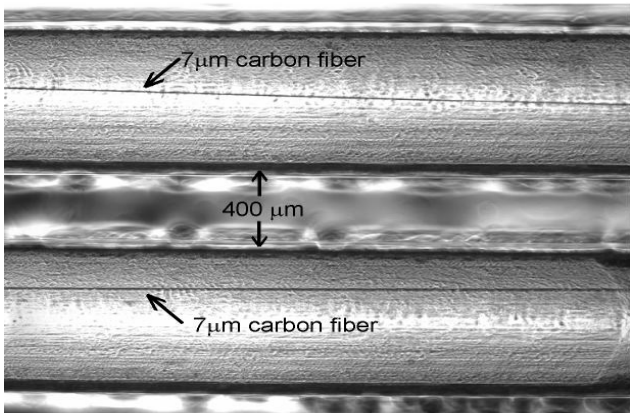


(b)

Figure 5.3: (a) Schematic drawing of the miniature cell structure; (b) A segment of the cell, consisting of two 7-μm diameter carbon fibers.

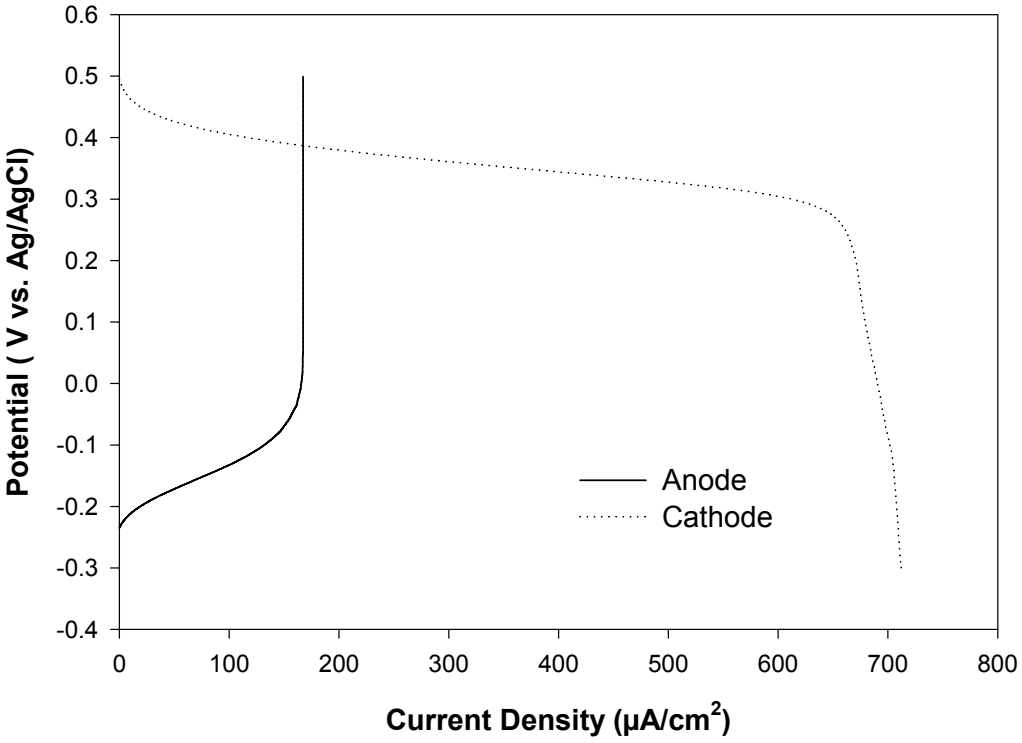


Figure 5.4: Polarization curves of the anode and cathode. Quiescent solution, under air, 37.5 °C, PBS buffer, 15 mM glucose.

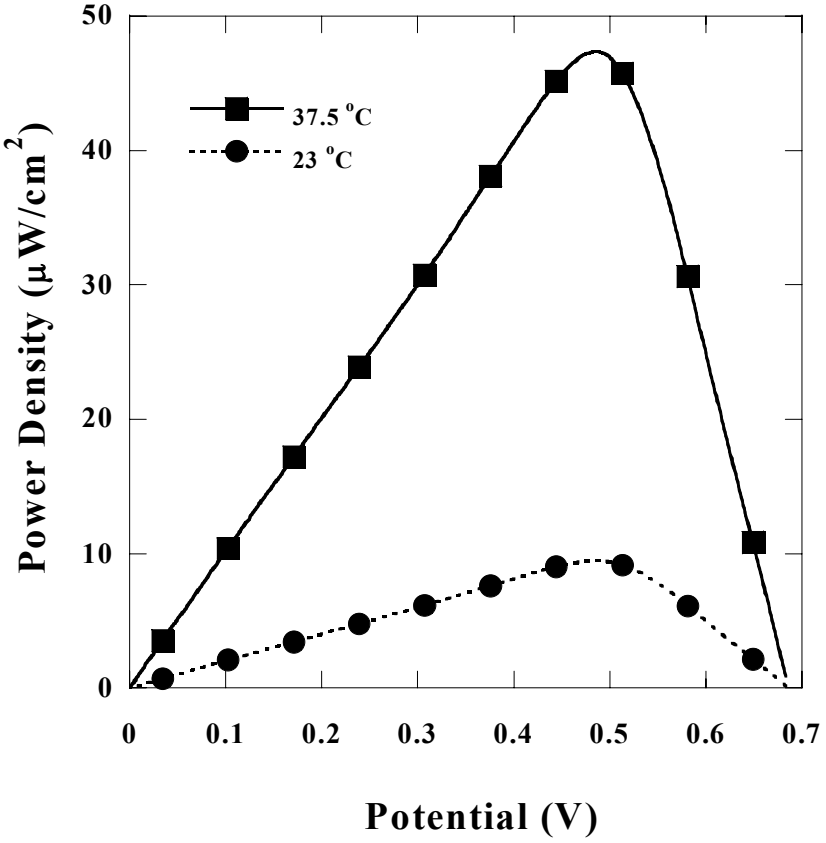


Figure 5.5: Dependence of the power density on the cell voltage. Quiescent solution, under air, PBS buffer, 15 mM glucose.

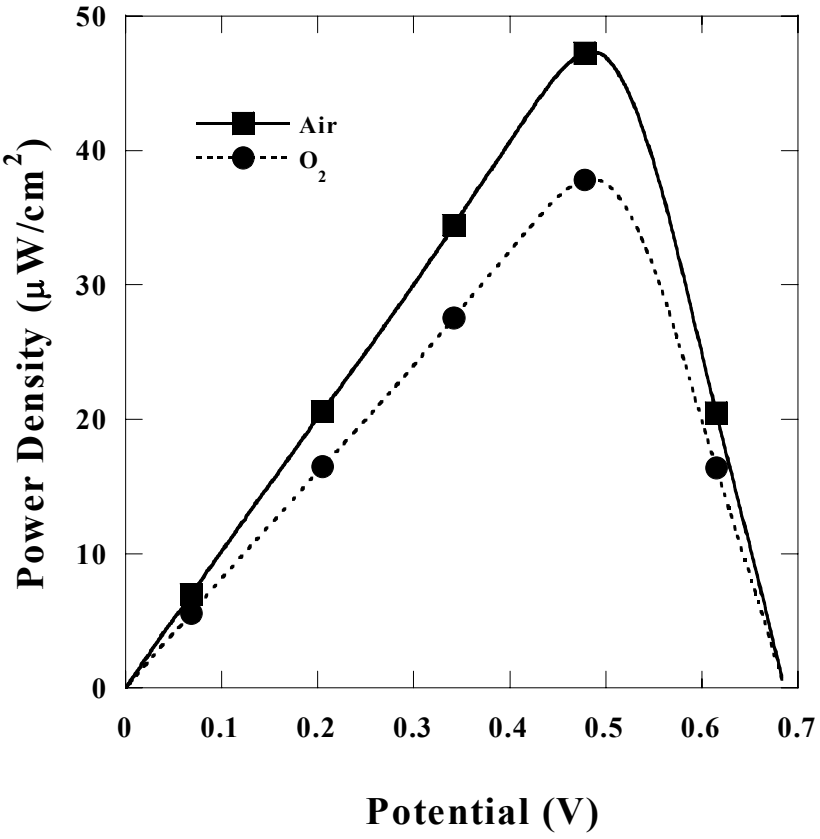


Figure 5.6: $O_2$ pressure dependence of the power density. Quiescent solution, under air, PBS buffer, 15 mM glucose, 37.5 °C.

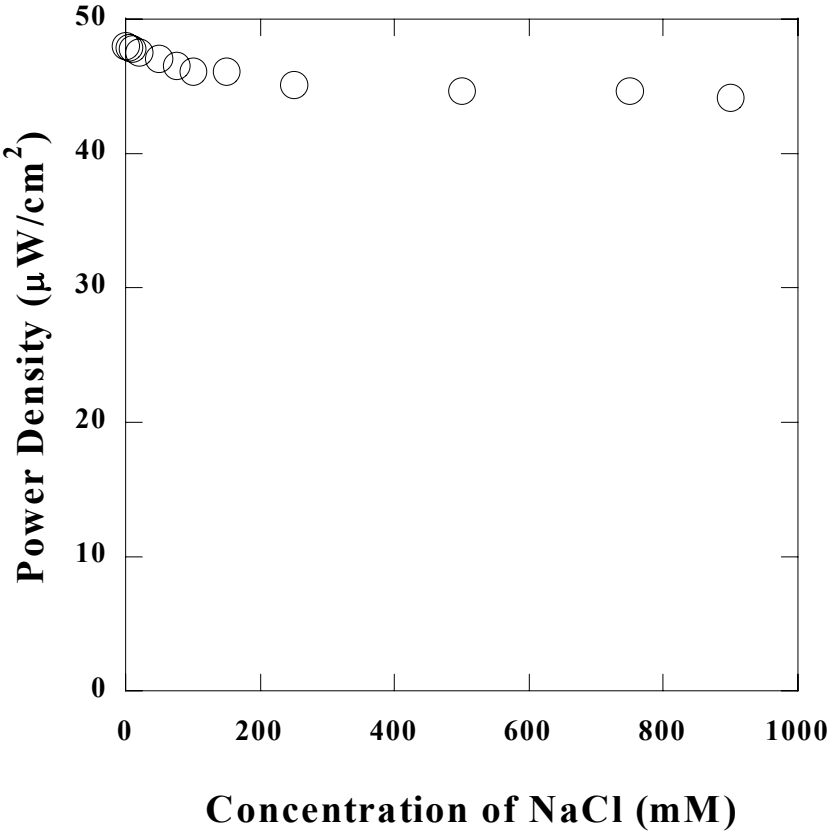


Figure 5.7: Dependence of the power density of the cell on the $Cl^-$ concentration. Quiescent solution, air, 37.5 °C, PBS buffer, 15 mM glucose.

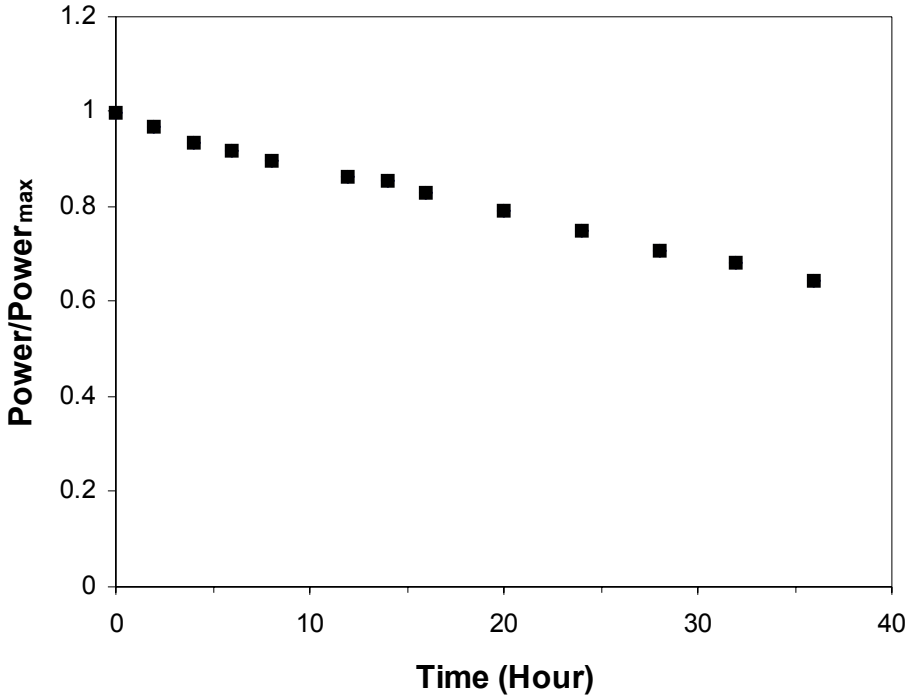


Figure 5.8: Stability of the biofuel cell operating at 0.5 V. Quiescent solution, air, 37.5 °C, PBS buffer, 15 mM glucose.

# Chapter 6: Charge Transfer Complexation of Ruthenium Tris-bipyridine by a Stable Carbene*

## 6.1 ABSTRACT

A stable carbene (**1**) interacts strongly with $[Ru(bpy)_3]^{2+}$ to form a paramagnetic charge transfer complex, which reverts to its components upon treatment with air. Absorption spectra and cyclic voltammetric studies confirms that carbene **1** reduces $[Ru(bpy)_3]^{2+}$ to a lower oxidation level in the complex.

## 6.2 INTRODUCTION

By their nature, carbenes are electron deficient and therefore electrophilic, although nucleophilic carbenes have been predicted, and later trapped, by Wanzlick and co-workers.[1-3] It was not until 1991 that the first stable nucleophilic carbene was successfully synthesized and isolated by Arduengo *et al.*[4] A variety of "stable carbenes", so called because of their extraordinary stability in the absence of oxygen and moisture, have since been prepared,[5-14] although little is known about their electrochemical properties or their tendency to participate in ground or excited state electron transfer reactions.

The range of typical organic reactions of the stable carbenes has been explored only modestly so far, although they do function as complexing ligands to transition metals and other complexes.[14-32] Both the complex and the

* The work in this chapter was conducted under the guidance of Prof. Marye Anne Fox.

uncomplexed ligands are largely nucleophilic.[33] Enders *et al.*[34,35] have shown, for example, that a stable triazol-5-ylidene reacts as a typical carbene, inserting to X-H bonds (X= O, N, S) and adding to activated double bonds. The electrochemical reduction of one such stable carbene has been reported.[36] The possibility that stable carbenes and their complexes might function as useful catalysts[31,37-44] has spurred great interest in their further characterization. The imidazol-2-ylidene carbenes do not react comparably as triazol-5-ylidenes. Although they may differ significantly from transient, highly reactive carbenes, their stability allows for more thorough characterization by spectroscopy than is possible for their highly reactive cousins.

We here report a study on the chemical reactivity of a stable carbene **1** in the imidazol-2-ylidene series which reduces $Ru(bpy)_3^{2+}$ readily. We provide evidence for formation of a contact charge transfer complex, the first such example, to our knowledge, describing the chemical oxidation of a stable carbene.

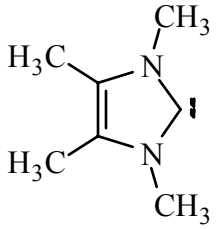

**1**

## 6.3 EXPERIMENTAL

### 6.3.1 Solvents and Chemicals.

Tetrahydrofuran (THF, Aldrich, regent grade) and toluene were distilled from Na/benzophenone prior to use and stored in a dry box. Acetonitrile ($CH_3CN$, B&J Brand), THF (Aldrich, spectrophotometric grade), dimethyl sulphoxide (DMSO, Aldrich, spectrophotometric grade) were purchased and stored in the dry box. $Ru(bpy)_3Cl_2$, $Ru(bpy)_2Cl_2$, N,N'-dimethylthiourea, 3-hydroxy-2-butanone, 1-hexanol, and potassium were used without further purification. Tetrabutylammonium hexafluorophosphate ($Bu_4NPF_6$) was recrystallized twice before being used as the electrolyte.

### 6.3.2 Instrumentation

All reactions and manipulations were carried out under an inert atmosphere, either in a Vacuum Atmospheres HE Dri-Lab glove-box or by using standard Schlenk techniques.

### 6.3.3 Synthesis of the Stable Carbene

Carbene **1** (1,3,4,5-tetramethylimidazol-2-ylidene) was synthesized according to the reported method,[45] as shown in Scheme 1. 1,3,4,5-tetramethylimidazole-2-thione (**2**) is a white crystal whereas **1** is a pale yellow solid. The NMR spectra of both the intermediate **2** and carbene **1** are in agreement with the literature values.

**Scheme 1**

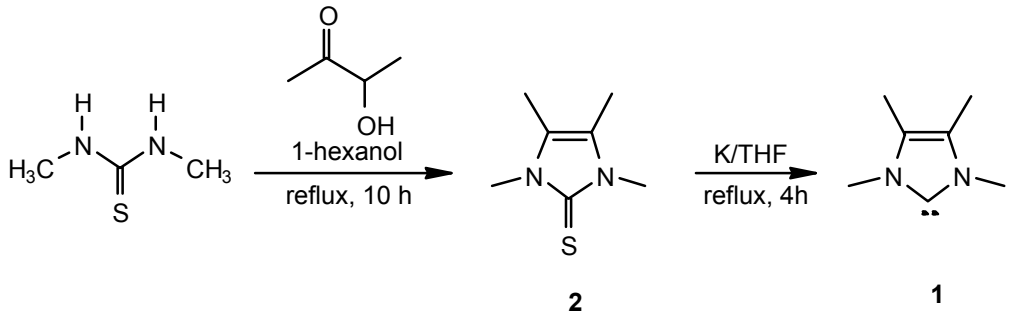


## 6.4 RESULTS AND DISCUSSION

### 6.4.1 Absorption and Fluorescence Spectra

Carbene **1** absorbs strongly below 300 nm in DMSO (Figure 6.1) and exhibits a weak band at about 350 nm that disappears upon exposure to air. Nucleophilic carbenes have been reported to react with chalcogens such as oxygen, sulfur, selenium, and tellurium,[2,35,46,47] and Schönherr *et al.*[3] have also noted a decomposition pathway for imidazol-2-ylidenes involving water and oxygen.

The carbene also shows weak fluorescence at about 460 nm, Figure 6.2. The emission band is quenched by addition of metal salts, completely disappearing, for example, when a 1:1 ratio of carbene-to-$Cu^{2+}$ is attained. With mercury ($Hg^{2+}$ as acetate), the band remains unshifted, Figure 6.3, in contrast with the quenching with copper, where a red-shift of about 10 nm accompanies the quenching. With $Fe^{2+}$ or $Eu^{3+}$, the carbene complex precipitates immediately.

The character of the complexation is more readily established in the complex formed by treating carbene **1** with $[Ru(bpy)_3]^{2+}$. The absorption spectrum of $[Ru(bpy)_3]Cl_2$ is characterized by an intense ligand-centered π-π* transition at 290 nm and a broad metal-to-ligand charge transfer (MLCT) d-π* transition centered at 450 nm (Figure 6.4, b).[48] When carbene 1 is added to a solution of $[Ru(bpy)_3]^{2+}$, a new band appears at between 500-550 nm (Figure 6.4, c), together with a drastic increase in the absorption at 350 nm. This band can not be attributed to a superposition of the separate absorptions of the carbene and $[Ru(bpy)_3]^{2+}$. Instead, the new spectrum is very similar to that reported in the electroreduction of $[Ru(bpy)_3]^{2+}$, successively to $[Ru(bpy)_3]^{1+}$, $[Ru(bpy)_3]^{0}$, and $[Ru(bpy)_3]^{1-}$.[49-51] Heath *et al*.[51,52] have assigned the two new bands (at 350 nm and 525 nm, respectively) to ligand-localized π-π* transitions. $[Ru(bpy)_3]^{1+}$and $[Ru(bpy)_3]^{0}$ are strong reducing agents,[50,51] and a rapid reaction is known to take place between $[Ru(bpy)_3]^{1+}$and $O_2$, quantitatively regenerating $[Ru(bpy)_3]^{2+}$.[49] In our study, upon exposure of the carbene **1**-$[Ru(bpy)_3]^{2+}$mixuture to air, this new band (500-550 nm) disappears and the characteristic absorption of $[Ru(bpy)_3]^{2+}$ at 450 nm reappears (Figure 6.4, d), as the band at 350 nm disappears. These absorption spectra suggest that carbene 1 reduces $[Ru(bpy)_3]^{2+}$ to a more active intermediate ($[Ru(bpy)_3]^{1+}$or $[Ru(bpy)_3]^{0}$), whish is reoxidized by $O_2$ to $[Ru(bpy)_3]^{2+}$, freeing the carbene which is oxidatively degraded by oxygen.

### 6.4.2 NMR Spectra

The complexation can also be followed by nuclear magnetic spectroscopy (NMR). $^{1}$H NMR spectra for 2,2'-bipyridine as a free ligand (bpy) and as complexed to ruthenium (II) ($[Ru(bpy)_3]^{2+}$) are easily distinguished because they exhibit different splitting patterns and chemical shifts in the aromatic region.[53] Figure 6.5 c is the $^{1}$H NMR spectrum of $[Ru(bpy)_3]^{2+}$ containing trace amount of free 2,2'-bipyridine.

The changes induced in this region by treatment of a sample of carbene **1** with a fixed concentration of $[Ru(bpy)_3]^{2+}$ containing ~5% free 2,2'-bipyridine, but with different carbene **1**-to-$[Ru(bpy)_3]^{2+}$ molar ratios (a, 0.5:1; b, 1:1), are shown in Figure 6.5. In the deaerated sample with a 0.5:1 carbene **1**-to-$[Ru(bpy)_3]^{2+}$ molar ratio, the $[Ru(bpy)_3]^{2+}$ signals at δ 7.52, 7.72, 8.17 and 8.85 have disappeared, being replaced by a broad unresolved signal centered at about 8.3 (Figure 6.5, a). Those signals from the free bpy also remain. When this ratio is increased to 1:1 this broad signal is shifted and broadened further (Figure 6.5, b); and with a 2.7:1 ratio (not shown here) the broad signal disappeared completely. The aliphatic regions of all samples are too complex to interpret.

When those carbene-treated samples are treated with air, the peaks assigned to $[Ru(bpy)_3]^{2+}$ reappear, but the aliphatic peaks assigned to the carbene become too complex for interpretation. They do duplicate, however, the complexity attained if the carbene is treated with air. Thus, the paramagnetic species responsible for the broadened signals in the deaerated sample is destroyed by air as $[Ru(bpy)_3]^{2+}$ is regenerated.[54] Since an electron spin has a magnetic

moment that is 657 times greater than that of a proton, it provides a relaxation pathway that is 500 000 times more efficient than by a proton. Therefore, significant broadening of the $^1$H NMR signals would be expected in a charge transfer complex produced by wlwctron donation from the carbene to the metal complex. In fact, sometimes the relaxation is so fast that the signals can not be detected. We conclude that a 1:1 charge transfer complex is formed between $[Ru(bpy)_3]^{2+}$ and carbene **1**, producing a paramagnetic species whose NMR spectrum disappears only to be restored upon exposure of $O_2$.

### 6.4.3 Cyclic Voltammetry

Figure 6.6 a is a cyclic voltammogram for carbene **1** in deaerated acetonitrile. One irreversible oxidation peak is observed at 1.0 V (vs. Ag/AgCl), suggesting that carbene **1** is capable of losing one electron to produce a radical cation, which undergoes a fast chemical reaction. No reverse reduction peak can be observed, irrespective of scan rate. After contact with air (Figure 6.6, b), the oxidation peak disappears, indicating that carbene **1** has decomposed.

A cyclic voltammogram for $[Ru(bpy)_3]^{2+}$, Figure 6.7 a, exhibits three reversible ligand-centered reduction peaks, corresponding to $[Ru(bpy)_3]^{2+}/[Ru(bpy)_3]^{1+}$, $[Ru(bpy)_3]^{1+}/[Ru(bpy)_3]^{0}$, and $[Ru(bpy)_3]^{0}/[Ru(bpy)_3]^{-1}$ respectively, and one quasi-reversible metal-centered oxidation peak ($Ru^{3+}/Ru^{2+}$). Spectroscopic and electrochemical studies[50,51,53,55-59] have shown that the extra electron density in $[Ru(bpy)_3]^{2+}$ and like complexes are carried by the ligands and that the orbitals of the ligands that accept electrons are spatially

isolated, i.e., electrons enter the π* orbitals of the three bpy ligand of $[Ru(bpy)_3]^{2+}$successively without delocalization when it is reduced by one, two, or three electrons, respectively. The reduced forms of $[Ru(bpy)_3]^{2+}$ would , therefore, better be expressed as $[Ru^{II}(bpy)_2(bpy^-)]^+$, $[Ru^{II}(bpy)(bpy^-)_2]^0$, and $[Ru^{II}(bpy^-)_3]^-$, respectively, all of which are paramagnetic. When carbene **1** is added to a solution of $[Ru(bpy)_3]^{2+}$, the three reduction peaks are still observed at roughly the same potentials (Figure 6.7, b). The fact that $[Ru(bpy)_3]^{2+}$disappears in the absorption spectrum and $^1H$ NMR spectrum upon complexation with carbene **1**, but is still observed by cyclic voltammetry, strongly supports the assertion that carbene **1** reduces $[Ru(bpy)_3]^{2+}$ to a paramagnetic intermediate that can be reoxidized to $[Ru(bpy)_3]^{2+}$, electrochemically or by oxygen.

Perhaps counter-intuitively, the reaction between $Ru(bpy)_2Cl_2$ and carbene **1** failed to produce analogous effects. Indeed, both the absorption spectrum and the $^1H$ NMR spectrum of the mixture show simple superposition of the components, indication that no redox or any other reactions transpire between them at all. This observation can be rationalized by the reduction potential of the complex: it is known that replacement of one of the bpy ligands by a halide shifts the reduction potentials negatively,[60] making $Ru(bpy)_2Cl_2$ much more difficult to reduce than $[Ru(bpy)_3]^{2+}$.

## 6.5 CONCLUSION

Carbene **1** reduces $[Ru(bpy)_3]^{2+}$ readily at room temperature, generating a paramagnetic ruthenium tris-bipyridine complex. Oxygen reoxidizes the reduced

intermediate and regenerates $[Ru(bpy)_3]^{2+}$. This is the first example of redox chemistry between a metal complex and a stable carbene.

## 6.6 REFERENCES


(1) Wanzlick, H. W. *Angew. Chem. Internat. Ed. Engl.* **1962**, *1*, 75.

(2) Wanzlick, H. W.; König, B. *Chem. Ber.* **1964**, *97*, 3513.

(3) Schönherr, H.-J.; Wanzlick, H. W. *Liebigs Ann. Chem.* **1970**, *731*, 176.

(4) Arduengo, A. J., III; Harlow, R. L.; Kline, M. *Journal of the American Chemical Society* **1991**, *113*, 361-363.

(5) Regitz, M. *Angew. Chem., Int. Ed. Engl.* **1991**, *30*, 674-676.

(6) Arduengo, A. J., III; Dias, H. V. R.; Harlow, R. L.; Kline, M. *J. Am. Chem. Soc.* **1992**, *114*, 5530.

(7) Dias, H. V. R.; Jin, W. *Tetrahedron Lett.* **1994**, *35*, 1365.

(8) Enders, D.; Breuer, K.; Raabe, G.; Runsink, J.; Teles, J. H.; Melder, J.-P.; Ebel, K.; Brode, S. *Angewandte Chemie, International Edition in English* **1995**, *34*, 1021-1023.

(9) Arduengo, A. J., III; Goerlick, J. R.; Marshall, W. J. *J. Am. Chem. Soc.* **1995**, *117*, 11027-11028.

(10) Alder, R. W.; Allen, P. R.; Murray, M.; Orpen, A. G. *Angew. Chem. Internat. Ed. Engl.* **1996**, *35*, 1121.

(11) Arduengo, A. J., III; Goerlick, J. R.; Marshall, W. J. *Liebigs Ann.* **1997**, 365.

(12) Arduengo, A. J., III; Davidson, F.; Dias, H. V. R.; Goerlich, J. R.; Khasnis, D.; Marshall, W. J.; Prakasha, T. K. *Journal of the American Chemical Society* **1997**, *119*, 12742-12749.

(13) Arduengo, A. J., III *Accounts of Chemical Research* **1999**, *32*, 913-921.

(14) Nakai, H.; Tang, Y.; Gantzel, P.; Meyer, K. *Chemical Communications (Cambridge, United Kingdom)* **2003**, 24-25.

(15) Arduengo, A. J., III; Dias, H. V. R.; Davidson, F.; Harlow, R. L. *J. Organomet. Chem.* **1993**, *462*, 13.

(16) Arduengo, A. J., III; Dias, H. V. R.; Calabrese, J. C.; Davidson, F. *Organometallics* **1993**, *12*, 3405.

(17) Arduengo, A. J., III; Gamper, S. F.; Calabrese, J. C.; Davidson, F. *J. Am. Chem. Soc.* **1994**, *116*, 4361.

(18) Arduengo, A. J., III; Tamm, M.; McLain, S. J.; Calabrese, J. C.; Davidson, F.; Marshall, W. J. *J. Am. Chem. Soc.* **1994**, *116*, 7927.

(19) Schumann, H.; Glanz, M.; Winterfeld, J.; Hemling, H.; Kuhn, N.; Kratz, T. *Angew. Chem., Int. Ed. Engl.* **1994**, *33*, 1733-1734.

(20) Schumann, H.; Glanz, M.; Winterfeld, J.; Hemling, H.; Kuhn, N.; Kratz, T. *Chemische Berichte* **1994**, *127*, 2369-2372.

(21) Kuhn, N.; Kratz, T.; Bläser, D.; Boese, R. *Inorg. Chim. Acta* **1995**, *238*, 179.

(22) Arduengo, A. J.; Harlow, R. L.; Marshall, W. J.; Prakasha, T. K. *Heterocycl. Chem.* **1996**, *7*, 421.

(23) Black, S. J.; Hibbs, D. E.; Hursthouse, M. B.; Jones, C.; Abdul Malik, K. M.; Smithies, N. A. *Journal of the Chemical Society, Dalton Transactions: Inorganic Chemistry* **1997**, 4313-4320.

(24) Desmurs, P.; Dormond, A.; Nief, F.; Baudry, D. *Bulletin de la Societe Chimique de France* **1997**, *134*, 683-688.

(25) Herrmann, W. A.; Schwarz, J.; Gardiner, M. G. *Organometallics* **1999**, *18*, 4082-4089.

(26) Abernethy, C. D.; Clyburne, J. A. C.; Cowley, A. H.; Jones, R. A. *Journal of the American Chemical Society* **1999**, *121*, 2329-2330.

(27) Zheng, X.; Herberich, G. E. *Organometallics* **2000**, *19*, 3751-3753.

(28) Clendenning, S. B.; Hitchcock, P. B.; Nixon, J. F.; Nyulaszi, L. *Chemical Communications (Cambridge)* **2000**, 1305-1306.

(29) Schumann, H.; Glanz, M.; Gottfriedsen, J.; Dechert, S.; Wolff, D. *Pure and Applied Chemistry* **2001**, *73*, 279-282.

(30) Cole, M. L.; Davies, A. J.; Jones, C. *Journal of the Chemical Society, Dalton Transactions* **2001**, 2451-2452.

(31) Niehues, M.; Kehr, G.; Erker, G.; Wibbeling, B.; Frohlich, R.; Blacque, O.; Berke, H. *Journal of Organometallic Chemistry* **2002**, *663*, 192-203.

(32) Denk, K.; Sirsch, P.; Herrmann, W. A. *Journal of Organometallic Chemistry* **2002**, *649*, 219-224.

(33) Regitz, M. *Angew. Chem. Internat. Ed. Engl.* **1996**, *35*, 725.

(34) Enders, D.; Breuer, K.; Runsink, J.; Teles, J. H. *Liebigs Annalen* **1996**, 2019-2028.

(35) Enders, D.; Breuer, K.; Teles, J. H.; Ebel, K. *Journal fuer Praktische Chemie/Chemiker-Zeitung* **1997**, *339*, 397-399.

(36) Enders, D.; Breuer, K.; Raabe, G.; Simonet, J.; Ghanimi, A.; Stegmann, H. B.; Teles, J. H. *Tetrahedron Letters* **1997**, *38*, 2833-2836.

(37) Teles, J. H.; Melder, J.-P.; Ebel, K.; Schneider, R.; Gehrer, E.; Harder, W.; Brode, S.; Enders, D. P.; Breuer, K.; Raabe, G. *Helv. Chim. Acta* **1996**, *79*, 61.

(38) Herrmann, W. A.; Reisinger, C.-P.; Spiegler, M. *Journal of Organometallic Chemistry* **1998**, *557*, 93-96.

(39) Gardiner, M. G.; Herrmann, W. A.; Reisinger, C.-P.; Schwarz, J.; Spiegler, M. *Journal of Organometallic Chemistry* **1999**, *572*, 239-247.

(40) Weskamp, T.; Kohl, F. J.; Hieringer, W.; Gleich, D.; Herrmann, W. A. *Angewandte Chemie, International Edition* **1999**, *38*, 2416-2419.

(41) Weskamp, T.; Bohm, V. P. W.; Herrmann, W. A. *Journal of Organometallic Chemistry* **1999**, *585*, 348-352.

(42) Schwarz, J.; Bohm, V. P. W.; Gardiner, M. G.; Grosche, M.; Herrmann, W. A.; Hieringer, W.; Raudaschl-Sieber, G. *Chemistry--A European Journal* **2000**, *6*, 1773-1780.

(43) Weskamp, T.; Bohm, V. P. W.; Herrmann, W. A. *Journal of Organometallic Chemistry* **2000**, *600*, 12-22.

(44) Simal, F.; Delfosse, S.; Demonceau, A.; Noels, A. F.; Denk, K.; Kohl, F. J.; Weskamp, T.; Herrmann, W. A. *Chemistry--A European Journal* **2002**, *8*, 3047-3052.

(45) Kuhn, N.; Kratz, T. *Synthesis* **1993**, 561.

(46) Kuhn, N.; Henkel, G.; Kratz, T. Z. *Naturforsch. B.* **1993**, *48*, 973.

(47) Kuhn, N.; Henkel, G.; Kratz, T. *Chem. Ber.* **1993**, *126*, 2047.

(48) Roundhill, D. M. *Photochemistry and Photophysics of Metal Complexes*; Plenum Press: New York, 1994.

(49) Anderson, C. P.; Salmon, D. J.; Meyer, T. J.; Young, R. C. *J. Am. Chem. Soc.* **1977**, *99*, 1980.

(50) Mulazzani, Q. C.; Emmi, S.; Fuochi, P. G.; Hoffman, M. Z.; Venturi, M. *J. Am. Chem. Soc.* **1978**, *100*, 981.

(51) Heath, G. A.; Yellowlees, L. J.; Braterman, P. S. *J. Chem. Soc., Chem. Comm.* **1981**, 287.

(52) Coombe, V. T.; Heath, G. A.; MacKenzie, A. J.; Yellowlees, L. J. *Inorg. Chem.* **1984**, *23*, 3423.

(53) DeArmond, M. K.; Myrick, M. L. *Acc. Chem. Res.* **1989**, *22*, 364.

(54) Iwen, P. C.; Hinrichs, S. H.; Rupp, M. E. In *Medical Mycology*, 2002; Vol. 40, pp 87-109.

(55) Vlcek, A. A. *Coord. Chem. Rev.* **1982**, *43*, 39.

(56) Ohsawa, Y.; DeArmond, M. K.; Hanck, K. W.; Morris, D. E.; Whitten, D. G.; Neveux, P. E. *J. Am.Chem. Soc.* **1983**, *105*, 6522.

(57) Motten, A. G.; Hanck, K.; DeArmond, M. K. *Chem. Phys. Lett.* **1981**, *79*, 541.

(58) Morris, D. E.; Hanck, K. W.; DeArmond, M. K. *J. Am. Chem. Soc.* **1983**, *105*, 3032.

(59) Boulas, P. L.; Gómez-Kaifer, M.; Echegoyen, L. *Angew. Chem. Internat. Ed. Engl.* **1998**, *37*, 216.

(60) Tan, S. L.; DeArmond, M. K.; Hanck, K. W. *J. Electroanal. Chem.* **1984**, *181*, 187.

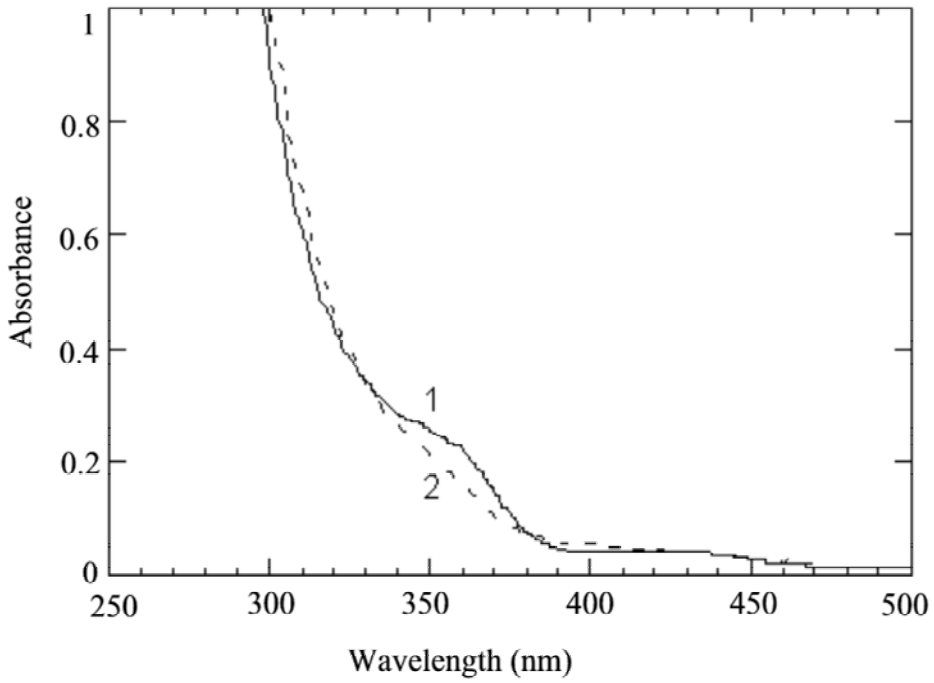


Figure 6.1: Absorption spectra of 5.4 mM carbene **1** in deaerated acetonitrile before (1) and after (2) exposure to air.

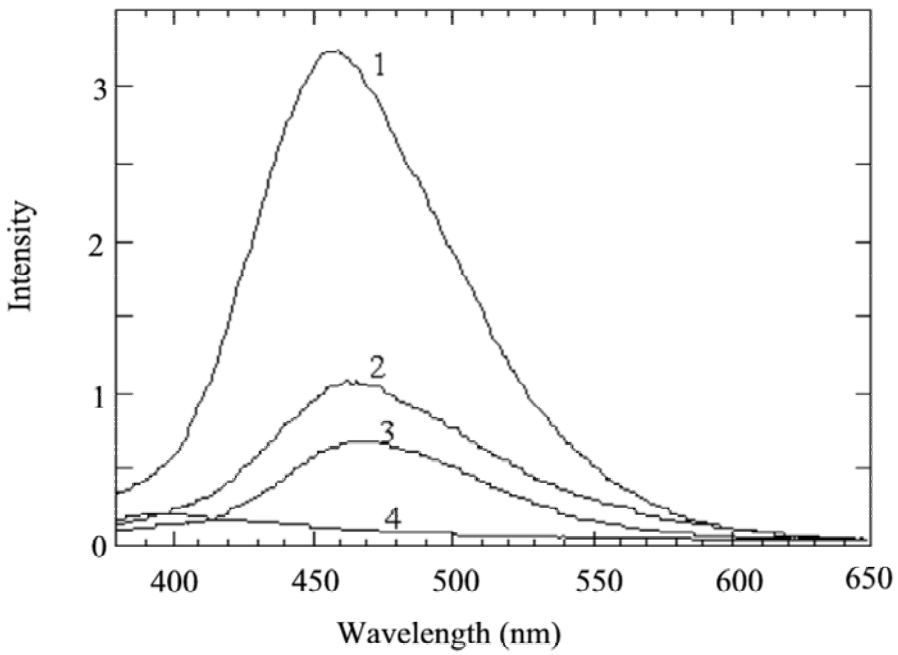


Figure 6.2: Emission spectra of a 2.7 mM solution of carbene **1** in deaerated THF with increasing amounts of $CuCl_2$. (1) No Cu2+; Carbene-to-$Cu^{2+}$ ratio : (2) 10:1; (3) 5:1; (4) 1:1. Excitation: 345 nm.

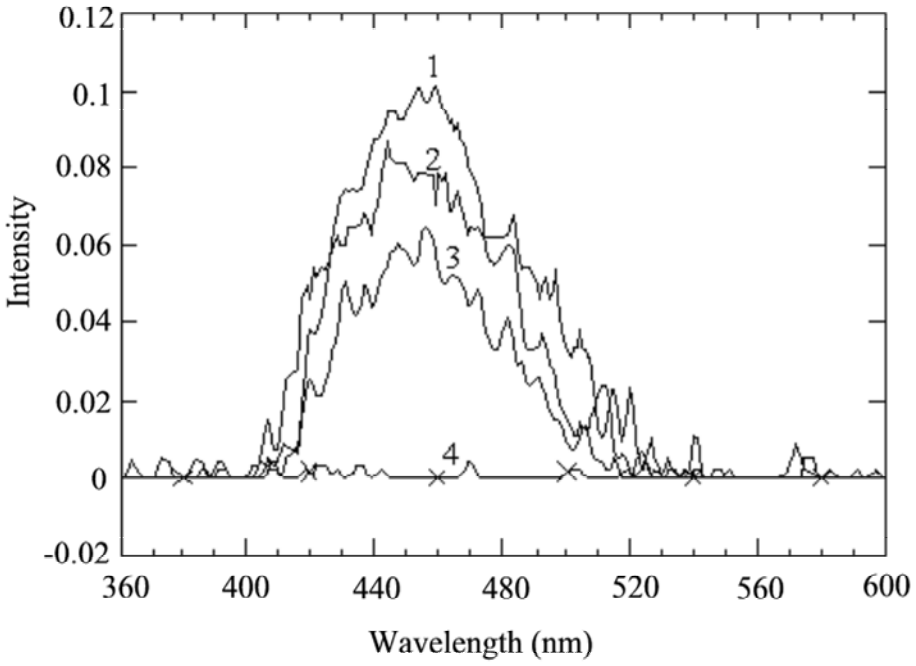


Figure 6.3: Emission spectra of a 4.0 mM solution of carbene **1** in deaerated THF with increasing amounts of $Hg(OAc)_2$: (1) 0; (2) 0.64 mM; (3) 1.6 mM; (4) 4.0 mM $Hg^{2+}$. Excitation: 345 nm.

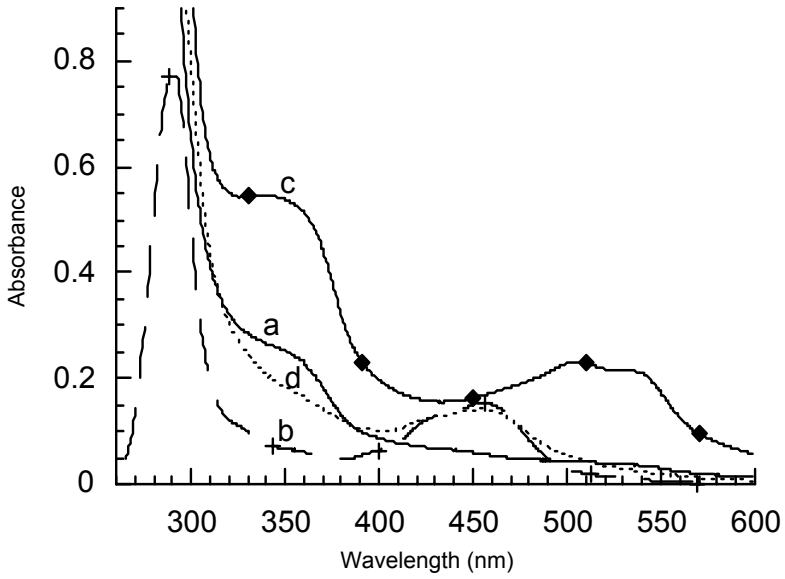


Figure 6.4: Absorption spectra of in deaerated DMSO of: (a) 1.4 mM carbene **1**; (b) 0.05 mM $[Ru(bpy)_3]^{2+}$; (c) mixture containing 1.4 mM carbene **1** and 0.05 mM $[Ru(bpy)_3]^{2+}$; and (d) sample c after treatment of air.

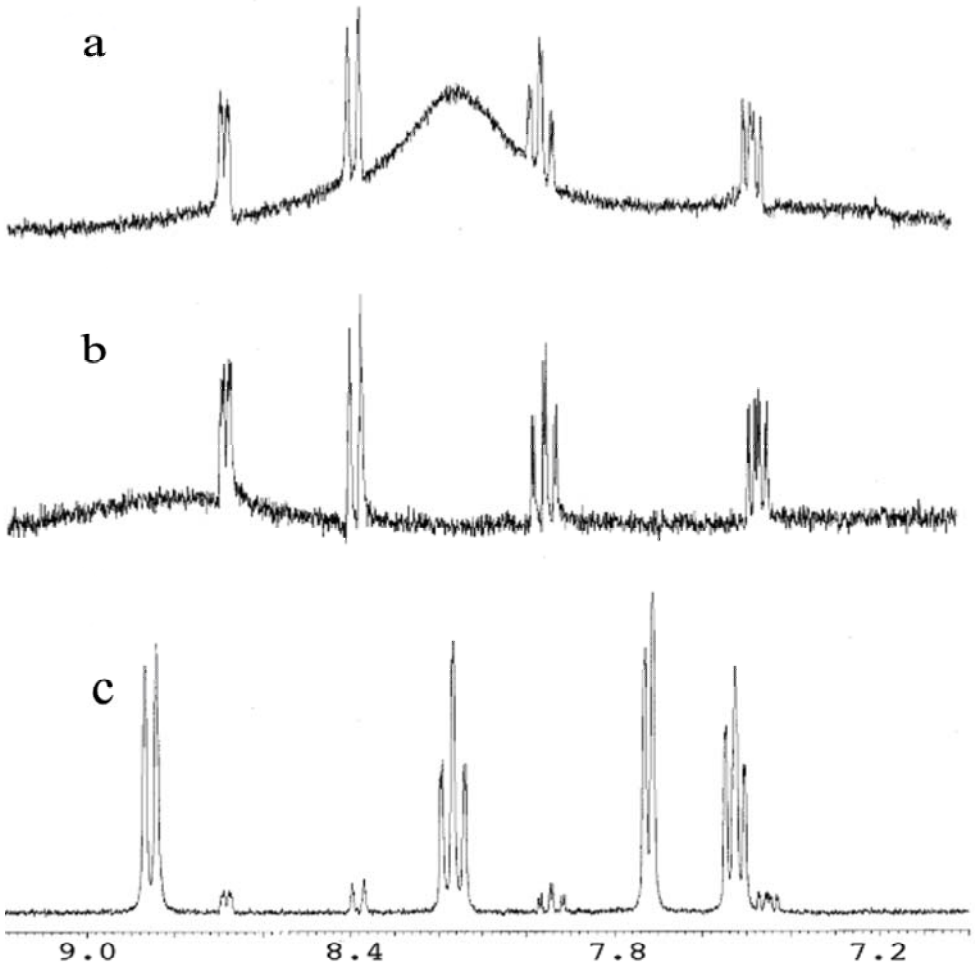


Figure 6.5: $^{1}$H NMR spectra of a 0.05 mM solution in deaerated DMSO-d6 of carbene **1** containing $[Ru(bpy)_3]^{2+}$ with a carbene-to-$[Ru(bpy)_3]^{2+}$ ratio of (a) 0.5:1; and (b) 1:1; and (c) $[Ru(bpy)_3]^{2+}$. All solutions contain trace amount of free 2,2'-bipyridine.

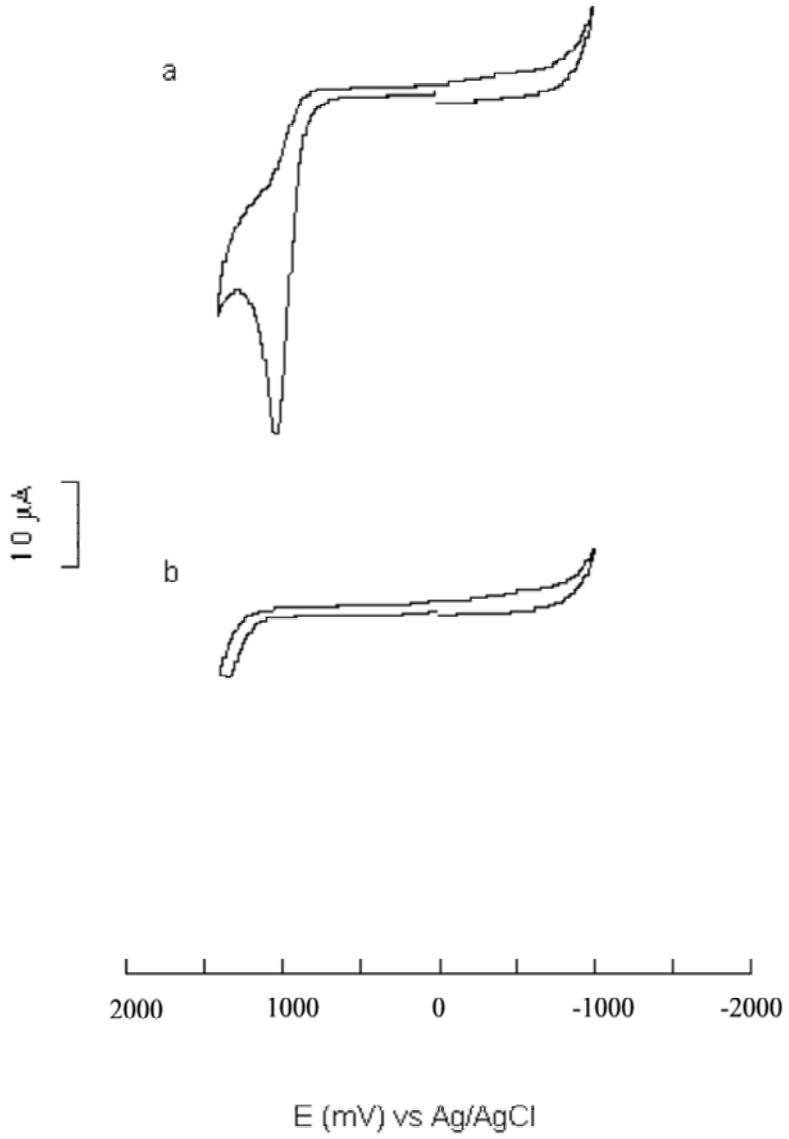


Figure 6.6: Cyclic voltammograms of a 2.0 mM carbene **1** solution in $CH_3CN$ before (a) and after (b) treatment of air. Electrolyte: 0.1 M $Bu_4 NPF_6$.

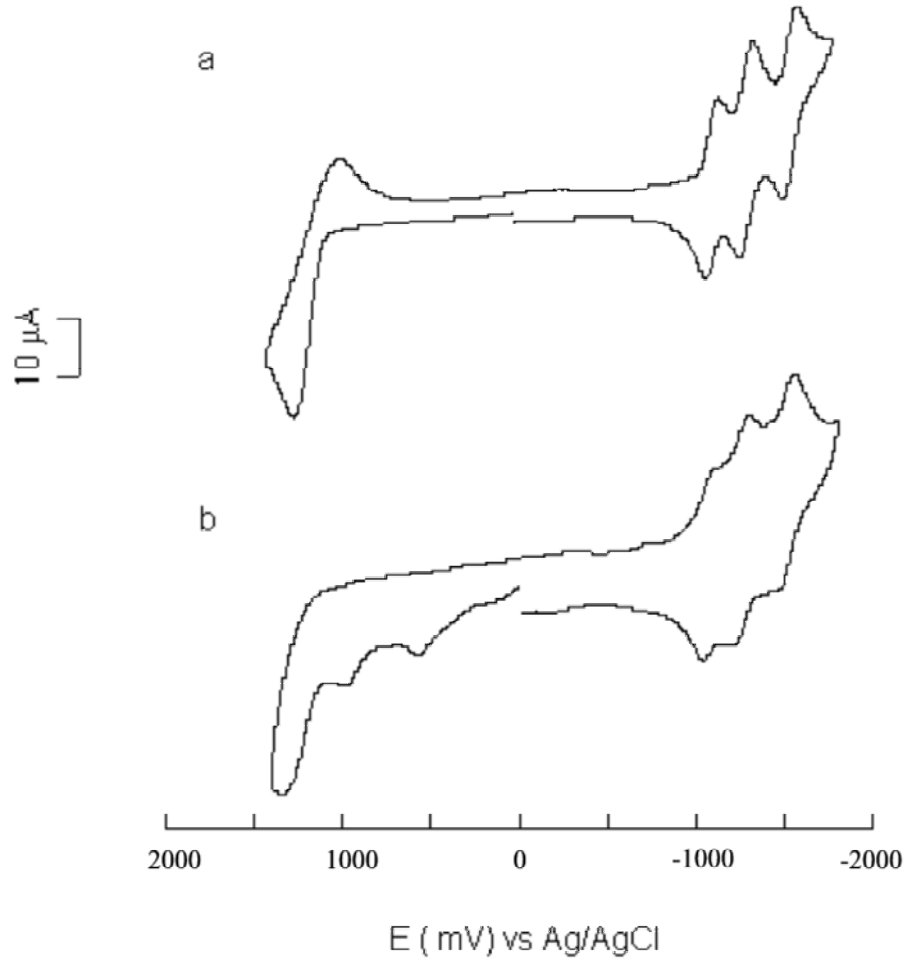


Figure 6.7: Cyclic voltammograms of (a) 0.8 mM $[Ru(bpy)_3]Cl_2$, and (b) a mixture of 0.8 mM $[Ru(bpy)_3]Cl_2$ and 1.6 mM carbene **1**. solvent: $CH_3CN$. Electrolyte: 0.1 M $Bu_4 NPF_6$.

# Bibliography


Abass, A. K., J. P. Hart, D. C. Cowell and A. Chappell. *Analytica Chimica Acta* **1998,** *373*, 1-8.

Abernethy, C. D., J. A. C. Clyburne, A. H. Cowley and R. A. Jones. *Journal of the American Chemical Society* **1999,** *121*, 2329-2330.

Actor, J. K., T. Kuffner, C. S. Dezzutti, R. L. Hunter and J. M. McNicholl. *Journal of Immunological Methods* **1998,** *211*, 65-77.

Albareda-Sirvent, M., A. Merkoci and S. Alegret. *Sensors and Actuators B: Chemical* **2000,** *69*, 153-163.

Alder, R. W., P. R. Allen, M. Murray and A. G. Orpen. *Angew. Chem. Internat. Ed. Engl.* **1996,** *35*, 1121.

Alexandre, I., N. Zammatteo, P. Moris, F. Brancart and J. Remacle. *Journal of Virological Methods* **1997,** *66*, 113-122.

Alfonta, L., A. K. Singh and I. Willner. *Anal. Chem.* **2001,** *73*, 91-102.

Anazawa, T., H. Matsunaga and E. S. Yeung. *Analytical Chemistry* **2002,** *74*, 5033-5038.

Anderson, C. P., D. J. Salmon, T. J. Meyer and R. C. Young. *J. Am. Chem. Soc.* **1977,** *99*, 1980.

Anderson, S., E. C. Constable, K. R. Seddon, E. T. Turp, J. E. Baggott and J. Pilling. *J. Chem. Soc. Dalton Trans.* **1985,** 2247.

Aoki, A. and A. Heller. *Jounal of Physical Chemistry* **1993,** *97*, 11014-11019.

Aoki, A., R. Rajagopalan and A. Heller. *Journal of Physical Chemistry* **1995,** *99*, 5102-10.

Arduengo, A. J., III. *Accounts of Chemical Research* **1999,** *32*, 913-921.

Arduengo, A. J., III, F. Davidson, H. V. R. Dias, J. R. Goerlich, D. Khasnis, W. J. Marshall and T. K. Prakasha. *Journal of the American Chemical Society* **1997,** *119*, 12742-12749.

Arduengo, A. J., III, H. V. R. Dias, J. C. Calabrese and F. Davidson. *Organometallics* **1993,** *12*, 3405.

Arduengo, A. J., III, H. V. R. Dias, F. Davidson and R. L. Harlow. *J. Organomet. Chem.* **1993,** *462*, 13.

Arduengo, A. J., III, H. V. R. Dias, R. L. Harlow and M. Kline. *J. Am. Chem. Soc.* **1992,** *114*, 5530.

Arduengo, A. J., III, S. F. Gamper, J. C. Calabrese and F. Davidson. *J. Am. Chem. Soc.* **1994,** *116*, 4361.

Arduengo, A. J., III, J. R. Goerlick and W. J. Marshall. *J. Am. Chem. Soc.* **1995,** *117*, 11027-11028.

Arduengo, A. J., III, J. R. Goerlick and W. J. Marshall. *Liebigs Ann.* **1997,** 365.

Arduengo, A. J., III, R. L. Harlow and M. Kline. *Journal of the American Chemical Society* **1991,** *113*, 361-3.

Arduengo, A. J., R. L. Harlow, W. J. Marshall and T. K. Prakasha. *Heterocycl. Chem.* **1996,** *7*, 421.

Arduengo, A. J., III, M. Tamm, S. J. McLain, J. C. Calabrese, F. Davidson and W. J. Marshall. *J. Am. Chem. Soc.* **1994,** *116*, 7927.

Armistead, P. M. and H. H. Thorp. *Analytical Chemistry* **2000,** *72*, 3764-3770.

Arnold, L. J., Jr., P. W. Hammond, W. A. Weise and N. C. Nelson. *Clin. Chem.* **1989,** *35*, 1588-1594.

Aston, W. J., R. E. Ashby, I. J. Higgins, L. D. L. Scott and A. P. F. Turner (1984). Charge and Field Effects in Biosystem. M. J. Allen and P. N. R. Usherwood. Tunbridge Wells, U.K., Abacus Press**:** 491.

Aston, W. J. and A. P. F. Turner. *Biotechnology & Genetic Engineering Reviews* **1984,** *1*, 89-120.

Ayala-Torres, S., Y. Chen, T. Svoboda, J. Rosenblatt and B. Van Houten. *Methods (Orlando, Florida)* **2000,** *22*, 135-147.

Azek, F., C. Grossiord, M. Joannes, B. Limoges and P. Brossier. *Analytical Biochemistry* **2000,** *284*, 107-113.

Bagel, O., C. Degrand, B. Limoges, M. Joannes, F. Azek and P. Brossier. *Electroanalysis* **2000,** *12*, 1447-1452.

Bard, A. and L. R. Faulkner. Electrochemical Methods: Fundamentals and Applications, John Wiley & Sons, Inc.: New York, 2001

Bartlett, P. N. and V. Eastwick-Field. *Electrochimica Acta* **1993,** *38*, 2515-2523.

Barton, S. C., H.-H. Kim, G. Binyamin, Y. Zhang and A. Heller. *Journal of the American Chemical Society* **2001,** *123*, 5802-5803.

Benecke, M. *Naturwissenschaften* **1997,** *84*, 181-188.

Black, S. J., D. E. Hibbs, M. B. Hursthouse, C. Jones, K. M. Abdul Malik and N. A. Smithies. *Journal of the Chemical Society, Dalton Transactions: Inorganic Chemistry* **1997,** 4313-4320.

Bontempelli, G., F. Magno, M. De Nobili and G. Schiavon. *J. Chem. Soc. Dalton Trans.* **1980,** 2288-2293.

Boon, E. M. and J. K. Barton. *Current Opinion in Structural Biology* **2002,** *12*, 320-329.

Boon, E. M., D. M. Ceres, T. G. Drummond, M. G. Hill and J. K. Barton. *Nature Biotechnology* **2000,** *18*, 1096-1100.

Boulas, P. L., M. Gómez-Kaifer and L. Echegoyen. *Angew. Chem. Internat. Ed. Engl.* **1998,** *37*, 216.

Burchill, S. A. and P. J. Selby. *Journal of Pathology* **2000,** *190*, 6-14.

Buttry, D. A. and M. D. Ward. *Chemical Reviews* **1992,** *92*, 1355-1379.

Byfield, M. P. and R. A. Abuknesha. *Biosensors and Bioelectronics* **1994,** *9*, 373-399.

Campbell, C. N., D. Gal, N. Cristler, C. Banditrat and A. Heller. *Anal. Chem.* **2002,** *74*, 158-162.

Candrian, U. *Journal of Microbiological Methods* **1995,** *23*, 89-103.

Cannon, D. M., Jr., N. Winograd and A. G. Ewing. *Annual Review of Biophysics and Biomolecular Structure* **2000,** *29*, 239-263, 2 Plates.

Cao, Y. C., R. Jin and C. A. Mirkin. *Science* **2002,** *297*, 1536-1540.

Caruana, D. J. and A. Heller. *J. Am. Chem. Soc.* **1999,** *121*, 769-774.

Caruso, F., E. Rodda, D. N. Furlong, K. Niikura and Y. Okahata. *Analytical Chemistry* **1997,** *69*, 2043-2049.

Casperson, M. E., R. W. Coughlin and E. M. Davis. *TrAC, Trends in Analytical Chemistry* **1991,** *10*, 133-6.

Chen, T., The Development and Application of Glucose Electrodes Based on "Wired" Glucose Oxidase; University of Texas: Austin, **2001**.

Chen, T., S. C. Barton, G. Binyamin, Z. Gao, Y. Zhang, H.-H. Kim and A. Heller. *Journal of the American Chemical Society* **2001,** *123*, 8630-8631.

Chiu, N. H. L. and T. K. Christopoulos. *Anal. Chem.* **1996,** *68*, 2304-2308.

Chiu, N. H. L., T. K. Christopoulos and J. Peltier. *ANALYST* **1998,** *123*, 1315-1319.

Christopoulos, T. K. *Anal. Chem.* **1999,** *71*, 425R-438R.

Clarke, J. R. *Expert Review of Molecular Diagnostics* **2002,** *2*, 233-239.

Clendenning, S. B., P. B. Hitchcock, J. F. Nixon and L. Nyulaszi. *Chemical Communications (Cambridge)* **2000,** 1305-1306.

Clyne, J. M., J. A. Running, M. Stempien, R. S. Stephens, H. Akhavan-Tafti, A. P. Schaap and M. S. Urdea. *Journal of Bioluminescence and Chemiluminescence* **1989,** *4*, 357-66.

Cole, M. L., A. J. Davies and C. Jones. *Journal of the Chemical Society, Dalton Transactions* **2001,** 2451-2452.

Coombe, V. T., G. A. Heath, A. J. MacKenzie and L. J. Yellowlees. *Inorg. Chem.* **1984,** *23*, 3423.

Cunningham, A. J. Introduction to Bioanalytical Sensors, John Wiley & Sons, Inc: New York, 1998

Dahlén, P., A.-C. Syvänen, P. Hurskainen, M. Kwiatkowski, C. Sund, J. Ylikoski, H. Söderlund and T. Lövgren. *Molecular and Cellular Probes* **1987,** *1*, 159-168.

Danielsson, B. and K. Mosbach (1989). Theory and application of calorimetric sensors. Biosensors: Fundamentals and Applications. A. P. F. Turner, I. Karube and G. S. Wilson. New York, Oxford University Press.

Davis, G., H. A. O. Hill, W. J. Aston, I. J. Higgins and A. P. F. Turner. *Enzyme and Microbial Technology* **1983,** *5*, 383-8.

De Lumley-Woodyear, T., C. N. Campbell and A. Heller. *J. Am. Chem. Soc.* **1996,** *118*, 5504-5505.

De Lumley-Woodyear, T., D. J. Caruana, C. N. Campbell and A. Heller. *Anal. Chem.* **1999,** *71*, 394-398.

DeArmond, M. K. and M. L. Myrick. *Acc. Chem. Res.* **1989,** *22*, 364.

DeFillipo, K. A. and M. L. Grayeski. *Analytica Chimica Acta* **1991,** *249*, 155-62.

Degani, Y. and A. Heller. *Journal of the American Chemical Society* **1988,** *110*, 2615-20.

Degani, Y. and A. Heller. *Journal of the American Chemical Society* **1989,** *111*, 2357-8.

Del Carlo, M., I. Lionti, M. Taccini, A. Cagnini and M. Mascini. *Analytica Chimica Acta* **1997,** *342*, 189-197.

Denk, K., P. Sirsch and W. A. Herrmann. *Journal of Organometallic Chemistry* **2002,** *649*, 219-224.

Dequaire, M., C. Degrand and B. Limoges. *Journal of the American Chemical Society* **1999,** *121*, 6946-6947.

Dequaire, M. and A. Heller. *Anal. Chem.* **2002,** *74*, 4370 -4377.

Desmurs, P., A. Dormond, F. Nief and D. Baudry. *Bulletin de la Societe Chimique de France* **1997,** *134*, 683-688.

Dias, H. V. R. and W. Jin. *Tetrahedron Lett.* **1994,** *35*, 1365.

Dunn, A. R. and J. A. Hassell. *Cell* **1977,** *12*, 23-36.

Durick, K. and P. Negulescu. *Biosensors & Bioelectronics* **2001,** *16*, 587-592.

Elbanowski, M. and B. Makowska. *Journal of Photochemistry and Photobiology A: Chemistry* **1996,** *99*, 85-92.

Enders, D., K. Breuer, G. Raabe, J. Runsink, J. H. Teles, J.-P. Melder, K. Ebel and S. Brode. *Angewandte Chemie, International Edition in English* **1995,** *34*, 1021-3.

Enders, D., K. Breuer, G. Raabe, J. Simonet, A. Ghanimi, H. B. Stegmann and J. H. Teles. *Tetrahedron Letters* **1997,** *38*, 2833-2836.

Enders, D., K. Breuer, J. Runsink and J. H. Teles. *Liebigs Annalen* **1996,** 2019-2028.

Enders, D., K. Breuer, J. H. Teles and K. Ebel. *Journal fuer Praktische Chemie/Chemiker-Zeitung* **1997,** *339*, 397-399.

Epstein, J. T., M. Lee and D. R. Walt. *Analytical Chemistry* **2002,** *74*, 1836-1840.

Erdem, A., K. Kerman, B. Meric, U. S. Akarca and M. Ozsoz. *Anal. Chim. Acta* **2000,** *422*, 139.

Erdem, A., K. Kerman, B. Meric and M. Ozsoz. *Electroanalysis* **2001,** *13*, 219.

Farb, A., F. D. Kolodgie, R. M. Jones, M. Jenkins and R. Virmani. *Journal of Molecular and Cellular Cardiology* **1993,** *25*, 343-353.

Ferguson, J. A., F. J. Steemers and D. R. Walt. *Analytical Chemistry* **2000,** *72*, 5618-5624.

Fisher, M., S. Harbron and C. J. Taylorson. *Analytical Biochemistry* **1997,** *251*, 280-287.

Forster, R. J. and J. G. Vos. *Macromolecules* **1990,** *23*, 4372.

Gambari, R. *Am J Pharmacogenomics* **2001,** *1*, 119-135.

Gao, Z., G. Binyamin, H.-H. Kim, S. C. Barton, Y. Zhang and A. Heller. *Angewandte Chemie, International Edition* **2002,** *41*, 810-813.

Gardiner, M. G., W. A. Herrmann, C.-P. Reisinger, J. Schwarz and M. Spiegler. *Journal of Organometallic Chemistry* **1999,** *572*, 239-247.

Girotti, S., M. Musiani, E. Ferri, G. Gallinella, M. Zerbini, A. Roda, G. Gentilomi and S. Venturoli. *Analytical Biochemistry* **1996,** *236*, 290-5.

Gmuender, H. *BioTechniques* **2002,** *32*, 152-154, 156, 158.

Gockel, A. and P. Berschick. *Nucleic Acids Isolation Methods* **2003,** 153-177.

Gregg, B. A. and A. Heller. *Journal of Physical Chemistry* **1991,** *95*, 5970-5.

Haas, O., M. Kriens and J. G. Vos. *J. Am. Chem. Soc.* **1981,** *103*, 1318-1319.

Habermuller, K., M. Mosbach and W. Schuhmann. *Fresenius Journal of Analytical Chemistry* **2000,** *366*, 560-568.

Hakala, H., E. Mäki and H. Lönnberg. *Bioconjugate Chem.* **1998,** *9*, 316-321.

Hakala, H., P. Virta, H. Salo and H. Lonnberg. *Nucl. Acids. Res.* **1998,** *26*, 5581-5588.

Han, S., J. Lin, F. Zhou and R. L. Vellanoweth. *Biochemical and Biophysical Research Communications* **2000,** *279*, 265-269.

Harry, M. R., R. Freedland and M. L. Roger. Biochemistry: A Short Course, Wiley-Liss, Inc.: New York, 1997

Hauber, R. and R. Geiger. *Nucleic Acids Research* **1988,** *16*, 1213.

He, L., M. D. Musick, S. R. Nicewarner, F. G. Salinas, S. J. Benkovic, M. J. Natan and C. D. Keating. *J. Am. Chem. Soc.* **2000,** *122*, 9071-9077.

Heath, G. A., L. J. Yellowlees and P. S. Braterman. *J. Chem. Soc., Chem. Comm.* **1981,** 287.

Heineman, W. R., J. N. Burnett and R. W. Murray. *Anal. Chem.* **1968,** *40*, 1970-1973.

Heller, A. *Accounts of Chemical Research* **1990,** *23*, 128-34.

Heller, A. *Journal of Physical Chemistry* **1992,** *96*, 3579-87.

Herrmann, W. A., C.-P. Reisinger and M. Spiegler. *Journal of Organometallic Chemistry* **1998,** *557*, 93-96.

Herrmann, W. A., J. Schwarz and M. G. Gardiner. *Organometallics* **1999,** *18*, 4082-4089.

Hershberger, J. W., C. Amatore and J. K. Kochi. *J. Organomet. Chem.* **1983,** *250*, 345-371.

Hiromi, K., S. Yamaguchi, Y. Sugiura, H. Iwamoto and J. Hirose. *J. Biosci. Biotech. Biochem.* **1992,** *56*, 1349.

Hirose, J., T. Inoue, H. Sakuragi, M. Kikkawa, M. Minakami, T. Morikawa, H. Iwamoto and K. Hiromi. *Inorganica. Chim. Acta* **1998,** *273*, 204.

Hirose, J., M. Minakami, K. Inoue, H. Watanabe, H. Iwamoto and K. Hiromi. *J. Inorg. Biochem.* **1995,** *59*, 718.

Homola, J., S. S. Yee and G. Gauglitz. *Sensors and Actuators B: Chemical* **1999,** *54*, 3-15.

Huang, L. and R. T. Kennedy. *TrAC, Trends in Analytical Chemistry* **1995,** *14*, 158-64.

Ianiello, R. M., T. J. Lindsay and A. M. Yacynych. *Anal. Chem.* **1982,** *54*, 1098.

Ihara , T., M. Nakayama , M. Murata , K. Nakano and M. Maeda. *Chem. Commun.* **1997,** 1609-1610.

Ishii, J. K. and S. S. Ghosh. *Bioconjugate Chem.* **1993,** *4*, 34-41.

Ivnitski, D., I. Abdel-Hamid, P. Atanasov and E. Wilkins. *Biosensors and Bioelectronics* **1999,** *14*, 599-624.

Janshoff, A., H.-J. Galla and C. Steinem. *Angewandte Chemie, International Edition* **2000,** *39*, 4004-4032.

Johnson, J. R. *J. Microbiol. Meth.* **2000,** *41*, 201-209.

Johnson, P. H., R. P. Walker, S. W. Jones, K. Stephens, J. Meurer, D. A. Zajchowski, M. M. Luke, F. Eeckman, Y. Tan, L. Wong, G. Parry, T. K. Morgan, Jr., M. A. McCarrick and J. Monforte. *Molecular Cancer Therapeutics* **2002,** *1*, 1293-1304.

Johnston, D. H., K. C. Glasgow and H. H. Thorp. *Journal of the American Chemical Society* **1995,** *117*, 8933-8.

Jung, R., K. Soondrum and M. Neumaier. *Clinical Chemistry and Laboratory Medicine* **2000,** *38*, 833-836.

Kambhampati, D. K. and W. Knoll. *Current Opinion in Colloid & Interface Science* **1999,** *4*, 273-280.

Kelley, S. C., G. A. Deluga and W. H. Smyrl. *Electrochem. Solid State Lett.* **2000,** *3*, 407.

Kelley, S. O., E. M. Boon, J. K. Barton, N. M. Jackson and M. G. Hill. *Nucleic Acids Research* **1999,** *27*, 4830-4837.

Kelley, S. O., N. M. Jackson, M. G. Hill and J. K. Barton. *Angewandte Chemie, International Edition* **1999,** *38*, 941-945.

Kenausis, G., C. Taylor, I. Katakis and A. Heller. *Journal of the Chemical Society, Faraday Transactions* **1996,** *92*, 4131-4136.

Kirk, J. R., D. Page, M. Prazak and V. Katovic. *Inorganic Chemistry* **1988,** *27*, 1956-1963.

Kleinjung, F., F. F. Bier, A. Warsinke and F. W. Scheller. *Analytica Chimica Acta* **1997,** *350*, 51-58.

Koudelka, G. B. and a. M. J. Ettinger. *J. Biol. Chem.* **1988,** *263*, 3698.

Koudelka-Hep, M. and P. D. Van der Wal. *Electrochimica Acta* **2000,** *45*, 2437-2441.

Kuhn, N., G. Henkel and T. Kratz. *Chem. Ber.* **1993,** *126*, 2047.

Kuhn, N., G. Henkel and T. Z. Kratz. *Naturforsch. B.* **1993,** *48*, 973.

Kuhn, N. and T. Kratz. *Synthesis* **1993,** 561.

Kuhn, N., T. Kratz, D. Bläser and R. Boese. *Inorg. Chim. Acta* **1995,** *238*, 179.

Laszik, A., A. Falus, L. Keresztury and P. Sotonyi. *Acta Biologica Hungarica* **1998,** *49*, 89-95.

Lindner, E. and R. P. Buck. *Analytical Chemistry* **2000,** *72*, 336A-345A.

Liu, X. and W. Tan. *Analytical Chemistry* **1999,** *71*, 5054-5059.

Lou, H. J. and W. Tan. *Instrumentation Science & Technology* **2002,** *30*, 465-476.

Lovatt, A. *Reviews in Molecular Biotechnology* **2002,** *82*, 279-300.

Maerker, G. and F. H. Case. *J. Am. Chem. Soc.* **1958,** *80*, 2475.

Malcolm, S. *European Journal of Biochemistry* **1990,** *194*, 317-21.

Mannelli, I., M. Minunni, S. Tombelli and M. Mascini. *Biosensors & Bioelectronics* **2003,** *18*, 129-140.

Mano, N., H.-H. Kim and A. Heller. *Journal of Physical Chemistry B* **2002,** *106*, 8842-8848.

Mano, N., H.-H. Kim, Y. Zhang and A. Heller. *Journal of the American Chemical Society* **2002,** *124*, 6480-6486.

Marazuela, M. D. and M. C. Moreno-Bondi. *Analytical and Bioanalytical Chemistry* **2002,** *372*, 664-682.

Mascini, M., I. Palchetti and G. Marrazza. *FRESENIUS JOURNAL OF ANALYTICAL CHEMISTRY* **2001,** *369*, 15-22.

Millan, K. M. and S. R. Mikkelsen. *Analytical Chemistry* **1993,** *65*, 2317-23.

Millan, K. M., A. Saraullo and S. R. Mikkelsen. *Analytical Chemistry* **1994,** *66*, 2943-8.

Miyawaki, O. and J. L. B. Wingard. *Biotech. Bioeng.* **1984,** *26*, 1364.

Montenegro, M. I., M. A. Queiros and J. L. Daschbach, Eds. (1991). Microelectrodes : Theory and Applications. Dordrecht ; Boston ; London, Kluwer Academic.

Morris, D. E., K. W. Hanck and M. K. DeArmond. *J. Am. Chem. Soc.* **1983,** *105*, 3032.

Motten, A. G., K. Hanck and M. K. DeArmond. *Chem. Phys. Lett.* **1981,** *79*, 541.

Mulazzani, Q. C., S. Emmi, P. G. Fuochi, M. Z. Hoffman and M. Venturi. *J. Am. Chem. Soc.* **1978,** *100*, 981.

Nagel, M., P. H. Bolivar, M. Brucherseifer, H. Kurz, A. Bosserhoff and R. Büttner. *Applied Optics* **2002,** *41*, 2074-2078.

Nagels, L. J. and E. Staes. *TrAC Trends in Analytical Chemistry* **2001,** *20*, 178-185.

Nakai, H., Y. Tang, P. Gantzel and K. Meyer. *Chemical Communications (Cambridge, United Kingdom)* **2003,** 24-25.

Napier, M. E., C. R. Loomis, M. F. Sistare, J. Kim, A. E. Eckhardt and H. H. Thorp. *Bioconjugate Chemistry* **1997,** *8*, 906-913.

Naqui, A. and S. D. Varfolomeev. *FEBS Lett.* **1980,** *113*, 157.

Nelson, N. C. and D. L. Kacian. *Clinica Chimica Acta* **1990,** *194*, 73-90.

Niehues, M., G. Kehr, G. Erker, B. Wibbeling, R. Frohlich, O. Blacque and H. Berke. *Journal of Organometallic Chemistry* **2002,** *663*, 192-203.

Ohara, T. J., R. Rajagopalan and A. Heller. *Analytical Chemistry* **1994,** *66*, 2451-7.

Ohsawa, Y., M. K. DeArmond, K. W. Hanck, D. E. Morris, D. G. Whitten and P. E. Neveux. *J. Am.Chem. Soc.* **1983,** *105*, 6522.

Olsen, J. E. *Food Research International* **2000,** *33*, 257-266.

Opalinska, J. B. and A. M. Gewirtz. *Nature Reviews Drug Discovery* **2002,** *1*, 503-514.

Ou, C. Y., S. H. McDonough, D. Cabanas, T. B. Ryder, M. Harper, J. Moore and G. Schochetman. *AIDS Research and Human Retroviruses* **1990,** *6*, 1323-9.

Palecek, E. *Talanta* **2002,** *56*, 809-819.

Palecek, E. and M. Fojta. *Analytical Chemistry* **2001,** *73*, 74A-83A.

Palmore, G. T. R. and H.-H. Kim. *Journal of Electroanalytical Chemistry* **1999,** *464*, 110-117.

Palmore, G. T. R. and G. M. Whitesides. *ACS Symposium Series* **1994,** *566*, 271-90.

Pancrazio, J. J., J. P. Whelan, D. A. Borkholder, W. Ma and D. A. Stenger. *Annals of Biomedical Engineering* **1999,** *27*, 697-711.

Park, S.-J., T. A. Taton and C. A. Mirkin. *Science* **2002,** *295*, 1503-1506.

Patolsky, F., A. Lichtenstein and I. Willner. *J. Am. Chem. Soc.* **2000,** *122*, 418 - 419.

Poljak, M., K. Seme and S. Koren. *Periodicum Biologorum* **1996,** *98*, 183-190, P.190.

Pollard-Knight, D., C. A. Read, M. J. Downes, L. A. Howard, M. R. Leadbetter, S. A. Pheby, E. McNaughton, A. Syms and M. A. W. Brady. *Analytical Biochemistry* **1990,** *185*, 84-9.

Popovich , N. D. and H. H. Thorp. *The Electrochemical Society Interface* **2002,** *11*, 30-34.

Raeymaekers, L. *Molecular Biotechnology* **2000,** *15*, 115-122.

Raeymaekers L. *Analytical Biochemistry* **1993,** *214*, 582-585.

Ramaraj, R. and P. Natarajan. *Journal of Polymer Science, Part A: Polymer Chemistry* **1991,** *29*, 1339-46.

Ramsay, G., Ed. (1998). Commercial Biosensors: Applications to Clinical, Bioprocess, and Environmental Samples. Chemical Analysis: A Series of Monographs on Analytical Chemistry and Its Applications. New York, John Wiley & Sons, Inc.

Ranki, M., A. Palva, M. Laaksonen, M. Virtanen and H. Söderlund. *Gene* **1983,** *21*, 77-85.

Rao, J. R., G. Richter, F. Von Sturm, E. Weidlich and M. Wenzel. *Biomedical Engineering* **1974,** *9*, 98-103.

Regitz, M. *Angew. Chem., Int. Ed. Engl.* **1991,** *30*, 674-676.

Regitz, M. *Angew. Chem. Internat. Ed. Engl.* **1996,** *35*, 725.

Reinhammer, B. R. M. *J. Inorg. Biochem.* **1981,** *15*, 27.

Roundhill, D. M. Photochemistry and Photophysics of Metal Complexes, Plenum Press: New York, 1994

Rule, G. S., R. A. Montagna and R. A. Durst. *Analytical Biochemistry* **1997,** *244*, 260-269.

Sayka, A. and J. G. Eberhart. *Solid State Technol.* **1989,** *32*, 69.

Schochetman, G. *Clinica Chimica Acta* **1992,** *211*, 1-26.

Schönherr, H.-J. and H. W. Wanzlick. *Liebigs Ann. Chem.* **1970,** *731*, 176.

Schuhmann, W. *Reviews in Molecular Biotechnology* **2002,** *82*, 425-441.

Schumacher, R. *Angewandte Chemie International Edition* **1990,** *29*, 329.

Schumann, H., M. Glanz, J. Gottfriedsen, S. Dechert and D. Wolff. *Pure and Applied Chemistry* **2001,** *73*, 279-282.

Schumann, H., M. Glanz, J. Winterfeld, H. Hemling, N. Kuhn and T. Kratz. *Angew. Chem., Int. Ed. Engl.* **1994,** *33*, 1733-1734.

Schumann, H., M. Glanz, J. Winterfeld, H. Hemling, N. Kuhn and T. Kratz. *Chemische Berichte* **1994,** *127*, 2369-72.

Schutzbank, T. E. and J. Smith. *Journal of Clinical Microbiology* **1995,** *33*, 2036-2041.

Schwarz, J., V. P. W. Bohm, M. G. Gardiner, M. Grosche, W. A. Herrmann, W. Hieringer and G. Raudaschl-Sieber. *Chemistry--A European Journal* **2000,** *6*, 1773-1780.

Sethi, R. S. *Biosensors and Bioelectronics* **1994,** *9*, 243-264.

Simal, F., S. Delfosse, A. Demonceau, A. F. Noels, K. Denk, F. J. Kohl, T. Weskamp and W. A. Herrmann. *Chemistry--A European Journal* **2002,** *8*, 3047-3052.

Smith, C. L., L. Kricka and U. J. Krull. *Genetic Analysis: Biomolecular Engineering* **1995,** *12*, 33-37.

Song, F., F. Zhou, J. Wang, N. Tao, J. Lin, R. L. Vellanoweth, Y. Morquecho and J. Wheeler-Laidman. *Nucl. Acids. Res.* **2002,** *30*, e72-.

Speiser, B. *Analytical and Bioanalytical Chemistry* **2002,** *372*, 29-30.

Stulik, K., C. Amatore, K. Holub, V. Marecek and W. Kutner. *Pure and Applied Chemistry* **2000,** *72*, 1483-1492.

Takagi, M. *Pure and Applied Chemistry* **2001,** *73*, 1573-1577.

Takenaka, S. *Bulletin of the Chemical Society of Japan* **2001,** *74*, 217-224.

Takenaka, S., K. Yamashita, M. Takagi, Y. Uto and H. Kondo. *Analytical Chemistry* **2000,** *72*, 1334-1341.

Tan, S. L., M. K. DeArmond and K. W. Hanck. *J. Electroanal. Chem.* **1984,** *181*, 187.

Tan, W., X. Fang, J. Li and X. Liu. *Chemistry--A European Journal* **2000,** *6*, 1107-1111.

Tarasevich, M. R., A. I. Yaropolov, V. A. Bogdanovskaya and S. D. Varfolomeev. *J. Electroanal. Chem. Interfacial Electrochem.* **1979,** *104*, 393.

Taton, T. A., G. Lu and C. A. Mirkin. *J. Am. Chem. Soc.* **2001,** *123*, 5164-5165.

Taton, T. A., C. A. Mirkin and R. L. Letsinger. *Science* **2000,** *289*, 1757-1760.

Tawata, M., K. Aida and T. Onaya. *Combinatorial Chemistry and High Throughput Screening* **2000,** *3*, 1-9.

Taylor, C., G. Kenausis, I. Katakis and A. Heller. *Journal of Electroanalytical Chemistry* **1995,** *396*, 511-15.

Teles, J. H., J.-P. Melder, K. Ebel, R. Schneider, Gehrer, E., W. Harder, S. Brode, D. P. Enders, K. Breuer and G. Raabe. *Helv. Chim. Acta* **1996,** *79*, 61.

Tsujimura, S., H. Tatsumi, J. Ogawa, S. Shimizu, K. Kano and T. Ikeda. *Journal of Electroanalytical Chemistry* **2001,** *496*, 69-75.

Turner, A. P. F. (1983). Biotech 83. London, Online Publ.**:** 643.

Turner, A. P. F., W. J. Aston, J. Bell, J. Colby, G. Davis, I. J. Higgins and H. A. O. Hill. *Anal. Chim. Acta* **1984,** *163*, 161.

Turner, A. P. F., W. J. Aston, I. J. Higgins, G. Davis and H. A. O. Hill. *Biotechnology and Bioengineering Symposium* **1982,** *12*, 401-12.

Turner, A. P. F., G. Ramsay and I. J. Higgins. *Biochem. Soc. Trans.* **1983,** *11*, 445.

Tyagi, S. and F. R. Kramer. *Nature Biotechnology* **1996,** *14*, 303-309.

Vercoutere, W. and M. Akeson. *Current Opinion in Chemical Biology* **2002,** *6*, 816-822.

Verhaegen, M. and T. K. Christopoulos. *Analytical Chemistry* **2002,** *74*, 4378-4385.

Vlcek, A. A. *Coord. Chem. Rev.* **1982,** *43*, 39.

Vreeke, M. S., K. T. Yong and A. Heller. *Analytical Chemistry* **1995,** *67*, 4247-9.

Wabuyele, M. B. and S. A. Soper. *Single Molecules* **2001,** *2*, 13-21.

Wang, J. *Chemistry-A European Journal* **1999,** *5*, 1681-1685.

Wang, J. *Nucl. Acids. Res.* **2000,** *28*, 3011-3016.

Wang, J. *TrAC, Trends in Analytical Chemistry* **2002,** *21*, 226-232.

Wang, J. *Analytica Chimica Acta* **2002,** *469*, 63-71.

Wang, J., P. E. Nielsen, M. Jiang, X. Cai, J. R. Fernandes, D. H. Grant, M. Ozsoz, A. Beglieter and M. Mowat. *Analytical Chemistry* **1997,** *69*, 5200-5202.

Wang, J., R. Polsky, A. Merkoci and K. L. Turner. *Langmuir* **2003,** *19*, 989-991.

Wang, J., D. Xu, A. Erdem, R. Polsky and M. A. Salazar. *Talanta* **2002,** *56*, 931-938.

Wanzlick, H. W. *Angew. Chem. Internat. Ed. Engl.* **1962,** *1*, 75.

Wanzlick, H. W. and B. König. *Chem. Ber.* **1964,** *97*, 3513.

Weskamp, T., V. P. W. Bohm and W. A. Herrmann. *Journal of Organometallic Chemistry* **1999,** *585*, 348-352.

Weskamp, T., V. P. W. Bohm and W. A. Herrmann. *Journal of Organometallic Chemistry* **2000,** *600*, 12-22.

Weskamp, T., F. J. Kohl, W. Hieringer, D. Gleich and W. A. Herrmann. *Angewandte Chemie, International Edition* **1999,** *38*, 2416-2419.

Willner, I., G. Arad and E. Katz. *Bioelectrochemistry and Bioenergetics* **1998,** *44*, 209-214.

Wolfbeis, O. S. *Analytical Chemistry* **2002,** *74*, 2663-2677.

Wood, S. and S. Langlois. *Journal of Chromatography* **1991,** *569*, 421-47.

Zakeeruddin, S. M., D. M. D. M. Fraser, M.-K. Nazeeruddin and M. Gratzel. *J. Electroanal. Chem.* **1992,** *337*, 253.

Zammatteo, N., S. Hamels, F. de Longueville, I. Alexandre, J.-l. Gala, F. Brasseur and J. Remacle. *Biotechnology Annual Review* **2002,** *8*, 85-101.

Zhang, Y., H.-H. Kim, N. Mano, M. Dequaire and A. Heller. *Anal. Bioanal. Chem.* **2002,** *374*, 1050-1055.

Zheng, X. and G. E. Herberich. *Organometallics* **2000,** *19*, 3751-3753.

Zoski, C. G. *Journal of Electroanalytical Chemistry and Interfacial Electrochemistry* **1990,** *296*, 317-33.

Zoski, C. G. *Electroanalysis* **2002,** *14*, 1041-1051.

# Vita

Yongchao Zhang was born in Hefei, Anhui, China on February 18, 1969, the son of Xiangzhong Zhang and Suqin Tao. In 1987, he entered Fudan University in Shanghai, China. He received the Degree of Bachelor of Science in Chemistry in 1991. He entered the State University of New York at Albany in 1994, and received a Master's Degree in Chemistry in 1996. In August of 1996 he entered the Graduate School of The University of Texas at Austin, and joined Professor Adam Heller's research group in August 1998.

Permanent address: 3363-D Lake Austin Blvd, Austin, TX 78703

This dissertation was typed by the author.